INFLUENCE OF CELL-ADHESIVE LAMININ PEPTIDES ON TUBULOGENESIS

Saniya Ali, Jennifer Saik, and Jennifer L. West
Department of Bioengineering, Rice University, Houston, TX
Saniya.Ali@rice.edu

Background and Objective:

The development of engineered tissues or organs has been limited due to their lack of functional vessels for providing nourishment and waste removal. We have investigated the influence of various cell-adhesive laminin derived peptides in the formation of vascular networks both *in vitro* and *in vivo*. Extracellular matrix-derived, bioactive peptides known to interact with cell surface receptors were incorporated into poly(ethylene glycol) (PEG) hydrogels. PEG hydrogels were utilized for the cell scaffold due to their well established biocompatibility, inherent resistance to protein absorption, and ease of biochemical modification [1]. A co-culture of human umbilical vein endothelial cells (HUVEC) and pericyte precursor cells (10T1/2) were encapsulated in the hydrogels. This co-culture of cells has lead to tubulogenesis with lumen-like structure development when encapsulated into three dimensional degradable gels [2]. In this study, we illustrate the effects of cell-adhesive laminin peptides YIGSR, IKVAV, and RGDS and their combinations on tubulogenesis.

Methods:

Poly(ethylene glycol) diacrylate (PEGDA) was synthesized as previously described [2]. The collagenase sensitive sequence GGGPQGIWGQGK (abbreviated PQ) was incorporated into the PEGDA polymer backbone to render the hydrogels sensitive to cell-secreted matrix metalloproteases for degradation. Bioactivity was incorporated into PEG materials by attaching the free amine of the peptide to a bifunctional PEG molecule, leaving the other end to crosslink into the hydrogel. Polymer solution was prepared in HBS (10 mM, pH 7.4) with a final formulation of 10% polymer weight MMP-sensitive PEG, 3.5 µmol/ml PEG-RGDS/PEG-YIGSR/PEG-IKVAV, and 0.3% weight/volume Eosin Y photoinitiator. Combinations of RGDS with IKVAV or YIGSR were incorporated at concentrations of 1 µmol/ml and 3.5 µmol/ml, respectively. Cells were encapsulated into three dimensional degradable gels at a ratio of 4:1 of HUVEC: 10T1/2 cells. A cell concentration of 30,000 cells/µl polymer solution was used. The polymer solution with cells was photopolymerized via UV light. Hydrogels were immersed in EGM-2 media before *in vitro* analysis or *in vivo* implantation. Tubulogenesis of encapsulated cells was studied *in vitro* and imaged using a DAPI stain for nuclei and phalloidin for actin fibers. Hydrogels with encapsulated cells were implanted into the mouse cornea to evaluate cell viability and tubulogenesis in *in vivo* for 7 days. Immunohistochemistry was performed to assess the accumulation of collagen IV and laminin proteins. Confocal images of gels were taken and the resulting vessels were quantified by percent shared borders of tubules, vessel diameter, vessel density, and branch points.

Results:

The type of adhesive peptides presented in polymer scaffolds influences cell adhesion and tubule formation as seen in Figures 1 and 2. There is a significant difference in tubule formation *in vitro* 7 days after cell encapsulation with the combination of YIGSR with RGDS as compared to the YIGSR alone or RGDS alone. Percent shared borders between tubules in gels with YIGSR and RGDS was 20% as compared to only 13% in gels with RGDS alone and 17% in gels with YIGSR alone. Collagen IV and laminin are both secreted and deposited by cell-formed tubes *in vivo* with the highest pixel intensity for laminin and collagen IV shown in Figure 2 in gels with both YIGSR and RGDS peptides. This ECM deposition is characteristic of more stable vessels [2].

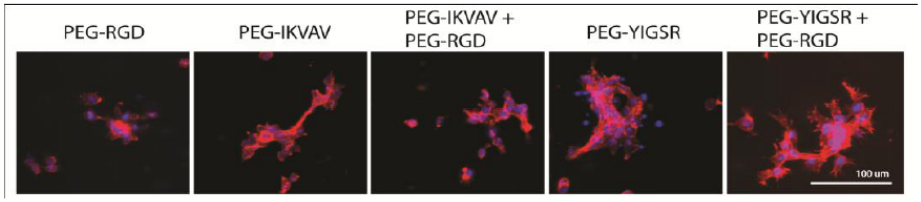

Figure 1: DAPI and Phalloidin staining of tubulogenesis *in vitro* in hydrogels with encapsulated HUVECs and 10T1/2 cells

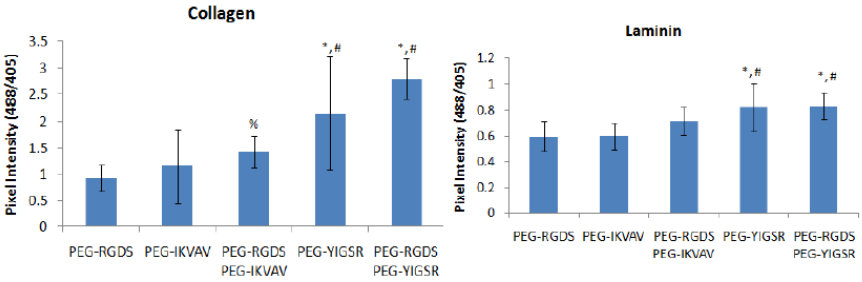

Figure 2: Laminin and collagen IV secretion and deposition from tubule formation *in vivo*

Conclusion:

Cell adhesion ligands (RGDS, IKVAV, and YIGSR) were covalently attached to PEG hydrogels. Different combinations of these ligands affected tubule formations to different degrees. Hydrogels containing the combination of RGDS with YIGSR peptide had the greatest of vessel density and tubule formation *in vitro* and *in vivo*. Further studies need to be conducted to evaluate tubulogenesis with combinations of these peptides at longer time points.

References:

[1] Nguyen KT, West JL. Photopolymerizable hydrogels for tissue engineering applications. Biomaterials. 2002;23:4307-14.
[2] Saik JE, Gould DJ, Watkins EM, Dickenson ME, West JL. Covalently immobilized platelet-derived growth factor-BB promotes angiogenesis in biomimetic poly(ethylene glycol) hydrogels. Acta Biomaterialia. 2011; 7:133-143.

NANOPOROUS PMMA-QD COMPOSITE FIBERS TOWARDS BIOMEDICAL APPLICATIONS

Anumandla, N; Sampathi, J; Rutman, D; Kucknoor, A; Li, Y and Wei, S*
Lamar University, Beaumont, TX 77710
suying.wei@lamar.edu

Here we report the fabrication and characterization of nanostructured polymer composite fibers towards biomedical applications. Poly (methyl methacrylate), PMMA was integrated with CdSe/ZnS Quantum Dots (QDs) via the simple process – solution electrospinning. Uniform and beads free PMMA-QDs composite fibers were prepared by adjusting the related parameters including mass percentage of the PMMA polymer in the solution, feed rate of the solution, applied voltage, and the distance between the ejection needle tip and the grounded fiber receiving substrate. Scanning electron microscopy (SEM) was used to characterize the surface morphology of the fibers and therefore to closely monitor and further guide the adjustment of the electrospinning process. The as-prepared composite fibers bear interesting nanopores in the range of 100-200 nm, while the fiber itself has a diameter between 3-5μm. Interactions between the polymer and the included QDs were explored by attenuated total reflectance infrared spectroscopy (ATR-FTIR) and X-ray photoelectron spectroscopy (XPS). Binding energy shifts were observed for both C 1s and O 1s high resolution spectra. Thermal stability and glass transition temperature were measured via thermogravimetric analysis (TGA) and differential scanning calorimetry (DSC) respectively. It was found that PMMA-QD composite fibers showed higher thermal stability and the glass transition temperature was also changed compared to the pristine PMMA. As the first step towards biomedical applications for the composite fibers, the Chinese hamster ovary (CHO) cell was used as a model epithelia cell type to explore the biocompatibility of PMMA-QD fibers and surface morphology effect on the cell growth. Our preliminary data proved that the PMMA-QDs composite fibers showed good biocompatibility with the cell, while the sharp and uniform fluorescence signal from the fiber provided additional visual advantage.

TAILORING THE PROPERTIES OF PEG-DA HYDROGEL SCAFFOLDS

+Bailey, B.M.; Fei, R.; Touchet, T.J.; Hui, V.; Grunlan, M.A.
Texas A&M University, Dept. of Biomedical Engineering,
Materials Science and Engineering Program, College Station, TX
brenb@neo.tamu.edu

Objective: In tissue engineering, a 3-D polymer scaffold creates an environment for cells to produce new tissue in a desired geometry. In healthy tissues, the native extracellular matrix (ECM) controls cell behavior, including regeneration, via signaling cascades involving not only specific binding events but also non-specific chemical and physical properties.[2] Limited knowledge exists regarding what precise scaffold chemical and physical properties produce cell behavior leading to the regeneration of tissues whose properties parallel that of native tissues (e.g. strength). Photopolymerized poly(ethylene glycol) diacrylate (PEG-DA) based hydrogels have been widely used as scaffolds for tissue engineering. They are particularly useful for controlled studies of cell-material interactions because they are "biological blank slates" – proteins and cells cannot adhere without the controlled introduction of adhesive ligands.[3] Scaffold chemical properties as well as physical properties such as porosity, hydration and modulus impact cell behavior.[4] Thus, hydrogel scaffolds which maintain the benefits of PEG-DA while tuning their properties over a broader range would allow us to establish predictive relationships between scaffold properties, cell regeneration and regenerated tissue properties. In this work, the chemical and physical properties of PEG-DA hydrogels were extended by introduction of inorganic methacrylated star polydimethylsiloxane ($PDMS_{star}$-MA) as well as use of dichloromethane (DCM, CH_2Cl_2) as the hydrogel fabrication solvent rather than water (**Table 1**).

Methods: *Macromer Synthesis:* $PDMS_{star}$-MA (M_n = 7k g/mol) PEG-DA (M_n = 3.4k and 6k g/mol) were prepared as previously reported (**Figure 1**).[5,6] *PEG-DA Hydrogel Fabrication in Water or DCM:* PEG-DA was dissolved in water or DCM at 5, 10, 15, 20, and 25wt% and 10 μL of photoinitiator solution (30 wt% solution of DMAP in NVP) added per 1 mL of solution followed by vortexing (1 min). *$PDMS_{star}$-PEG Hydrogel Fabrication in Water or DCM:* $PDMS_{star}$-MA:PEG-DA (0:100, 5:95, 10:90, 15:85, and 20:80 wt% ratio) were combined in water or DCM at 10 wt% total concentration and photoinitiator was added. The mixtures were vortexed for 1 min after addition of each component. For all hydrogels, the precursor solution was cured in a planar mold comprised of two clamped microscope slides separated by polycarbonate spacers (1 mm) via exposure to UV light (6 mW/cm^2, 365 nm) for 6 min. In the case of hydrogels fabricated in DCM, the resulting slab was allowed to air dry overnight and then soaked in water for 3 days. Hydrogels fabricated in water were similarly allowed to soak in water prior to testing. Swelling, morphology, mechanical properties and degradation rates were investigated.

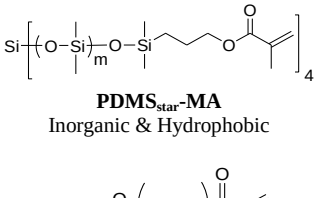

Fig. 1. Structures of $PDMS_{star}$-MA and PEG-DA.

Table 1: Tuning Properties of $PDMS_{star}$-PEG Hydrogels

M_n of PEG-DA (3k and 6k g/mol)
M_n of $PDMS_{star}$-MA (7k g/mol)
Wt ratio of PEG:PDMS (0:100 to 20:80)
Total concentration of macromer in precursor solution (5 to 25 wt%)
Fabrication solvent: water or DCM

Results: When fabricated in DCM, all hydrogels exhibited enhanced swelling versus the corresponding hydrogel fabricated in water. SEM images of hydrogels fabricated in DCM (**Figure 2**) revealed macroporous morphology. In addition, the storage moduli (DMA) of hydrogels fabricated in DCM were greater than that of the corresponding hydrogel fabricated in water. Degradation studies showed that PEG-DA hydrogels (10 wt%) fabricated in DCM degraded in approximately half the time compared to those fabricated in water. For $PDMS_{star}$-PEG hydrogels fabricated in DCM, CLSM images (**Figure 3**) revealed a macroporous network as well as a more uniform distribution of PDMS. When fabricated in DCM, storage modulus values increased and swelling ratio decreased with increase amounts of $PDMS_{star}$-MA.

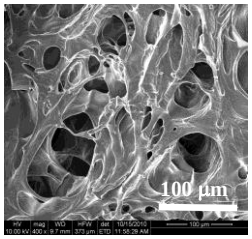

Fig. 2. SEM image of PEG-DA (3k g/mol) hydrogel fabricated from a 10 wt% CH_2Cl_2 solution and then dried and hydrated with water.

Conclusions: Fabrication of pure PEG-DA and $PDMS_{star}$-PEG hydrogels from DCM-based solutions (rather than water) followed by subsequent hydration resulted in significant alterations in chemical and physical properties. This library of scaffolds having tunable properties is expected to be useful to study cell-material interactions to establish predictive relationships leading to a better tissue engineering outcome.

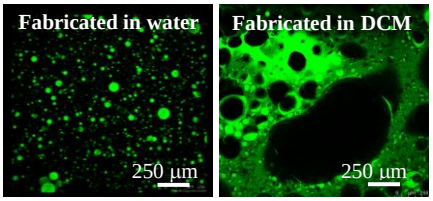

Fig. 3. CLSM images of hydrated hydrogels [20:80 wt% ratio PDMS (7k): PEG(6k)].

References:

1. Langer, R.; Vacanti, J. P. *Science* **1993,** 260, 920-926.
2. Kleinman, H.K.; Philp, D.; Hoffman, M.P. *Curr. Opin. Biotechnol.* **2003**, *14*, 526-532.
3. Burdick, J. A.; Anseth, K. S. *Biomaterials* **2002**, 23, 4315-4323.
4. Dutta, R. C.; Dutta, A. K. *Biotech. Adv.* **2009**, 27, 334-339.
5. Hou, Y.; Schoener, C.A.; Regan, K.R.; Munoz-Pinto, D.; Hahn, M.S.; Grunlan, M.A. *Biomacromolecules* **2010**, *11*, 648-656.
6. Hahn, M.S.; Miller, J.S.; West, J.L. *Adv Mater* 2005, *17*, 2939–2942.

MULTILAYER VASCULAR GRAFTS BASED ON COLLAGEN-MIMETIC HYDROGELS

M.B. Browning, D. Dempsey, R. Nezarati, V. Guiza, S. Becerra, M. Höök, B. Russell, J. Dong, A. Bergeron, F. Clubb, M. Miller, T. Fossum, M. Hahn, E.M. Cosgriff-Hernandez
Texas A&M University, College Station, Texas
mbrowning28@gmail.com

Objective: Current synthetic options for small diameter (<4mm) vascular grafts have high rates of re-occlusion due to poor cell-material interactions and compliance mismatch. A thromboresistant small-caliber vascular graft that promotes endothelialization and provides mechanical properties that match native vasculature could fulfill this rapidly growing clinical need. Streptococcal collagen-like protein Scl2.28, or Scl2, has many properties that could promote its success in this application. It has the triple helical structure of collagen, but unlike collagen, Scl2 is a non-thrombogenic protein that can be modified to have selective cell adhesion. We have developed the methodology to incorporate Scl2 into a poly(ethylene glycol) (PEG) based hydrogel matrix. These bioactive hydrogels provide a non-thrombogenic surface with unique control over both substrate modulus and biochemical landscape. However, scaffold properties that promote desirable cell-material interactions may not be consistent with the mechanical properties necessary to withstand physiological loading. We have decoupled these two requirements by reinforcing Scl2/PEG hydrogels with an electrospun polyurethane mesh. This multilayer vascular graft design will allow us to optimize the bioactivity of the intimal layer while matching arterial mechanical properties.

Methods: Scl2 proteins were functionalized with acrylate-PEG-N-hydroxysuccinimide to form photocrosslinking sites. Funtionalized Scl2 and PEG diacrylate were combined and crosslinked into hydrogels under UV light. ***Multilayer Graft Fabrication:*** 4 mm inner diameter polyurethane meshes were fabricated utilizing a rotating mandel electrospinning setup. They were placed into a cylindrical mold with a 3mm glass mandrel in the center. Hydrogel solution was pipetted between the mandrel and the pre-wetted mesh then crosslinked under UV light. Composite delamination was evaluated after 4 weeks of pulsatile flow, and compliance, burst pressure, and suture retention were measured. ***Thrombogenicity:*** Platelet adhesion to Scl2/PEG hydrogels after exposure to Yucatan miniature pig whole blood for 2 minutes in a parallel plate flow chamber or for 6 hours in a bioreactor. Platelet adhesion was assessed via measurement of levels of lactate dehydrogenase (LDH) released from adherent cells after forced cell lysis. Platelet aggregation was qualitatively assessed using brightfield microscopy. ***Platelet Activation:*** Flow cytometry was utilized to determine P-selectin expression of activated platelets in human blood after contact with Scl2/PEG hydrogels for 2 hours.

Results: No delamination or changes in construct thickness were seen in multilayer grafts after 4 weeks of pulsatile flow. Biomechanical testing indicated that the constructs can acheive burst pressure, compliance, and suture retention values comparable to autologous grafts currently used in bypass surgeries and that these properties can be optimized by varying polyurethane chemistry and mesh thickness. ***Thrombogenicity:*** After the 2 minute study, the level of platelet adhesion on the PEG/Scl2 hydrogels was statistically comparable to PEG hydrogels and less than collagen coated TCPS positive control. Bioreactor tests qualitatively showed low levels of adhesion on the Scl2/PEG hydrogels, comparable to PEG hydrogels. The Dacron vascular graft clinical control occluded within one hour of flow and showed much higher levels of adhesion and aggregation. ***Platelet Activation:*** Scl2/PEG hydrogels did not induce significant platelet activation over baseline.

Conclusions: Scl2/PEG hydrogels provide a highly tunable non-thrombogenic intimal layer that can be integrated with a reinforcing electrospun polyurethane mesh. This results in a vascular graft with desirable cell-material interactions and biomechanical properties that are comparable to current autologous grafts. These findings demonstrate the great potential of this multilayer design as an off-the-shelf graft for small-caliber arterial prostheses that improves on current synthetic options.

ENVIRONMENTALLY RESPONSIVE POLYMERIC CARRIER SYSTEMS FOR ORAL DELIVERY OF CHEMOTHERAPEUTICS

M. Caldorera-Moore[1,2], and N. Peppas[1,2,3]
[1]Department of Chemical Engineering, [2]Department of Biomedical Engineering, [3]Division of Pharmaceutics,
University of Texas at Austin, Austin, TX, 78712, USA
mcmoore@mail.utexas.edu

OBJECTIVE

In the work presented here, poly (methacrylic acid grafted ethylene glycol) (P(MAA-g-EG) nanoparticles with hydrophobic polymer tethers of *tert*-butyl methacrulate (*t*-BMA) were synthesized using emulsion photo-polymerization for the development of pH responsive carriers for oral delivery of hydrophobic chemotherapeutic agents. When these carriers are exposed to the pH increase from the stomach to the upper small intestine, the particles swell leading to controlled release of the hydrophobic drugs encapsulated within the carriers.

EXPERIMENTAL METHODS

Poly (methacrylic acid grafted ethylene glycol) (P(MAA-g-EG)) nanoparticles with *tert*-butyl methacrylate (t-BMA) hydrophobic polymer tethers were synthesized using emulsion photo-polymerization. The particles were composed of a 1:1 molar ratio of methacrylic acid (MAA) to poly(ethylene glycol) methyl ether methacrylate, crosslinked with 1 mol% of the hydrophobic UV crosslinker tetra (ethylene glycol) dimethacrylate (TEGDMA), with 30 mol% of *t*-BMA. Sodium dodecyl sulfate and Brij-30 surfactants (30%mol) were added to the solution to stabilize the hydrophobic monomers in the continuous phase of deionized water. Irgacure 2959 photoinitiator (0.05% wt) was used to initiate free-radical polymerization of the hydrogel network. The precursor solution was sonicated using a sonicator probe to form the nanoparticle. The precursor solution reaction flask was then purged for 20 minutes with nitrogen and then exposed to 2.5 hours of UV using a UV point-source at 100 mW/cm^2 to polymerize the nanoparticles. The particles were then purified, dialyzed, and freeze dried.

Dynamic Light Scattering (DLS) was used to verify the diameters of the synthesized nanoparticles' as the particles were exposed to an increase in pH, as they would be exposed to when they move from the stomach to the upper lower intestine. Loading and release efficiency of hydrophobic drugs *in vitro* is currently under way. Dried particles were re-hydrated in phosphate buffer saline (PBS) at pH 7 for 24 hours. DLS was performed using the Malvern Zetasizer with auto titrator system. The particles zeta potential and size was monitored as a function of pH.

Cell proliferation in the presence of synthesized particles was evaluated in Caco 2 cells to determine if the particles would have any *in vitro* cytotoxicity effects on the intestinal lining. Cells were incubated for 2 hours with various concentrations of particles (0.5-5 mg/mL). After the incubation period, MTS assay solution (CellTiter 96 AQueous One Solution Cell Proliferation Assay kit) was added to each well of cells. The cells were incubated for an additional 4 hour at 37^{o}C. The optical density of the cell suspension was measured.

RESULTS AND DISCUSSION

Successful synthesis of P(MAA-g-EG) carriers with hydrophobic tethers was evaluated using scanning electron microscopy (SEM) and transmission electron microscopy (TEM). As observed in Figure 1, the particle size is significantly affected by post synthesis steps. Particle diameter is significantly decreased after freeze dry lyophilization. From DLS measurements of freeze dried particles that were re-hydrated in PBS (shown in Figure 2), despite the particle mean diameters being smaller after drying, the particles are still swelling as predicted. When the particles are exposed to increased pH, around 4.8 (pKa of MAA) the particle diameters are significantly increasing, signifying that the particles are swelling. Cellular proliferation studies demonstrated that the synthesized grafted hydrogel nanoparticles did not have a significant cytotoxicity effects on cells.

CONCLUSION

Here we have demonstrated the ability to synthesize pH responsive hydrogel materials that can be used for oral delivery of hydrophobic therapeutic agents. The designed pH responsive networks will protect the chemotherapeutic drug while in the harsh environment of the stomach and, in response to the pH change in the intestine, allow for the drug to be released. Experimental evaluation of particles' *in vitro* loading and release of hydrophobic therapeutic agents and contrast agents are currently being investigated. Ultimately, once these hydrogel networks are incorporated into nanoparticles they will allow for toxic chemotherapeutic agents to be efficiently delivered to diseased sites, therefore eliminating the need to systemically administrate chemotherapeutic agents.

ACKNOWLEDGMENTS

This work was supported by a grant from the Nattional Institutes of Health (U54 program)

LIPOSOMES RECOGNIZE B-GLUCAN OF *ASPERGILLUS FUMIGATUS*

Neelam L. Chavan,[1] Lili Cui,[1] Mohamed I. Nounou,[1] Russell Lewis[2] and Malavosklish Bikram[1,*]

[1]Department of Pharmacological & Pharmaceutical Sciences, College of Pharmacy, University of Houston, Houston, TX 77030

[2]Clinical Sciences & Administration, College of Pharmacy, University of Houston, Houston, TX 77030

*Corresponding author: mbikram@central.uh.edu

Objective: Liposomal formulations of Amphotericin B including AmBisomes® (Astellas, Inc) are used as potent drug carriers for the treatment of invasive pulmonary aspergillosis (IPA). Previously, it has been observed that liposomes showed significant binding to *Aspergillus fumigatus* hyphae but there have been no studies to explore why these lipid carriers bind with such high affinity.[1] In this study, we have investigated the mechanism by which liposomes are able to bind to the fungal hyphae of *Aspergillus*. These findings would be important since this would lay the foundation for the development of new and novel targeted drug delivery systems with higher efficacies compared to conventional therapies. The fungal hyphae is composed of four major polymers: chitin, galactomannan, branched b-1,3/b-1,6 glucans, and linear b-1,3/b-1,4 glucans. The b-glucans are present at primary and the secondary septum.[2] From our preliminary data, it was observed that liposomes were specifically bound to the tips and septa of the hyphae in serum, which indicated possible interaction of the liposomes with the glucans present on the surface of the hyphae. To prove this hypothesis, we carried out some binding assays with: (*1*) caspofungin that inhibits the enzyme β(1,3)-D-glucan synthase; (*2*) laminarin that is a storage glucan; and (*3*) Candida hyphae that possesses a higher percentage of glucans on its surface compared to the hyphae of *Aspergillus fumigatus*.

Methods: Fluorescently labeled liposomes consisting of DPPC, DPPE, cholesterol, DPPC-rhodamine and PEG-550-PE (8:1:1:0.2:0.4) were prepared by reverse phase evaporation. To study the binding of liposomes to the fungal hyphae, two assays were conducted with *Aspergillus fumigatus* 293 and one with Candida hyphae. In all three assays, the hyphae were grown on glass cover slips in 24-well plates to which RPMI media without serum was added and incubated at 37 °C for 12 hrs. In the first binding study with Aspergillus, the hyphae were grown in media containing caspofungin (500 ng/ml) and washed with 1X PBS buffer prior to use. The fungal hyphae were then incubated with 10% serum for 1 hr and washed twice before incubating with the liposomes for an additional 30 min. The hyphae were again washed twice with 1X PBS buffer and viewed under confocal microscopy (Olympus DSU BX51WI) to determine the degree of liposomal binding to the hyphae. In the second study with Aspergillus, the fabricated liposomes were first incubated with laminarin (1 mg/ml) for 1 hr prior to use. The hyphae grown on the cover slips were then washed with 1X PBS buffer and 10% serum was added and incubated for 1 hr. The hyphae were then treated with the liposomes and incubated for an additional 30 min. After this time, the hyphae were then washed and imaged as before. In the binding study with Candida, the hyphae were similarly grown on glass cover slips, washed and incubated with 10% serum for 1 hr and then treated with the liposomal formulation for 30 min and viewed under the confocal microscope after washing twice with buffer.

Results: Confocal images showed increased fluorescence when *Aspergillus fumigatus* hyphae were grown in the presence of caspofungin and treated with fluorescently labeled liposomes, as the integrity of the fungal cell wall was disturbed exposing additional glucans on the its surface.[3] Similarly, increased fluorescence was observed in the case of Candida hyphae as it has more glucans on surface compared to *Aspergillus fumigatus*. In contrast, when the fluorescently labelled liposomes were incubated with laminarin, the confocal images showed significantly decreased binding to the fungal hyphae since laminarin coated the liposomes and inhibited liposomal interaction with the b-glucans.

Conclusions: Thus, we have shown that the presence of b-glucan on the fungal hyphae cell wall influences the binding of liposomes to *Aspergillus fumigatus*. To further confirm our findings, we will be investigating the therapeutic efficacy of the fabricated liposomes with the broad-spectrum fungicide, amphotericin B.

Reference:

1] Lestner J. M., Howard S. J., Goodwin J., Gregson L., Majithiya J., Walsh T. J., Jensen G. M., and Hope W. W. **2010** "Pharmacokinetics and Pharmacodynamics of Amphotericin B Deoxycholate, Liposomal Amphotericin B, and Amphotericin B Lipid Complex in an *In Vitro* Model of Invasive Pulmonary Aspergillosis" *Antimicrobial agents and chemotherapy,* 54 (8), 3432-3441.

2] Clavaud C., Aimanianda V., Latge J., "*Chemistry, Biochemistry and Biology of (1-3)-β-glucans and related polysaccharides*", 2009.

FABRICATION OF PDMS-LIKE NANOFILMS THAT PROMOTE PROTEIN ADSORPTION AND MAMMALIAN CELL INTERACTIONS

Ramon E. Coronado[1*], Karin Y. Chumbimuni-Torres[2], Adelphe M. Mfuh[2], Maria Fernanda Silva[3], George R. Negrete[2], Rena Bizios[1] and Carlos D. Garcia[2]

[1] *Department of Biomedical Engineering, UT San Antonio, San Antonio, TX, USA*
[2] *Department of Chemistry, UT San Antonio, San Antonio, TX, USA*
[3] *School of Agronomic Sciences, National University of Cuyo, Mendoza, Argentina*
[*] *Corresponding author and presenter: recs84@gmail.com*

Objective: The objective of the present study was to investigate the adsorption of select proteins, mediators of subsequent cell interactions, using a novel nano-film made of n- dimethylsiloxane.

Materials and Methods: Fabrication of PDMS-like nano-films were realized on standard silicon wafers which were cleaned, dried at 80°C for 4 hours, and immersed, under gentle stirring, in solutions containing n-dimethylsiloxane (dissolved in dichloromethane) for 3 hours. This approach is simpler and faster than others previously reported and resulted in uniform layers of PDMS and is thus compatible with ellipsometric measurements. The PDMS-like nanofilms produced in the present study using deposition of 1,7-dicholoro-octamethyltetrasiloxane were characterized by nuclear magnetic resonance (500 MHz ^{1}H-NMR), reflectance Fourier-transformed infrared spectroscopy (FTIR), reflectance UV-vis spectrophotometry, scanning electron microscopy (SEM), atomic force microscopy (AFM), and spectroscopic ellipsometry. Dynamic adsorption of various proteins specifically, fibrinogen, collagen type-I, and bovine serum albumin, was investigated as a function of protein concentrations and pH values and measured using an ellipsometer. Adhesion of human dermal micovascular cells onto the PDMS-like nanofilms in the presence of each pre-adsorbed protein was also investigated.

Results and Discussion: Films fabricated with n-dimethysiloxane deposition produced a uniform layer with average thickness of 2 ± 0.1 nm (as determined by an optical model). The amount and arrangement of proteins adsorbed onto nanofilms were similar (if not identical) to those properties of commercially available PDMS. In agreement with literature reports, the highest amount of protein was adsorbed when the pH of the buffer solution was close to, or near, the isoelectric point of the respective protein. Measurements of the initial adsorption rate were achieved using a small amount of protein and were completed in a relatively short (~20 min) time; maximizing the adsorption rate is an effective way to minimize structural rearrangements (such as spreading) of the adsorbing protein molecules. On the other hand, measurements of protein saturation required significantly longer (~175 min) time periods. Furthermore, the importance of hydrophobic interactions in the adsorption of the proteins tested is evidenced by the strong adsorption observed even under unfavorable electrostatic conditions. Although the number of adhering cells was similar on all substrate surfaces tested, differences in cell morphology were observed. Cells adhering onto PDMS-like surfaces modified with either absorbed collagen type-I or fibrinogen at 0.01 mg/mL or 0.0001 mg/mL concentrations exhibited more spread-out morphology than cells adhering onto either unmodified silicon, PDMS-like without adsorbed protein, or PDMS-like with pre-adsorbed bovine serum albumin at all concentrations tested.

NEAR-INFRARED ABSORBING GOLD NANOSHELLS FOR PROSTATE CANCER CELL THERAPY

Andrew J. Coughlin, André M. Gobin, James J. Moon, and Jennifer L. West
Department of Bioengineering, Rice University, Houston, TX
andrew.coughlin@rice.edu

Background and Objective: While many cancer therapeutics do not discriminate between healthy and diseased tissue, nanotechnology offers the potential to more specifically treat tumors through targeting mechanisms. Herein, we report the use of ephrinA1 to target metal nanoshells to the EphA2 receptor, a tyrosine kinase receptor overexpressed on many prostate cancer cell surfaces.[1] Gold nanoshells, composed of a gold shell over a dielectric core, can interact with near-infrared (NIR) light, where transmission through human tissue is maximal, either by scattering for diagnostic purposes or absorption for photothermal ablation.[2,3] In this study, we characterize both gold-silica and gold-gold sulfide nanoshells for targeted photothermal ablation of prostate cancer cells.

Methods:

Particle Synthesis

Gold-silica and gold-gold sulfide shell-core nanoshells were fabricated as previously described.[4,5] Silica cores 120 nm in diameter were functionalized with amine groups, upon which gold colloid (~3 nm) was adsorbed and nucleated the growth of a complete gold shell in the presence of reduced $HAuCl_4$ (Alfa Aesar). Gold-gold sulfide nanoshells were synthesized by mixing Na_2S (Sigma-Aldrich) and $HAuCl_4$, followed by removal of the sulfur source via centrifugation to cease particle growth. Particles were characterized with transmission electron microscopy (TEM) and UV-Vis spectroscopy.

Particle Functionalization

Mouse ephrinA1/Fc chimera (R&D Systems) was conjugated to nanoshells with a hetero-bifunctional poly(ethylene glycol) (PEG) linker (Creative PEGWorks), containing an N-hydroxysuccinimide end-group for protein conjugation and a disulfide end-group for attachment to gold. Particle surfaces were further coated with PEG-SH (MW = 5000 Da, Laysan) to prevent non-specific cell binding. As a control, nanoshells were conjugated to PEG-SH only.

Photothermal Ablation

EphrinA1-conjugated nanoshells or PEG-SH coated nanoshells were incubated with PC3 cells, which overexpress the EphA2 receptor.[6] The cells were washed with PBS to remove unbound nanoshells and then irradiated (808 nm, 80 W/cm^2, 5-7 min). Calcein AM (live) and ethidium homodimer-1 (dead) staining (Invitrogen) were used to characterize cell viability under fluorescent microscopy.

Results: Both gold-silica and gold-gold sulfide nanoshells, with approximate diameters of 150 and 45 nm respectively, were designed to absorb NIR light with peak absorption near 800 nm (Figure 1). EphrinA1 loading on nanoshell surfaces successfully targeted the particles to PC3 cells for photothermal ablation as shown in Figure 2. PEG-SH coated nanoshells did not bind PC3 cells, and as a result, cell death did not occur after laser irradiation.

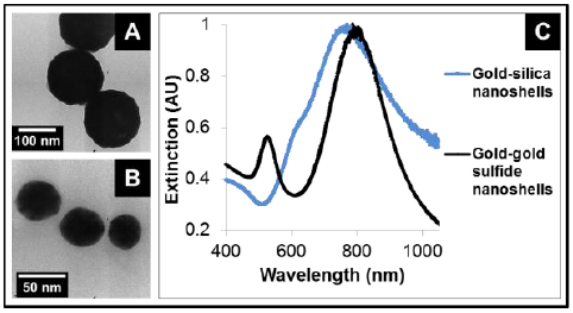

Figure 1: TEM images of (A) gold-silica and (B) gold-gold sulfide nanoshells. (C) The particles are designed to maximally absorb NIR light.

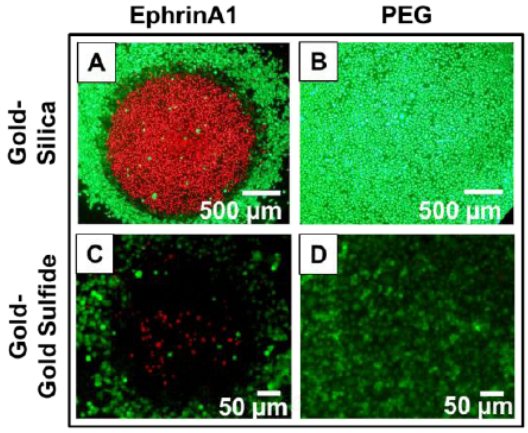

Figure 2: Live/dead (green/red) staining after NIR ablation of PC3 cells incubated with (A and B) gold-silica and (C and D) gold-gold sulfide nanoshells. (A and C) Area of laser exposure after cells incubated with targeted ephrinA1-conjugated and (B and D) control PEG-conjugated nanoshells.

Conclusions: NIR absorbing particles can induce cancer cell death as light is converted to heat. EphrinA1 targeting offers an alternative to antibody targeting for cancer cell types overexpressing the associated Eph receptor. Further work will include combined imaging and therapy studies *in vivo*, including characterization of particle biodistribution, which may vary with nanoshell diameter.

References: 1. Surawska H. Cytokine Growth Factor Rev. 2004; 15: 419–433.
2. Weissleder R. Nat Biotechnol. 2001; 19: 316-317.
3. Loo C. Nano Lett. 2005; 5: 709-711.
4. Oldenburg SJ. Chem Phys Lett. 1998; 288: 243-247.
5. Averitt RD. J Opt Soc Am B. 1999; 16: 1824-1832.
6. Gobin AM. Int J Nanomedicine. 2008; 3: 351-358.

DESIGN OF A FLOW PERFUSION BIOREACTOR FOR OSTEOCHONDRAL TISSUE ENGINEERING ON BIOMATERIAL SCAFFOLDS

+*Dahlin, RL; *,**Meretoja, VV; *Kasper, FK; *Mikos; AG

*Dept. of Bioengineering, Rice University, Houston, TX
**Institute of Dentistry, University of Turku, Finland
+email: rld3@rice.edu

Objective: Cell growth on three-dimensional scaffolds is often limited by the diffusion of nutrients and waste products to and from the interior of the construct. Consequently, flow perfusion bioreactors are commonly used to improve the mass transport and in turn the cell growth within the scaffold pores. Furthermore, flow induced shear stress has been shown to promote the chondrogenic or osteogenic differentiation of progenitor cells, given the correct culture conditions. For these reasons, flow perfusion bioreactors have great utility when culturing cells on biomaterial scaffolds. As such, the objective of this work was to design a flow perfusion bioreactor for osteochondral tissue engineering.

Methods: Design requirements of the system were the ability to provide a consistent and controllable media flow rate through the scaffolds, while eliminating air bubbles before reaching the scaffolds. Minimizing the volume of media necessary for culture was desirable, as chondrogenic culture media is often supplemented with growth factors. Additionally, all parts must be autoclavable and easily handled and assembled under sterile conditions.

Results: Each bioreactor system has four main components, shown in Figure 1. The media reservoir consists of a custom-made stainless steel base (A) and lid (B), held together with screws. The inlet and outlet ports are centered on the lid and base, respectively. Also on the lid is a syringe filter for gas exchange and a rubber stopper for media changes. A custom-made polycarbonate scaffold holder (C) is positioned within the media reservoir, and o-rings are compressed on each side by the lid and base to restrict the path of the media to the scaffolds only. Ten scaffolds are press-fit in the sample holder and supported from underneath by a titanium mesh. Culture media is pumped with a peristaltic pump through gas permeable tubing (D), into the media reservoir, and through the scaffolds from the top to bottom surfaces. A total of twelve systems, each with ten scaffolds, can be run with one peristaltic pump allowing for high throughput cultures.

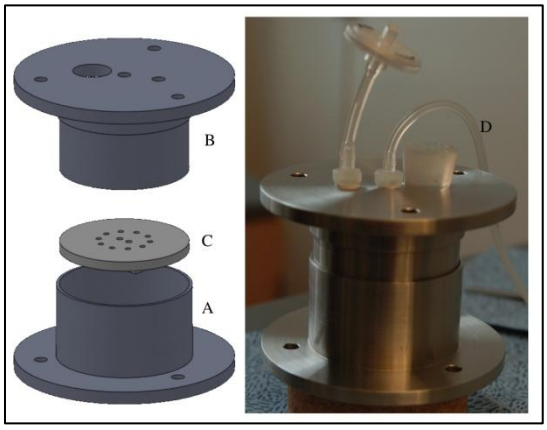

FIGURE 1. BIOREACTOR SCHEMATIC AND PROTOTYPE

Conclusions: The bioreactor design described above meets all of the stated design requirements. The simplicity of the design and the ability to culture a large number of samples are significant advantages over other bioreactor designs. The bioreactor is intended for osteochondral tissue engineering, and further testing of the system with osteogenic and chondrogenic cultures is underway.

EVALUATION OF PEG-DA MOLECULAR DYNAMICS THROUGH COMPUTER SIMULATIONS

Alina Daszkowski, Cheng Zhang, Jennifer West
Rice University, Houston, TX
ADasz@rice.edu

Poly(ethylene glycol) diacrylate (PEG-DA) , a polymer with a hydrophilic polyethylene glycol (PEG) chain and dual hydrophobic acrylate ends. PEG-DA is often fabricated into hydrogels via photo-induced crosslinking of the acrylate groups. These hydrogels serve as blank scaffolds for tissue engineering. The purpose of this research was to evaluate the molecular dynamics of unreacted PEGDA molecules in water through computer simulations using GROMACS, a free molecular dynamics simulation package often used for biomolecular systems with proteins and lipids. It was hypothesized that the hydrophobic ends of PEG-DA will interact with each other and the polymers will arrange in an organized manner to minimize energy loss. If PEG-DA polymers are shown to arrange like micelles or a reverse lipid membrane, they could be considered for drug delivery vehicles, as PEG can act as a shield from the immune system and slow the clearance rate. The molecular dynamics of PEG-DA were simulated using polymers of varying length (n = 16, 32, 47 monomers) in a system with varying amounts of total number of polymers (polymers = 14, 20, 27). These numbers were chosen to keep the system and simulation time relatively small while still allowing for the visualization of the resulting trends. Visual Molecular Dynamics (VMD) was used to visually inspect the PEGDA polymer arrangement. A PEG polymer control group simulation will also be run using the same system sizes as the PEGDA polymer group in order to compare the contribution of the hydrophobic acrylate ends of PEG-DA. As was done with a computer simulation, the distances between all the starting and terminal carbon atoms of individual PEGDA and PEG systems will be calculated in vitro, and if the simulation results prove correct, the distances in the PEGDA systems will be shorter than the distances in the PEG systems. Future experiments will be done to confirm computer simulation findings with longer polymers (n = 47, 82, 147).

ACCELERATED BIODEGRADATION OF SEGMENTED POLYURETHANES

D. Dempsey[1]; P. Gray[2]; E. Cosgriff-Hernandez[1]
[1]Texas A&M University, College Station, TX
[2]DSM Biomedical, Berkeley CA
davedemp@tamu.edu

Objective: Segmented polyurethanes have been a popular choice for biomedical devices because of their established biocompatibility and highly tunable mechanical properties. In devices where biostability is a critical factor such as pacemaker leads and breast implants, polyurethanes have failed due to degradation of the oxidatively labile soft segment. Thus controlling the degradation profile has been one of the main focal points in developing new polyurethanes for biomedical devices. Poly(carbonate urethanes) have been developed to better withstand oxidative degradation for prolonged biostability after implantation. In this study we present the degradation profile of three poly(carbonate urethanes) (PCUs) in comparison with a poly(ether urethane) (PEU) developed by DSM Biomedical: Bionate® (SB), Bionate® with an alternative polyol (SBA), Bionate® II (SB II), and Elasthane™ (SE). Based on previous work, the *in vitro* accelerated degradation experiment should simulate an approximate 15 month *in vivo* period.[1]

Methods: *In vitro degradation:* Extruded films of SB, SBA, SB II, and SE were cut to 15x40x0.25mm dimensions. Unstrained films were submerged in oxidative solutions of 0.3M $CoCl_2$/20%H_2O_2 at 37°C with solution changes every 3 days. Films were removed every 6 days to examine chemical and physical degradation.

Materials Characterization: Surface chemistry was monitored with Attenuated Total Reflectance-Fourier Transform Infrared spectroscopy (ATR-FTIR). Percent soft segment loss was calculated using changes in the 1250cm^{-1} peak (C-O, carbonate) for PCUs and 1110cm^{-1} peak (C-O-C, aliphatic ether) for PEU relative to the stable hard segment 1591cm^{-1} peak (C=C, aromatic ring). Surface crosslinking was monitored using the emerging 1174cm^{-1} peak (C-O, branched ether). Changes in molecular weight and polydispersity were measured with Gel Permeation Chromatography (GPC). Analysis of physical damage to specimens was conducted on unstrained and strained to failure specimens using Scanning Electron Microscopy (SEM). Finally, a standard swelling test in deionized water and 20% H_2O_2 was conducted on untreated films.

Results: ATR-FTIR analysis indicated evidence of soft segment loss (reduced peak height) and crosslinking (new branched ether peak at 1174 cm) and hard segment chain scission (new degradation product peak at 1650 cm) in all polyurethanes tested. Quantification of spectral changes indicated decreased soft segment loss of the PCUs as compared to the PEU; however, no significant difference was observed between the three PCUs tested. Molecular weight changes monitored with GPC confirmed the greater susceptibility of PEU to oxidative chain scission, **Table 1.**

Table 1. Molecular weight data before and after *in vitro* biodegradation.

	Untreated		30 Days		
	M_W (kDa)	PDI	M_W (kDa)	PDI	%M_W Lost
SB	205±5	3.0±0.2	180±7	3.4±0.3	12.2±3.5
SBA	202±4	3.0±0.4	180±4	3.4±0.3	11.8±1.7
SB II	205±6	3.1±0.3	184±6	3.7±0.8	9.8±2.7
SE	172±9	2.7±0.2	69±3	9.7±2.6	66.1±1.4

(average ± standard deviation; n=8)

Surface pitting was observed on all specimens due to solubilization of polymer chains after chain scission. Strained PEU specimens displayed significant cracking indicating a much thicker degradation layer than the PCU specimens, **Figure 1**. Swelling studies indicate that PEU absorb an increased concentration of hydrogen peroxide which facilitates chain transfer of oxidative radicals into the polyurethane bulk.

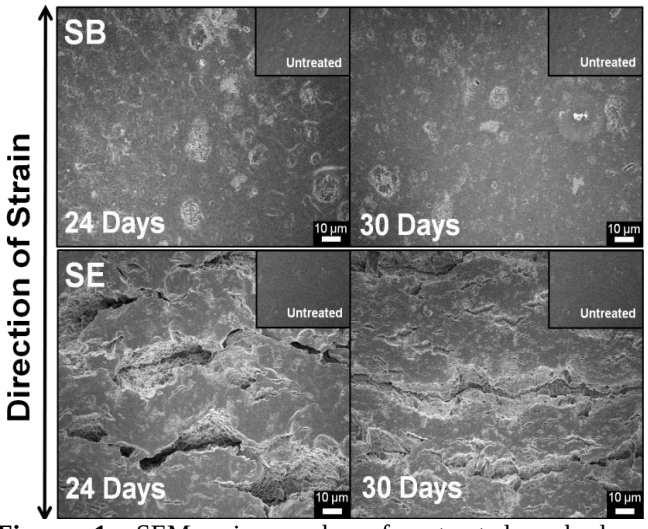

Figure 1. SEM micrographs of untreated and degraded specimens strained to failure.

Conclusions: This study demonstrates that both PEU and PCU are susceptible to oxidative degradation; however, the decreased permeability of the PCU limits the depth of degradation and prevents surface cracking. Given that environmental stress cracking is the dominant mechanism of polyurethane device failure, this resistance to cracking makes PCU preferable over traditional PEU elastomers.

[1] Christenson et al. JBMR A, 70A(2): 245-255. 2004

THERMORESPONSIVE DOUBLE NETWORK HYDROGELS: INTRODUCTION OF ELETROSTATIC FORCES

+Fei, R; George, J. T.; Park, J; Grunlan, M.A.
+Texas A&M University, Dept. of Biomedical Engineering, College Station, TX
rfei@neo.tamu.edu

Objective: Crosslinked poly (*N*-isopropylacrylamide) (PNIPAAm) hydrogels have been shown to release cultured cells when thermally cycled though its volume phase transition temperature (VPTT) from a swollen to deswollen state.[1] In order to utilize PNIPAAm hydrogels as "self-cleaning" membranes for implanted biosensors, the extent and rate of swelling/deswelling (i.e. thermosensitivity) as well as mechanical properties need to be enhanced. These properties are typically enhanced for double network (DN) hydrogels versus conventional, "single network" hydrogels.[2] Towards this goal, we prepared thermoresponsive double network (DN) hydrogels in which included "electrostatic comonomer" 2-acrylamido-2-methylpropanesulfonic acid (AMPS) which will introduce electrostatic repulsive forces to the network.

Methods: DN hydrogels were prepared in two sequential steps. The 1st network was obtained by the photocure of aqueous precursor solutions containing NIPAAm and AMPS monomer (total weight equal to 1.0 g) (**Table 1**), BIS crosslinker (0.04 g), and Irgacure-2959 photoinitiator (0.08 g) and DI water (7.0 g). Hydrogel sheets (1.5 mm thick) were prepared by pipetting the solution between two clamped glass microscope slides (75 x 50 mm) separated by polycarbonate spacers. The mold was submerged in an ice water bath (~7 °C) and exposed to UV light (6 mW/cm^2, 365 nm) for 30 min. The hydrogel sheet was rinsed was soaked in DI water for 1 day with to remove impurities and then soaked in a solution of NIPAAm (6 g), Irgacure-2959 (0.24 g), BIS (0.012 g) and DI water (21.0 g) for 1 day at 7 °C. The hydrogel sheet was transferred to similar mold (4.0 mm thick) and likewise photocured. The impact of AMPS on mechanical properties, kinetic swelling, deswelling and morphology were evaluated.

Results: DSC confirmed introduction of AMPS did not alter the VPTT of PNIPAAm hydrogels. As the AMPS content was increased, both swelling and deswelling kinetics were enhanced (**Figure 1**). In addition, the compressive strength of the DN hydrogels was increased with AMPS levels (**Figure 2**).

Table 1. DN hydrogel composition.

Notation	1st network: Weight of AMPS	1st network: Weight of NIPAAm
0%	--	--
5%	0.05 g	0.95 g
25%	0.25 g	0.75 g
50%	0.50 g	0.50 g
60%	0.60 g	0.40 g
75%	0.75 g	0.25 g

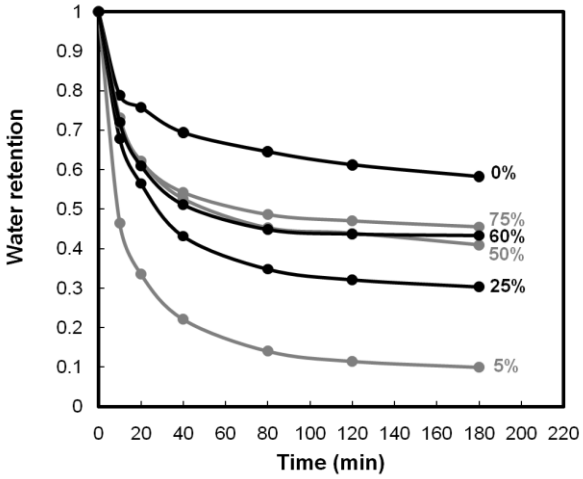

Figure 1. Deswelling kinetics of DN hydrogels.

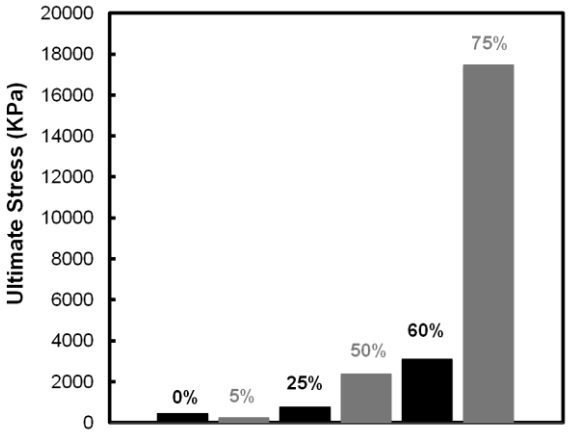

Figure 2. Compression strength of DN hydrogels.

Conclusions: Thermoresponsive AMPS-based DN hydrogels were successfully synthesized in two steps via *in situ* photopolymerization. Because of their enhanced swelling and deswelling kinetics and mechanical properties, they may be particularly useful in applications requiring rapid cell-release such for biosensor membranes which self-clean in response to thermal modulation.

References:

1. Yamato, M.; Akiyama, Y.; Kobayashi, J.; Yang, J.; Kikuchi, A.; Okano, T. *Prog. Polym. Sci.* **2007**, *32*, 1123-1133.
2. Gong, J. P.; Katsuyama, Y.; Kurokawa, T.; Osada, Y. *Adv. Mater.* 2003, 15, 1155-1158.

AMPHIPHILIC PEG-SILANES: ENHANCING CLOT-RESISTANCE OF SILICONES

+Giese, M.L.; Grunlan, M.A.
+Texas A&M University, Department of Biomedical Engineering, College Station, TX
gies67@neo.tamu.edu

Objective: Silicones are widely used in biomedical applications due to their flexibility, thermal and oxidative stability and gas permeability. Many blood-contacting devices are fabricated from silicones including hemodialysis catheters, pacemaker components, heart valve leaflets and even stent coatings.[1] Unfortunately, as a result of their extreme hydrophobicity, blood proteins are readily adsorbed which initiates platelet adhesion and eventually thrombus formation.[2] This ultimately leads to diminished performance or even failure. In contrast, poly(ethylene oxide) (PEO; or poly(ethylene glycol) PEG) is a neutral, hydrophilic polymer which exhibits high protein resistance due to its hydrophilicity as well as configurational mobility.[3] In this work, silicones were modified with a novel PEG-silane amphiphile via surface-grafting as well as bulk-crosslinking (**Figure 1**). The PEG-silane amphiphile consists of a PEG segment distanced from the grafting/crosslinking $(EtO)_3Si$- group by a hydrophobic, highly flexible siloxane tether. This strategic PEG design combines molecular mobility and amphiphilicity to synergistically reduce thrombosis.

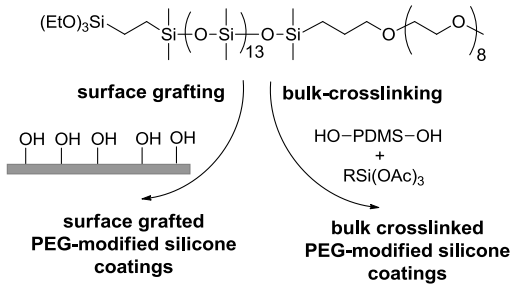

Figure 1. Surface and bulk modification of silicones with PEG-silane amphiphile.

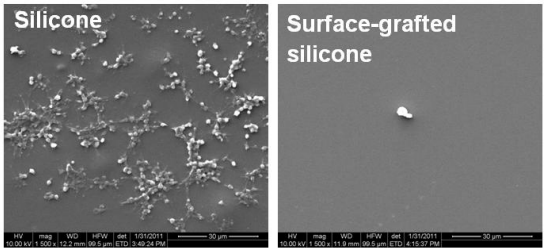

Figure 2. Whole blood (pig) adhesion under flow conditions (15 min).

Methods: *PEG-Silane Amphiphile Synthesis*: The PEG-silane amphiphile was prepared as previously reported.[4] *Surface-grafted Coatings*: NuSil MED-1137, an acetoxy-cure silicone (20 wt% silica) whose composition closely parallels hemodialysis catheters, was solvent cast (33 wt% in hexane) onto glass microscope slides. Following plasma treatment (1 min, air), the coated slide was exposed to 0.005 -0.05 M grafting solution (toluene or ethanol) for 2h followed by rinsing and/or sonication with EtOH/water. Finally, coatings were dried *in vacuo* (36 in. Hg, RT, 12 hr). *Bulk-crosslinked Coatings*: NuSil MED-1137 was combined with hexane (1:3, wt:wt) and the PEG-silane at varying wt% based on silicone wt (0, 1, 5, 10, 15, 20%). The mixture was applied to glass microscope slides as described above. Six types of PEG-modified silicone films were prepared by curing a silicone material which mimics common catheter materials with varying wt% of PEG-silane: 0, 1, 5, 10, 15, 20%. *Protein Adhesion*: Fibrinogen adhesion studies were conducted as previously reported.[4,5] *Whole Blood Adhesion*: Under static conditions, 1 mL of whole blood (pig) was applied to a silicone isolator (diameter = 23 mm) for 1h. Coatings were exposed to whole blood under flow conditions using a parallel plate flow chamber. For 15 min, blood flow was maintained at 0.825 mL/min which generated a mean wall shear stress of 60 dyne/cm^2. Following exposure to whole blood, these surfaces were imaged using scanning electron microscopy (SEM) to visualize platelet adhesion and aggregation. *Surface Characterization*: Surface properties were examined via contact angle analysis (KSV CAM-200). *Mechanical properties*: Mechanical properties of bulk-crosslinked coatings were determined by performing tensile tests (Instron 3345) at a strain rate of 500 mm/min.

Results: Surface-grafted coatings resulted in significantly reduced amounts of adhered platelets upon exposure to whole blood compared to the silicone control (**Figure 2**). Contact angle results showed a lack of hydrophobic recovery or stability of the hydrophilic properties of the bulk-crosslinked coatings with minimal restructuring of the silicone over time. Tensile testing of bulk-crosslinked coatings revealed a decrease in modulus and tensile strength and an increase in elongation when increasing amounts of PEG-silane were introduced into the silicone.

Conclusions: The PEG-silane amphiphiles are useful to improve the clot resistance of silicones. It may be effectively incorporated exclusively at the silicone surface which may be useful for modification of existing devices (e.g. hemodialysis catheters). Alternatively, bulk modified silicones may be produced as thick coatings applied to a given substrate.

References:

(1) Curtis, J.; Colas, A., Medical applications of silicones. In *Biomaterials Science: An Introduction to Materials in Medicine*, 2nd ed.; Ratner, B. D.; Hoffman, A. S.; Schoen, F. J.; Lemons, J. E., Eds. Elsevier Academic Press: San Diego, CA, 2004; pp 697-707.
(2) Pitt, W. G.; Park, K.; Cooper, S. L. *J. Colloid Interface Sci.* **1986,** 111, 343-362.
(3) Jeon, S. I.; Andrade, J. D. *J. Colloid Interface Sci.* **1991,** 142, 159-166.
(4) Murthy, R.; Cox, C.D.; Hahn, M.S.; Grunlan, M.A. *Biomacromolecules*, **2007**, *8*, 3244.
(5) Murthy, R.; Shell, C.E.; Grunlan, M.A. *Biomaterials*, **2009**, *30*, 2433-2439.

SHAPE MEMORY POLYMERS WITH NOVEL PROCESSING CAPABILITIES FOR BIOMEDICAL DEVICE APPLICATIONS

Keith Hearon[1,2], Thomas S. Wilson[2], and Duncan J. Maitland[1,2]
[1]Texas A&M University, College Station Texas; [2]Lawrence Livermore National Laboratory, Livermore, CA
hearon.keith@tamu.edu

Objectives: Shape memory polymers (SMPs) are advanced smart materials that have the ability to actuate from a metastable geometry or geometries to a primary geometry when introduced to a stimulus such as heat or moisture. Because SMP-based biomedical implant devices can change their geometries after insertion in the body, SMPs are being considered for numerous biomedical applications.[1] Although covalently crosslinked SMPs have excellent thermo-mechanical properties, these thermoset materials cannot be mass-manufactured into complex geometries by thermoplastic processing methods such as injection molding or solution casting.[2] Consequently, the mass-manufacture of complex thermoset SMP-based medical devices is neither economically favorable nor time-efficient.[3] Our goal was to synthesize polyurethane SMPs with tunable mechanical properties that could be made into thermoplastic polymers, processed into complex thermoplastic precursors, and later crosslinked in a final curing step using electron beam irradiation to fix a permanent primary geometry.

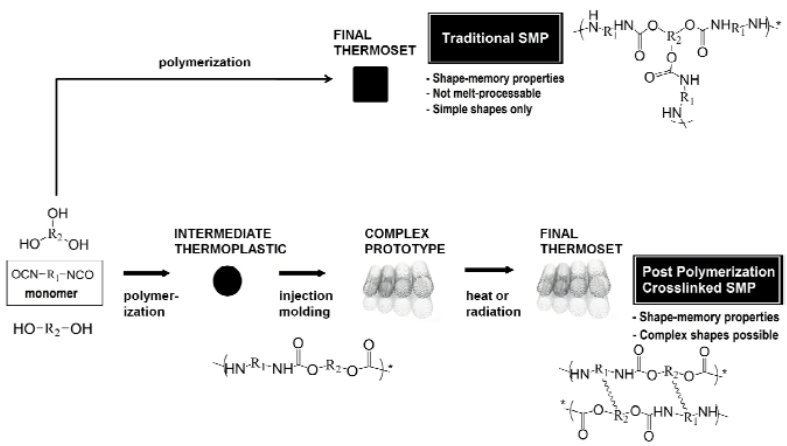

Methods: We hypothesized that a thermoplastic polyurethane SMP series based on 2-butene-1,4-diol would be susceptible to radiation crosslinking because of the resonance stabilization of e-beam-induced α-carbamate radicals by adjacent unsaturated groups in the polymer backbone. We investigated the effects of radiation dose and radiation sensitizer composition on the crosslink density (and corresponding rubbery moduli) of the irradiated SMPs. Tris[2-(acryloyloxy)ethyl] isocyanurate (TAcIC) was solution blended in THF in 2.5-25 mole % ratios with thermoplastic polyurethanes made from 2-butene-1,4-diol and trimethylhexamethylene diisocyanate (TMHDI). Samples were then irradiated at 5-100 kGy. Sol/gel analysis and dynamic mechanical analysis (DMA) experiments were run to determine if covalent crosslinking occurred during irradiation. Differential scanning calorimetry (DSC), tensile testing, and various shape recovery experiments were run to evaluate the biomedical relevance of the new SMPs.

Results: Sol/gel analysis and DMA results (pictured in Figure 1) provided concrete evidence that covalent crosslinking occurred during irradiation. Gel fractions approaching 100% were achievable with doses as low as 5 kGy. Rubbery moduli were tailorable between 0.1 and 72.0 MPa and could be controlled by varying both radiation dose and radiation sensitizer composition, as Figure 2 demonstrates. Further mechanical characterization demonstrated other outstanding mechanical properties, including tailorable glass transitions between 25 and 80°C, cyclic recoverable strains approaching 100%, failure strains of over 500% at T_g, and toughness values as high as 50.2 MJ/m^3.

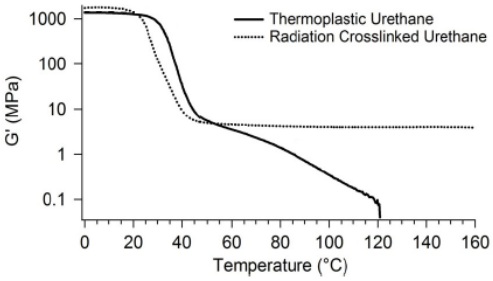

Figure 1: Confirmation of crosslinking by DMA

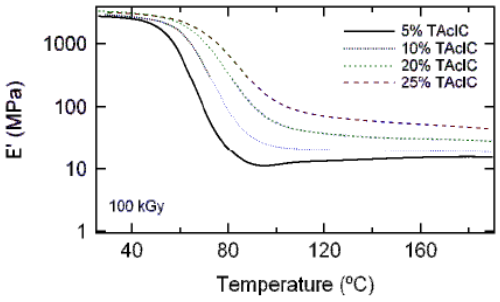

Figure 2: Rubbery moduli tailorable with increasing sensitizer

Conclusions: We developed novel polyurethane SMPs that can be made into thermoplastic precursors and later crosslinked using electron beam irradiation. Consequently, the mass-manufacture of complex SMP-based biomedical implant devices may become more economically feasible. Furthermore, mechanical characterization of this new SMP system demonstrated that high crosslink densities and correspondingly high rubbery moduli are achievable upon irradiation. Since the recovery stress of SMPs is proportional to rubbery modulus, it is believed that this SMP system will be potentially useful in applications that demand high recovery stresses, such as self-deploying cardiovascular stents.

[1] Small IV, et al. J Mater Chem 17, 3356 2010.
[2] Voit, et al. Adv Func Mater 20, 162 2010.
[3] Ware, et al. Radiat Phys Chem 79, 446 2010.

ENGINEERING AN EX VIVO HEPATIC NICHE: PHOTOPATTERNING BIOACTIVE PEG HYDROGELS

*Higbee, SJ; *Cuchiara, MP; *West, JL.
*Rice University, Houston, TX
sh19@rice.edu

Objective: Within tissues, cell behavior is dictated by a variety of chemical and mechanical cues present within the cellular microenvironment, an elaborate organization of different cell types, matrix components, and bioactive factors. Consequently, precise spatial control over cells, matrix, and bioactive factors is desirable to direct biomimetic tissue formation *in vitro*. In this work, mask projection photolithography was used for the directed fabrication of biomimetic hydrogels, encapsulating multiple cell types in order to recapitulate key aspects of tissue structure and function.

Methods: Human hepatocellular carcinoma cells (HepG2s) were seeded in a 96-well plate (1,000 per well) in the following groups: HepG2s alone and HepG2s with 400 human umbilical vein endothelial cells (HUVECs) and 100 pericyte precursor cells (10T½ cells. The HUVEC-10T½ co-culture has been shown to form microvascular tubes in culture. 7-Ethoxy-4-trifluoromethylcoumarin (EFC) was added to the media and its degradation by cytochrome P450 enzymes was measured fluorescently (ex. 385 nm, em. 502 nm). This metabolic assay was repeated with identical cell numbers encapsulated in hydrogels consisting of a 5% (w/v) proteolytically degradable poly(ethylene glycol) (PEG) diacrylate (incorporating MMP-sensitive peptide GGGPQGIWGQGK into the polymer backbone) with 2 mM PEG-RGDS. These hydrogels were photopolymerized, in the presence of a photoinitiator (Irgacure 2959), with long-wavelength UV light. Hepatic tissue analogues were generated using mask projection photolithography. Prepolymer solutions were prepared in HBS (HEPES buffered saline) using 2.5% degradable PEG diacrylate, 2 mM PEG-RGDS, photoinitiator (Eosin Y), and cells. HUVECs were encapsulated at $2.25*10^7$ cells/mL, 10T½ cells at $7.5*10^6$ cells/mL, and HepG2s at $1*10^6$ cells/mL. Spatial control of hydrogel formation was achieved by inserting a photomask into the light path of an inverted fluorescence microscope, using the mercury arc lamp to photopolymerize the prepolymer solutions. Multiple PEG hydrogel microstructures were synthesized using an iterative process, which allowed the structures to differ in cellular and/or molecular composition. Additional tissue analogues were generated through self-organization of HUVECs ($2.25*10^7$ cells/mL), 10T½ cells ($7.5*10^6$), and HepG2s ($1*10^6$). Fluorescent cell trackers were used for real time imaging of tissue analogues, while immunohistochemistry was used for most endpoint imaging. PECAM was used as a marker for HUVECs, α-smooth muscle actin was used for 10T½ cells, and FoxA2/HNF3β for HepG2s.

Results: 2D cell culture and 3D encapsulation in hydrogels demonstrated that HepG2 cells exhibit enhanced metabolic activity when co-cultured with HUVECs and 10T½ cells (Fig. 1a). Mask projection photolithography was successfully used to fabricate spatially patterned hydrogel structures (Fig 1b). The spontaneous cellular organization of the HepG2-HUVEC-10T½ tri-culture was also observed in bioactive hydrogels. Figure 1c depicts the spontaneous organization of the HepG2-HUVEC-10T½ tri-culture in a cell-degradable and cell-adhesive PEG hydrogel; a microvascular-like network formed around hepatocyte islands.

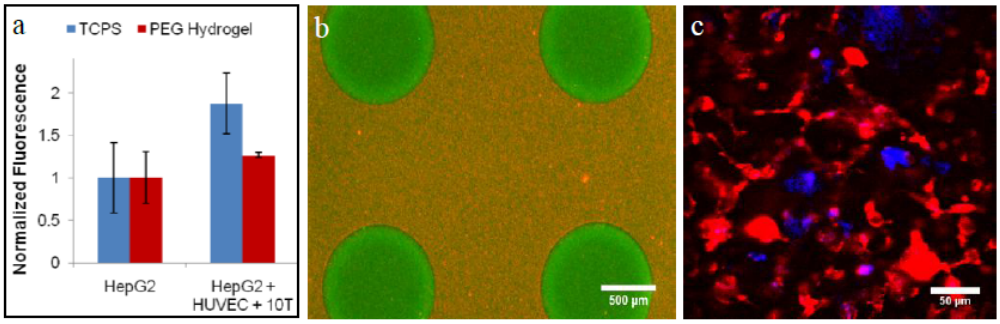

Figure 1. (a) Metabolic activity of HepG2 cells cultured on TCPS and in cell-adhesive PEGDA hydrogels. Culture with HUVECs and 10T½ cells increased metabolic activity ($p < 0.05$). (b) Hydrogel structures patterned using mask projection photolithography. (c) Fluorescent image of HepG2s (blue), HUVECs (red), and 10T½ cells (unlabeled) in a cell-degradable PEG hydrogel. HUVECs and 10T½ cells form microvascular tubes, which surround groups of HepG2s that cluster in "hepatocyte islands."

Conclusions: The ability to precisely control the spatial organization of cells and their matrix allows for development of *ex vivo* microenvironments that mimic native tissue in structure and function. These studies demonstrate cellular behavior in engineered hepatic tissues, especially as it relates to the role of microvasculature on hepatocytes.

HIGH POROSITY POLYHIPES AS INJECTABLE BONE GRAFTS

Jennifer Holm, Robert Moglia, and Elizabeth Cosgriff-Hernandez
Biomedical Engineering, Texas A&M University, College Station, Texas 77843
Jholm2009@gmail.com

Objective: Tissue engineered bone grafts have the potential to repair critical size defects when traditional transplants are unavailable or fail. The ability to match the irregular geometries of bone defects is necessary to promote osseointegration and full healing. Injectable grafts that cure *in situ* are preferable to more costly and time-consuming computer-aided design molds. However, researchers have been challenged to develop a scaffold fabrication method that is injectable and porous, yet retains high mechanical strength. Emulsion templating is a relatively new method for the production of high porosity scaffolds which involves the template polymerization of high internal phase emulsions (HIPEs). Recently, we have identified appropriate macromers and surfactants that enable the utilization of emulsion templating as injectable bone grafts. Scaffold architecture is a key determinant in the clinical success of bone grafts. Specifically, modulation of pore size and interconnectivity is necessary to promote osteoblast proliferation and nutrient/waste transport. We expand on our previous work with injectable propylene fumarate dimethacrylate macromer (PFDMA) polyHIPEs by assessing the ability of key processing variables to modulate pore architecture. Initial biodegradability and mechanical properties of this new class of injectable, high porosity bone grafts is also reported.

Methods: PFDMA was synthesized according to a protocol adapted from Christenson et al. [1] ***HIPE Fabrication:*** PFDMA was mixed with 10 wt % PGPR prior to emulsification. Once thoroughly mixed, the aqueous solution of calcium chloride (1% v/v) and ammonium persulfate (5 wt %) was added to the organic phase and mixed in a FlackTek Speedmixer DAC 150 FVZ-K. HIPEs were then cured in a 37°C aluminum bead bath for 12 hours. The resulting polyHIPE foams were dried under vacuum for 24 hrs prior to characterization. ***SEM Analysis:*** Scanning electron microscopy (JEOL JSM-7500F) was utilized to characterize polyHIPE pore architecture. Circular specimens were sectioned into quarters, fractured at the center of the quarter, sputter-coated with gold and imaged. Quantification of pore sizes was conducted via measurements of the first 10 pores along the micrograph median of each specimen. Average pore sizes for each polyHIPE composition are reported (n=150). ***Mechanical Testing:*** Mechanical properties of the resulting scaffolds were tested with an Instron 3300 equipped with a 1000-N load cell according to ASTM method D1621-04a. The test specimens (n = 3) were cut into flat rectangular shapes (9 x 9 x 3 mm) and compressed at 50 µm/s. ***Accelerated Degradation Study***: PolyHIPE specimens were immersed in 0.1 M NaOH for 4 weeks to accelerate hydrolytic degradation. Specimens were cut, dried, and their initial weights recorded before submersion in the base solution. Each week, three specimens were removed, rinsed with RO water, and dried for 48 hours prior to monitoring mass loss.

Results and Discussion: All PFDMA polyHIPEs resulted in stable monoliths with closed pore architectures and porosities between 75-85%. Pore sizes ranged from 1-30 microns with an average compressive modulus of 30 MPa. A decrease in pore size was observed with an increase in mixing speed, **Figure 1**. We hypothesize that the lower mixing speeds corresponded to decreased shear forces that deform water droplets resulting in the observed increase in pore diameter. An increase in volume fraction resulted in a decrease in pore size and wall thickness. Matrix erosion and surfactant extraction from the scaffolds resulted in 35% mass loss after one week in 0.1 M NaOH. Hydrolytic degradation led to continued mass loss over the 4 week incubation period with 60% mass loss after 4 weeks.

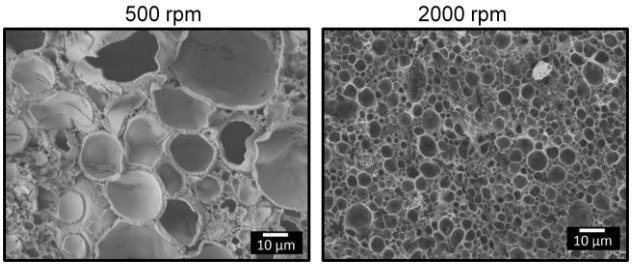

Figure 1: Effect of mixing speed on PolyHIPE pore architecture; 500 and 2000 rpm in FlackTek Speedmixer

Conclusion: Our recent work demonstrated the feasibility of using emulsion templating to generate injectable, high porosity PFDMA bone grafts. This study illustrates the tunability of the resulting architecture by modulating processing variables. In addition, the mechanical properties and hydrolytic degradation of the PFDMA polyHIPEs are appropriate for bone graft applications. Current experiments are investigating the cytocompatibility and osteoblastic differentiation of mesenchymal stem cells on these promising new grafts.

References: 1. Christenson, E.M., et al., *Biodegradable fumarate-based polyHIPEs as tissue engineering scaffolds.* Biomacromolecules, 2007. 8: p. 3806-3814

HIGH POROSITY POLYHIPES AS INJECTABLE BONE GRAFTS

Jennifer Holm, Robert Moglia, and Elizabeth Cosgriff-Hernandez
Biomedical Engineering, Texas A&M University, College Station, Texas 77843
Jholm2009@gmail.com

Objective: Tissue engineered bone grafts have the potential to repair critical size defects when traditional transplants are unavailable or fail. The ability to match the irregular geometries of bone defects is necessary to promote osseointegration and full healing. Injectable grafts that cure *in situ* are preferable to more costly and time-consuming computer-aided design molds. However, researchers have been challenged to develop a scaffold fabrication method that is injectable and porous, yet retains high mechanical strength. Emulsion templating is a relatively new method for the production of high porosity scaffolds which involves the template polymerization of high internal phase emulsions (HIPEs). Recently, we have identified appropriate macromers and surfactants that enable the utilization of emulsion templating as injectable bone grafts. Scaffold architecture is a key determinant in the clinical success of bone grafts. Specifically, modulation of pore size and interconnectivity is necessary to promote osteoblast proliferation and nutrient/waste transport. We expand on our previous work with injectable propylene fumarate dimethacrylate macromer (PFDMA) polyHIPEs by assessing the ability of key processing variables to modulate pore architecture. Initial biodegradability and mechanical properties of this new class of injectable, high porosity bone grafts is also reported.

Methods: PFDMA was synthesized according to a protocol adapted from Christenson et al. [1] ***HIPE Fabrication:*** PFDMA was mixed with 10 wt % PGPR prior to emulsification. Once thoroughly mixed, the aqueous solution of calcium chloride (1% v/v) and ammonium persulfate (5 wt %) was added to the organic phase and mixed in a FlackTek Speedmixer DAC 150 FVZ-K. HIPEs were then cured in a 37°C aluminum bead bath for 12 hours. The resulting polyHIPE foams were dried under vacuum for 24 hrs prior to characterization. ***SEM Analysis:*** Scanning electron microscopy (JEOL JSM-7500F) was utilized to characterize polyHIPE pore architecture. Circular specimens were sectioned into quarters, fractured at the center of the quarter, sputter-coated with gold and imaged. Quantification of pore sizes was conducted via measurements of the first 10 pores along the micrograph median of each specimen. Average pore sizes for each polyHIPE composition are reported (n=150). ***Mechanical Testing:*** Mechanical properties of the resulting scaffolds were tested with an Instron 3300 equipped with a 1000-N load cell according to ASTM method D1621-04a. The test specimens (n = 3) were cut into flat rectangular shapes (9 x 9 x 3 mm) and compressed at 50 µm/s. ***Accelerated Degradation Study***: PolyHIPE specimens were immersed in 0.1 M NaOH for 4 weeks to accelerate hydrolytic degradation. Specimens were cut, dried, and their initial weights recorded before submersion in the base solution. Each week, three specimens were removed, rinsed with RO water, and dried for 48 hours prior to monitoring mass loss.

Results and Discussion: All PFDMA polyHIPEs resulted in stable monoliths with closed pore architectures and porosities between 75-85%. Pore sizes ranged from 1-30 microns with an average compressive modulus of 30 MPa. A decrease in pore size was observed with an increase in mixing speed, **Figure 1**. We hypothesize that the lower mixing speeds corresponded to decreased shear forces that deform water droplets resulting in the observed increase in pore diameter. An increase in volume fraction resulted in a decrease in pore size and wall thickness. Matrix erosion and surfactant extraction from the scaffolds resulted in 35% mass loss after one week in 0.1 M NaOH. Hydrolytic degradation led to continued mass loss over the 4 week incubation period with 60% mass loss after 4 weeks.

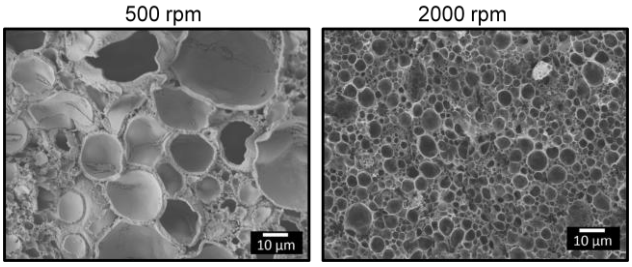

Figure 1: Effect of mixing speed on PolyHIPE pore architecture; 500 and 2000 rpm in FlackTek Speedmixer

Conclusion: Our recent work demonstrated the feasibility of using emulsion templating to generate injectable, high porosity PFDMA bone grafts. This study illustrates the tunability of the resulting architecture by modulating processing variables. In addition, the mechanical properties and hydrolytic degradation of the PFDMA polyHIPEs are appropriate for bone graft applications. Current experiments are investigating the cytocompatibility and osteoblastic differentiation of mesenchymal stem cells on these promising new grafts.

References: 1. Christenson, E.M., et al., *Biodegradable fumarate-based polyHIPEs as tissue engineering scaffolds.* Biomacromolecules, 2007. 8: p. 3806-3814

SCULPTING HYDROGEL SCAFFOLDS WITH EMBEDDED 3D VASCULATURE

Jen-Huang Huang, Jeongyun Kim, Arul Jayaraman, and Victor M. Ugaz*
Artie McFerrin Department of Chemical Engineering, Texas A&M University,
College Station, TX, USA
jenhuang@tamu.edu

Abstract

Living systems face a fundamental challenge of orchestrating exchange of nutrients, oxygen, and waste throughout three dimensional spaces in order to satisfy their metabolic needs. Vascular networks play a critical role in satisfying these needs by incorporating a highly branched fractal-like architecture that is efficiently space-filling while minimizing the energy required to sustain transport. But the complex 3-D arrangement of these networks makes them challenging to fabricate inside biomaterial scaffolds. We have recently developed a novel process based on electrostatic discharge to embed 3-D vasculature inside polymeric materials, and here we present recent progress aimed at applying this method toward biomaterials relevant for tissue engineering. First, a biodegradable substrate (e.g., poly(lactic acid)) containing the 3-D network is heated and injected with pressurized gas to inflate the interior microchannels, yielding a global increase in diameter and smoother sidewall profile. Next, a low melting temperature metal is injected to create a sacrificial replica of the microchannel architecture upon dissolving the surrounding biodegradable substrate. A hydrogel can then be cast around this metal replica, after which the metal is easily removed in a 37 °C incubator. The end result is a hydrogel scaffold containing an embedded functional vasculature that enables greatly enhanced transport throughout a large 3-D volume. Unlike conventional techniques, this process enables 3-D flow networks containing a broad hierarchy of diameters with physiologically-mimicking branching characteristics to be embedded in a variety of hydrogels relevant for tissue engineering applications.

MULTIFUNCTIONAL POLYMERIC MICELLES FOR MR IMAGING AND TARGETED CHEMOTHERAPY ON LUNG CANCER

[†]Gang Huang, [†]Su-Geun Yang, [†]Lei Wu, [†]Jagadeesh Setti Guthi, [†]Shunzi Li, [†]Chalermchai Khemtong, [†]Chase W. Kessinger, [‡]Osamu Togao, [*]Michael Peyton, [*]John D. Minna, [‡]Masaya Takahashi, [†]Kathlynn C. Brown, and [†]Jinming Gao

†Simmons Comprehensive Cancer Center, ‡Advanced Imaging Research Center, * Hamon Center for Therapeutic Oncology Research, University of Texas Southwestern Medical Center, Dallas, TX 75390

Email*:* gang.huang@utsouthwestern.edu

Objective: Lung cancer is the leading cause of cancer-related death for both men and women in the USA. Despite advances in standard therapies such as chemotherapy, radiation and surgery, the 5 year survival for patients is below 15%. Recently, nanomedicine with integrated imaging and therapeutic functions has the potential to offer paradigm-shifting solutions to improve the outcome of cancer diagnosis and therapy. In this study, we report the development of multi-functional micelles based on polyethylene glycol-co-poly(D,L-lactide) copolymers with integrated MR imaging and therapeutic delivery capabilities. The surface of the micelles was encoded with lung cancer targeting peptide H2009.1 (LCP, with the sequence of RGDLATLRQL), which specifically bind to intergrin $\alpha_v\beta_6$ over-expressed in many human non-small cell lung carcinomas. We hypothesize that LCP-encoded polymer micelles will promote the tumor-specific delivery of imaging probes and therapeutic agents in lung cancer treatment.

Methods: Amphiphilic block copolymer methoxy-poly(ethylene glycol)-co-poly(D,L-lactic acid) (MeO-PEG-PLA) and maleimide terminated polymer Mal-PEG-PLA were synthesized by ring opening polymerization and used for micelle formation. The density of lung cancer targeting peptides on the surface of the micelles was controlled by the amount of the maleimide PEG-PLA introduced on the micelles. anticancer drugs and superparamagnetic iron oxide (SPIO) nanoparticles were loaded inside the core of micelles. Targeting and cytotoxicity tests of different micelle formulations were examined in the $\alpha_v\beta_6$(+) H2009 and $\alpha_v\beta_6$(-) H460 lung cancer cells, respectively. For MR imaging, H2009 and H460 lung cancer cells were subcutaneously injected on each flank of scid mice. The images were taken before and after intravenous injection of LCP-encoded micelles with 6 mg/kg of iron concentration under 4.7 T scanner. ^{3}H labeled polymer micelles were synthesized to evaluate pharmacokinetics and biodistribution profile of micelles in H2009 tumor bearing mice. *In vivo* antitumor efficacy of micelles was also examined on SCID mice containing subcutaneous H2009 lung tumors.

Results: For comparison, scrambled peptide (SP) with the sequence of DALRLQGTLR was also conjugated on the surface of micelles. The resulting micelles showed a mean size of 60-70 nm with narrow size distribution. Significantly increased amount of LCP-encoded MFM was observed in $\alpha_v\beta_6$(+) H2009 lung cancer cells over the $\alpha_v\beta_6$(-) H460 cells, demonstrated by confocal laser scanning microscope. We also evaluated the *in vivo* MR imaging specificity by i.v. injection of LCP-encoded micelles to the mice bearing H2009 and H460 tumor xenografts. Only signal intensity of H2009 tumors dropped significantly 2 hours after micelle injection, while H460 tumor still kept the same signal intensity. Biodistribution studies of ^{3}H-labelled micelles 24 hours after i.v. administration demonstrated 2.6 fold increase of LCP-encoded MFM accumulated in H2009 tumors than SP-encoded micelles. In addition, antitumor efficacy studies showed a better tumor response to micelles loaded with paclitaxel than doxorubicin, and moreover, higher growth inhibition for LCP-encoded micelles over Scramble peptide (SP)-encoded and PBS controls.

Conclusions: A theranostic polymer micelle nanoplatform with effective cancer imaging and therapeutic modalities is successfully established. LCP-encoded micelles showed specific targeting efficiency and ultrasensitive MR detection towards the H2009 lung tumor model *in vitro* and *in vivo*. The LCP-encoded micelles inhibited the tumor growth better than the SP-encoded micelles and PBS control. By combining tumor targeting, imaging and therapy function in an all-in-one system, these theranostic nanoparticles can provide a promising target-specific, imaging-guided treatment of lung cancer.

NOVEL LYSINE-BASED NONVIRAL CARRIER SYSTEM FOR THE TREATMENT OF MYOCARDIAL INFARCTION

Mohamed Ismail Nounou[1], Cori Wijaya[1], Andrea Diaz[1], Dongling Li[1], Sahr Ahmed[1], Sameer Saifuddin[1], Daniel Garcia[2], Yi Zheng[2], Guilherme V. Silva[2], Bradley K. McConnell[1], and Malavosklish Bikram[1,*]

[1] Department of Pharmacological and Pharmaceutical Sciences, College of Pharmacy, University of Houston, Houston, TX, 77030.

[2] Department of Cardiology Research, Texas Heart Institute, Stem cell center, St. Luke's Episcopal Hospital, Houston, TX 77030.

* Author of Correspondence: mbikram@uh.edu

Background: Despite advancement in the various surgical and pharmacological techniques, ischemic heart disease (IHD) or coronary artery disease (CAD) remains a leading cause of death in the United States †. The poor prognosis of IHD is directly related to a build-up of atherosclerotic plaque that produces narrowing of the coronary artery lumen. Current treatments include bypass surgery, angioplasty, stent implantation, and pharmacotherapy but unfortunately many patients with IHD remain refractory to pharmacological treatments and are unsuitable candidates for surgical interventions. Also, restenosis of the vessel lumen due to neointimal hyperplasia is a recurrent problem. Gene therapy is a promising alternative to conventional treatment strategies since the delivery of angiogenic cytokines such as vascular endothelial growth factor ($VEGF_{165}$) can stimulate angiogenesis in a process known as therapeutic angiogenesis as well as neovascularisation.

Objective: Treatment of myocardial infarction through the use of gene therapy to generate genetically modified stem cells that are able to produce angiogenic cytokines to promote revascularization of an infarcted region of the heart, which can reduce myocardial damage and scar formation.

Methods: To transfect the cells, reducible novel linear L-lysine modified copolymers (LLCs) were designed and synthesized as an alternative to high molecular weight non-degradable poly(L-lysine) (PLL) for nonviral gene delivery. The transfection efficiencies of the polyplexes as determined with luciferase and ELISA assay showed that LLC polyplexes produced over 20 times higher transfection efficiencies and lower cytotoxicities in human mesenchymal stem cells (hMSCs) as compared to the optimal PLL control. The hMSCs transfected with the LLC/$VEGF_{165}$ gene were then injected into the infarcted area of the heart of severe combined immunodeficient (SCID) mice. The myocardial infarction (MI) was created by permanent ligation of the left anterior descending artery (LAD). At time points (1-week and 2-weeks) following MI induction and cell injection, cardiac hemodynamic analysis was performed and then the mice were sacrificed for immunohistochemistry analysis.

Results: Hemodynamic studies showed that hearts, injected with LLC/$VEGF_{165}$ transfected hMSCs following the MI, had 1.5 times cardiac contractility, as defined by the maximum and minimum rate of pressure change in the left ventricle (LV dP/dt max and dP/dt min, respectively), as compared to untreated cell controls. Moreover, immunohistochemistry staining of tissue sections for differentiation of hMSCs into cardiomyocytes showed well defined tubular like structures that were stained positive for human cardiac troponin T (TnT) and human alpha smooth muscle actin (α-SMA). These data indicated potential differentiation of hMSCs into myocardial-like cells as well as neovascular transformation of the modified injected cells respectively.

Conclusions: Ex vivo gene therapy of hMSCs with the nonviral LLC vectors hold great potential for the treatment of myocardial ischemia. Our data suggest that this novel therapeutic strategy can be used to advance the field of nanotherapeutics and hence their applications to cardiovascular disease.

† Gepstein L.; Ann N Y Acad Sci.; 2010 Feb;1188:32-8.

DESIGN OF ANIMAL MODEL FOR EVALUATION OF VERTICAL BONE AUGMENTATION WITH HYDROGEL SCAFFOLDS

+*Kinard, LA; *Chu, C; **Kasper, FK; *,**Mikos, AG
Rice University, Houston, TX
* Department of Chemical and Biomolecular Engineering
** Department of Bioengineering
+ email: lak2@rice.edu

Objective:

Tissue engineering scaffolds for bone repair are extensively evaluated in animal models before advancing to the stage of human clinical trials. A significant portion of bone engineering biomaterials are evaluated in critical sized defects (CSDs) in the cranium of rats (8 mm) and rabbits (15 mm). It is often advantageous to proceed with rabbit testing only following a demonstration of efficacy in rats since using rats is ethically favorable and relatively inexpensive. However, problems have arisen when implanting hydrogels into defects of the calvarium due to intracranial pressure (ICP) exerted by the contents of the skull on surrounding bone. ICP can displace the hydrogel through force generated by relaxing of the brain into the defect space and subsequent migration results in lack of apposition between hydrogel and bone preventing osteoconduction and osteoinduction into the implant. Furthermore, minimal thickness of the cranium (0.8-1 mm) limits volume for hydrogel swelling, which results in dimensional disparity between hydrogel and defect. The objective of this research was to develop a method for evaluating the capacity of hydrogels to improve new bone formation using vertical bone augmentation in rats.

Methods:

Design criteria for vertical bone augmentation model in the rat: enable the implantation of two hydrogels per animal, increase the overall volume of the implant compared to CSD (8 mm diameter x 1 mm thickness), prevent migration and micromotion, secure hydrogel to the cranium with minimal morbidity, minimize compressive force on implant resulting from tension in scalp, prevent the conduction of fibrous tissue into the implant from cranial sutures, and minimize inflammatory response. Feasibility of the envisioned animal model was tested in a rat necropsy.

Results:

The designed implantation materials consist of a thin-walled poly(methyl methacrylate) (PMMA) cylinder open at one end. The dimensions of the cylinder are such that two cylinders can be placed side-by-side on the rat calvarium (ID: 6 mm, OD: 7 mm, void height: 2 mm, total height: 2.5 mm). The dimensions of the cylinders enable an increase in implant volume of 12.5% compared to CSD. According to rat necropsy it was determined that two suitable fixation mechanisms exist for the PMMA cylinders. Cylinders can be attached using miniature self-tapping screws with stainless steel fixation plates. Alternatively, a circular groove 0.5 mm in depth can be created using a trephine burr (ID: 6 mm, OD: 7 mm), the PMMA cylinder placed accordingly, and secured with a small volume of clinical-grade bone cement.

Conclusions:

The designed vertical bone augmentation model enables more ethically favorable and cost-effective use of rats for evaluation of the efficacy of hydrogel tissue engineering scaffolds to enhance new bone formation *in vivo*. The design represents an improved model for bone augmentation as a result of its geometry, which requires new bone apposition beyond the skeletal envelope.

Rapid Degrading Crosslinked Urethane-doped Block Polyester Elastomers

Aleksey Kolasnikov, Richard T. Tran, and Jian Yang

Bioengineering Department, The University of Texas at Arlington, Arlington, TX 76019

Early efforts in vascular tissue engineering have focused on the use of biodegradable synthetic polymers, such as polylactic acid, polyglycolic acid, and their copolymers, to support extracellular matrix production. Unfortunately, these materials have not achieved success in developing scaffolds for vascular tissue engineering due to their lack of strength and elasticity causing a mismatch in compliance [1]. In an effort to address the challenges on developing soft, elastic, yet strong biodegradable polymers, our lab has recently reported on a novel platform biomaterial, crosslinked urethane doped polyesters (CUPEs) [2]. Although CUPEs have shown potential as a soft, elastic and strong scaffolding material, better control over balancing the degradation rate and mechanical strength must be addressed for better serving as a platform biomaterial for tissue engineering applications. Herein, we report on the development of a new biodegradable elastomer, crosslinked urethane-doped block polyesters (CUBPEs). Introducing hydrophilic blocks into the CUPE network maintained excellent material mechanical properties while providing better control over the degradation rate. The mechanical properties and degradation rates of CUBPEs could be widely controlled by varying the percentage of hydrophilic blocks, the concentration of urethane bonds in the polymer, and the crosslinking conditions compared to the previous CUPE. The introduction of CUBPEs provides new avenues to meet the versatile requirements of tissue engineering.

References

1. Kim, B.S.; Nikolovski J.; Bonadio J.; Smiley E.; Mooney D.J. Engineered smooth muscle tissues: regulating cell phenotype with the scaffold. *Exp Cell Res* **1999**, *251*(2), 318-28.
2. Dey, J.; Xu H.; Shen J.; Thevenot P.; Gondi S.R.; Nguyen K.T.; Sumerlin B.S.; Tang L.; Yang J. Development of biodegradable crosslinked urethane-doped polyester elastomers. *Biomaterials* **2008**, *29*(35), 4637-49.

PROTEIN CONFORMATIONAL STUDIES FOR MOLECULARLY IMPRINTED POLYMERS

Kryscio, DK; Fleming, MQ; Peppas, NA
University of Texas at Austin, Austin, TX
dkryscio@che.utexas.edu

Objective:

Molecularly imprinted polymers (MIPs) are crosslinked polymer networks that act as synthetic antibody mimics. MIP networks are formed via polymerization in the presence of a template biomolecule of interest. These systems can be designed to specifically recognize physiologically relevant macromolecule biomarkers and are advantageous over their biological counterparts because they mimic biological recognition pathways while at the same time exhibiting abiotic properties, such as stability in harsh environments. In spite of the successes of MIPs used for recognition of small MW molecules, macromolecular recognitive MIPs have yet to reach their vast potential. The objective of this research is to investigate conformational instability of protein templates under polymerization conditions as a reason for the lack of success in this field to date.

Methods:

Circular Dichroism (CD) is a well-established spectroscopic technique for studying protein secondary structures in solution and can be employed to illustrate global changes in protein conformation as a result of various environmental conditions. Proteins have a characteristic CD spectra it in their natural state and relative percentages of secondary structural elements can be estimated based on the shape of this spectra compared to standard curves. In this research, CD was used to quantify changes in native secondary structures of bovine serum albumin (BSA), a common protein template, upon systematic addition of frequently used monomers from the literature.

Results:

Studies conducted to date have clearly shown a marked decrease in the alpha-helical % of BSA from its native level of 60% for the five most commonly used monomers – acrylamide, methacrylic acid, 3-aminophenylboronic acid, acrylic acid, and N-isopropylacrylamide. The figure below, a plot of % alpha-helix as a function of molar ratio of acrylamide to BSA, shows a significant decrease in BSA helical content above a ratio of 200:1. Studies with the other monomers show similar results. These results are significant because molar ratios seen in the literature for monomer to protein templates are commonly above 1000, which is indicated in the figure to be well-away from the protein's native state.

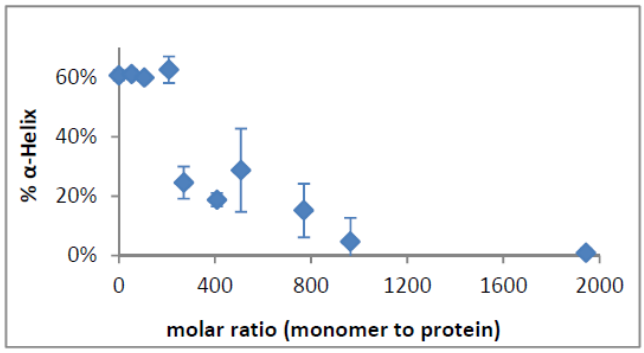

Conclusions:

Based on this work, protein conformational changes in the presence of monomers is potentially a major reason for the lack of success to date with protein MIPs. This is because if the protein template is put into a different conformation prior to polymerization, the binding sites formed during polymerization would be specific to this alternate conformation. When the polymer is re-exposed to the protein in its native state at a later time, specific recognition will not be observed. Studies with other common protein templates and monomers are currently underway.

RAPIDLY DEGRADABLE DUAL-RESPSONSIVE NANOSCALE HYDROGELS FOR siRNA DELIVERY

Liechty, W.B.; Scheuerle, R.L.; Peppas, N.A.

The University of Texas at Austin, Department of Chemical Engineering, Austin, TX, 78731
Liechty@che.utexas.edu

OBJECTIVE

Several recent efforts have explored the utility of responsive nanoscale hydrogel carriers in drug delivery[1-4], demonstrating release of biological therapeutics such as insulin and imaging agents such as gold. Nanoscale hydrogels are increasingly attractive as drug delivery agents owing to their facile manufacture, tunable physicochemical characteristics, and repeatable release. Furthermore, their covalent crosslinking endows them with mechanical integrity not available in their self-assembled counterparts. Our current work aims to develop nanogel-based platform technologies for delivery of small interfering RNA. Theoretically, RNAi mediated by small interfering RNA (siRNA) could be used as a powerful and versatile treatment modality to treat nearly any disease resulting from aberrant gene expression. Owing to its remarkable potency and low therapeutic dosage, siRNA holds extraordinary promise as a new biological therapeutic. However, efficient delivery has been implicated as the major hurdle to its widespread clinical application[5]. Though much effort has been directed toward synthetic polymer carriers for siRNA, there remains a paucity of data on the development of oral delivery systems. The goal of our work is to develop a novel hydrogel platform for oral siRNA delivery, a synthetic polymer carrier capable of providing siRNA to disease targets, specifically those along the gastrointestinal tract.

METHODS

Nanoscale hydrogels were synthesized via facile photoemulsion polymerization as described in previous reports from our laboratory[1, 2]. Bis(2-methacryloyloxyethyl) disulfide (SSXL) was synthesized according to a previous report[6]. The hydrodynamic diameter and effective surface ζ - potential of the polymer networks wer measured using a Malvern Zetasizer NanoZS. TEM micrographs were collected using a FEI Tecnai Transmission Electron Microscope. Particles were stained with 2% uranyl acetate immediately prior to imaging. DLS measurements of particle size and pH-responsive behavior were conducted in PBS and electrophoretic light scattering measurements of the surface ζ-potential were collected in 5 mM sodium phosphate. Hemolysis assays were conducted to assess pH- and concentration-dependant endosomolytic activity of nanogels. Cytoxicity experiments were conducted using standard MTS assays following 90 min exposure to nanogels.

RESULTS

A panel of polycationic nanoscale hydrogels comprised of a crosslinked core of poly[2-(diethylaminoethyl) methacrylate] surface grafted with poly(ethylene glycol) (PTEB30 and PDESSB30) was synthesized using photoemulsion polymerization. Polymer composition was varied to determine the effect of cross-linking density and core hydrophobicity on physicochemical properties and drug delivery efficacy.

Light scattering and analysis of TEM micrographs reveal disulfide crosslinked nanoscale hydrogels are rapidly degradable in reductive milieu, including aqueous solutions of glutathione and dithiothreitol. DLS studies clearly indicate the influence of hydrophobic moiety incorporation in the polymer network. The addition of *t*-BMA shifts the onset of pH-dependent swelling from ~7.4 to pH 7.0. All formulations exhibited a collapsed hydrodynamic diameter of 70 - 100 nm as determined by dynamic light scattering. Hemolysis experiments suggest these nanogels have utility in intracellular delivery applications as polymers mediate erythrocyte membrane disruption in a concentration- and pH-dependant manner. At pH 6.50, nanoscale hydrogels demonstrate excellent hemolytic ability, lysing over 80% of erythrocytes at 1 μg/mL and nearly 100% at 100 μg/mL. These data, coupled with cytotoxicity results, indicate these nanoscale hydrogels are promising agents for siRNA delivery. They are non-toxic to Caco-2 cells at concentrations up to 0.25 mg/mL. Preliminary results indicate these networks are efficient vectors for intracellular delivery, increasing the uptake of fluorescently labeled siRNA over 7-fold in HT-1080 cells.

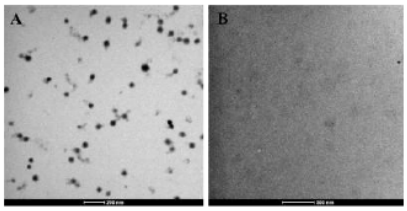

Figure 1 - Representative transmission electron microscopy images of bis(2-methacryloyloxyethyl) disulfide-crosslinked poly(DEAEMA-co-*t*-BMA-g-PEGMA) incubated for 2 hours in (A) DI water and (B) 10 mM glutathione solution. Particles stained with uranyl acetate and images collected at 26,500×.

CONCLUSION

Physicochemical properties of nanoscale hydrogel networks, including volume swelling ratio, critical swelling pH, and zeta potential were investigated using electron microscopy and dynamic and electrophoretic light scattering. As expected, these properties can be modulated by tuning the polymer composition. Nanogels synthesized with t-BMA exhibit favorable pH-responsive behavior for intracellular delivery and offer an excellent combination of hemolytic ability and cytocompatibility.

REFERENCES

1. Fisher, O., et al., *Macromolecules* **2009,** *42* (9), 3391-3398.
2. Fisher, O., et al., *Pharm Res.* **2009,** *26* (1), 51-60.
3. Marek, S. R., et al.,. *Polymer* **2010,** *51* (6), 1237-1243.
4. Owens, D. E., et al., *Macromolecules* **2007,** *40* (20), 7306-7310.
5. Whitehead, K. A., et al., *Nat Revs Drug Discov* **2009,** *8* (2), 129-138.
6. Gao, H., et al., *Macromolecules* **2005,** *38* (14), 5995-6004.

DIELECTROPHORETIC ALIGNMENT OF FIBROUS SILK FIBROIN-CHITOSAN SCAFFOLDS

Wang L; Iyyanki T; Hubenak, J; Reece, GP; Mathur AB
Tissue Regeneration and Molecular Cell Engineering Labs, Departments of Plastic Surgery,
The University of Texas M. D. Anderson Cancer Center, Houston, Texas 77030, USA
amathur@mdanderson.org

Objectives: Silk fibroin-chitosan (SFCS) scaffolds, with physiological compatibility and mechanical pliability, have been successfully applied in *in vivo* and *in vitro* models by our group for abdominal wall reconstruction, skin wound healing and bone regeneration. First generation of SFCS scaffolds formed stacked smooth sheets structure, and lacked the nano-micro-combined structural features of the extracellular matrix sheets found *in vivo*. These features provide strength to *in vivo* tissues and also the necessary local architecture for the cellular interface. Dielectrophoresis (DEP), through which protein molecules could be patterned in the AC electric fields, has been applied to align structures within the SFCS scaffolds in a two-dimensional (2D) manner (monolayer formation). We have previously studied endothelial and stem cell interactions in co-cultures using the aligned SFCS scaffolds.

Methods: We aligned SFCS scaffolds by DEP and studied the effects from AC frequency (100 kHz, 1 MHz, 10 MHz) and solution conductivity (with or without NaCl (5 mM) in the solution) on scaffold fabrication. Silk fibroin alignment was studied by polarized light microscopy (PLM). PLM images were analyzed with ImageJ software. Scaffolds topography and architecuture were studied using scanning electron microscopy (SEM).

Results: Application of the dielectrophoretic field for aligning 3D fibrous SFCS (50:50) scaffolds, silk fiber alignment could be influenced by AC frequency. Aligned SFCS scaffolds prepared under 10 MHz had significantly larger aligned area (34±9%) than those prepared under 100 kHz (25±8%) or 1 MHz (20±11%). The presence of NaCl increased the aligned area significantly. For example, alignment area of 100 kHz sample increased to 38±12% after adding NaCl. Within the 5 mM NaCl group, 10 MHz samples (46±15%) had a significantly larger aligned area than 1 MHz samples (32±8%).

Conclusions: At a given frequency (e.g. 10 MHz), DEP effect may work synergistically with intermolecular force (hydrogen bond) for parallel alignment. Presence of NaCl may disrupt the intermolecular hydrogen bonding and enhance aligned fibers formation. The modeling of the electrode design parameters shows an effect of design on distribution of frequency in a given space. Future studies will include optimizing electrode design by simulation, optimizing fabrication parameters (e.g. AC frequency, conductivity).

DEVELOPMENT AND APPLICATION OF DECORIN SCAFFOLDS FOR *IN VIVO* VENTRAL HERNIA REPAIR

Wang L; Iyyanki TS; Hubenak J; Butler CE; Mathur AB
Tissue Regeneration and Molecular Cell Engineering Labs, Department of Plastic Surgery,
The University of Texas M. D. Anderson Cancer Center, Houston, Texas 77030, USA
amathur@mdanderson.org

Objectives: Musculofascial defects of the anterior abdominal wall, such as ventral hernias, are a difficult surg problem with wound healing, infection complications, and hernia recurrence as one of the most mor complications. In fact, even small, routine hernias have a 46% recurrence rate at 10 years if it is closed w sutures alone. Mesh repair reduces recurrences by approximately half, however, implantation of surgical mesh increase other complications such as adhesion and infection; particularly synthetic, prosthetic meshes such polypropylene, polyethylene, and polytetrafluoroethylene. Bioprosthetics mesh (e.g. human acellular der matrix (HADM), porcine small intestinal submucosa, and porcine acellular dermal matrix (PADM)) provide effective alternative for abdominal wall reconstruction with good tensile strength, fewer bowl adhesions and lo risk of infection. Bioprosthetic mesh becomes revascularized, recellularized, and remodeled by the surround host tissue allowing tissue regeneration unlike the scar tissue response of synthetic mesh. However, they expensive, limited maximal surface area available, long remodeling times, poor interfacial strength, and prov limited control of architecture per patient specific geometry or control over initial mechanical properties. propose an alternative option to abdominal wall repair that involves engineering the microstructure, architectu and mechanical properties of a biomimetic or biologically derived polymer system in order to improve the ini mechanical strength of the repaired mechanically-loaded host site and provide patient specific control of tis regeneration at the same time. We hypothesized that the initial mechanical strength of the silk fibroin ba scaffolds will increase with decorin and would result in higher tensile strength of the regenerated tis characterized by seamless integration at the repair site such that the integrity of the repair site is not compromi over the entire period of remodeling.

Methods: SF based (pure SF and SFCS) scaffolds blended with various concentrations of decorin are prepared a the mechanical properties and architecture using mechanical testing and scanning electron microscopy, respectiv are assessed. Silk fibroin-decorin scaffolds (decorin concentration of 28.6 ug/mL) (n = 7) are used alone combined with PADM (n=7) for ventral hernia repair in an established *in vivo* guinea pig ventral hernia rep model. Polypropylene meshes (n = 7) and PADM (n = 7) are used as negative and positive controls, respectiv Repair outcomes including bowel adhesion to the repair site, mechanical properties of the implant-tissue interfa tissue regeneration (with cellular infiltration, neovascularization collagen deposition) and amount of biomate degradation at the repair site are evaluated.

Results: Increasing the concentration of decorin in SFCS scaffolds decreased their ultimate tensile strength. each concentration of decorin in SFCS versus the corresponding concentration in SF, the elastic modulus and str at failure were decreased in the SFCS. SF-decorin scaffolds at 28.6 μg/mL decorin had significantly the hig ultimate tensile strength than all other decorin concentrations in SF-decorin blends. SEM showed that that decorin at 28.6 μg/mL decorin results in entangled fibrillar structures and increasing the decorin concentrat further to 56 μg/mL results in embedded grape-like clusters in the existing fibrils. At concentrations higher t 28.6 μg /mL, the grapelike clusters would represent failure points and could be the cause of reduced mechani strength. SFCS–decorin blends forms flat sheet scaffolds similar to SFCS only scaffolds that are weaker mechanical strength as compared to SF-decorin blends.

Conclusions: Thus, decorin increased the ultimate tensile strength of pure SF scaffolds. The improvement in mechanical strength of SF scaffolds with decorin provides a viable solution in developing a patient-specific design for musculofascia reconstruction. The results of the ongoing *in vivo* work are hypothesized to show tissue regenerative capacity of SF-decorin scaffolds.

INJECTABLE BONE GRAFTS: SURFACTANT EFFECTS ON PORE MORPHOLOGY

Robert Moglia, Jennifer Holm, Nick Sears, Elizabeth Cosgriff-Hernandez
Biomedical Engineering, Texas A&M University, College Station, Texas 77843
robert.moglia@gmail.com

Introduction: Tissue engineered bone grafts have the potential to repair critical size defects when traditional transplants are unavailable or fail. Recent efforts have focused on fabricating a scaffold with suitable mechanical properties which is still biodegradable and injectable. The process of emulsion templating allows for creation of high internal phase emulsions (HIPEs) that upon polymerization form highly porous scaffolds (polyHIPEs) with tunable properties. Previous polyHIPEs have all used diluents to decrease the organic phase viscosity which facilitates emulsification. These diluents are highly toxic to the body and are the primary obstacle in creating injectable HIPEs. Surfactant selection is critical in determining polyHIPE pore morphology, particularly pore size and interconnectivity. Tuning pore architecture is necessary to promote osteoblast proliferation and nutrient/waste transport. In this study, we successfully fabricated injectable and biodegradable polyHIPEs using propylene fumarate dimethacrylate (PFDMA) macromer. PFDMA's low viscosity allows for emulsification without the use of toxic diluents. The effect of surfactant choice and concentration on polyHIPE formation and structure is also presented.

Methods: PFDMA was synthesized according to a protocol adapted from Christenson et al. [1] ***Surfactant Selection:*** Sorbitan monooleate (Span 80), Tween 80, and PGPR 4125 were studied to observe their effect on PFDMA HIPE formation. Each surfactant had different hydrophilic-lipophilic balance (HLB) values and different hydrogen bond donor sites. PFDMA, surfactant, and DI water (2, 0.4, and 8g respectively) were vortexed for 5 minutes. The compositions which resulted in HIPEs were fabricated full-scale (described below) to investigate the effect of surfactant structure on pore architecture. ***HIPE Fabrication:*** Surfactant concentration was varied by mixing PFDMA with 5, 10, 15, and 20 wt% PGPR prior to emulsification. Once thoroughly mixed, an aqueous solution of calcium chloride (1% v/v) and ammonium persulfate (5 wt %) was added to the organic phase and mixed in a FlackTek Speedmixer DAC 150 FVZ-K. HIPEs were then cured in a 37°C aluminum bead bath for 12 hours. The resulting polyHIPE foams were dried under vacuum for 24 h prior to characterization. ***SEM Analysis:*** Scanning electron microscopy (JEOL JSM-7500F) was utilized to characterize polyHIPE pore architecture. Circular specimens were sectioned into quarters, fractured at the center of the quarter, sputter-coated with gold and imaged. Quantification of pore sizes was conducted via measurements of the first 10 pores along the micrograph median of each specimen. Average pore sizes for each polyHIPE composition are reported (n=150). ***Mechanical Testing:*** Mechanical properties of the resulting scaffolds were tested with an Instron 3300 equipped with a 1000-N load cell according to ASTM method D1621-04a. Wet specimens (n = 3) were cut into flat rectangular shapes (9 x 9 x 3 mm) and compressed at 50 µm/s.

Results and Discussion: ***Surfactant Selection:*** Of the three surfactants tested, only PGPR 4125 formed stable PFDMA HIPEs. Analysis of surfactant chemical structures of Span 80 and Tween 80 revealed hydrogen bond donor sites in the polar "heads," where PGPR 4125 does not. PFDMA has numerous hydrogen bond acceptor sites which appear to be interacting with the Span 80 and Tween 80 heads, preventing the surfactants from "anchoring" into the aqueous phase of the HIPE and resulting in emulsion separation. ***Effect of PGPR Concentration:*** All PFDMA HIPEs polymerized to rigid monoliths at 37ºC within 2 hours. These polyHIPEs had closed pore structures with an average compressive modulus and strength of 33 and 5 MPa. Prior to polymerization, all HIPEs had a mayonnaise-like consistency capable of flowing through a large gauge syringe. Increasing PGPR concentration decreased average pore diameter in PFDMA polyHIPEs from 29 to 4 µm. We hypothesize that the decreased pore sizes are a result of increasing HIPE stability with increasing PGPR 4125 concentration.

Conclusion: We have successfully fabricated an injectable polyHIPE without the use of toxic diluents. The polyHIPEs had tunable pore sizes and mechanical properties suitable for bone graft applications. Furthermore, surfactants with hydrogen bond donor sites in the polar head may not be suitable for use with biodegradable polymers because they frequently have hydrogen bond acceptors in their backbones. Current studies focus on creating an open pore structure and fabricating an interpenetrating polymer network polyHIPE to improve mechanical properties.

References: 1. Christenson, E.M., et al., *Biodegradable fumarate-based polyHIPEs as tissue engineering scaffolds.* Biomacromolecules, 2007. 8: p. 3806-3814

$PDMS_{star}$-PEG Hydrogels for Directed MSC Differentiation

Dany J. Munoz-Pinto[1],Yaping Hou[2], Melissa A. Grunlan,[2] Mariah S. Hahn[1]
Department of Chemical Engineering, Texas A&M University, College Station, Texas
Department of Biomedical Engineering, Texas A&M University, College Station, Texas

Statement of Purpose: The use of mesenchymal stem cells (MSC) for bone regeneration requires the identification of osteoinductive scaffolds. Hydrophobic biomaterials such as poly(propylene fumarates) and polyanhydrides have shown promise as osteoinductive matrices, and recently, hydrophilic polyethylene glycol (PEG) hydrogels were employed as bone regeneration scaffolds. Thus, tuning scaffold hydrophobicity may be a potent method for optimizing the formulation of bone tissue engineering matrices. Furthermore, an extensive body of literature indicates that appropriately tailoring scaffold inorganic composition (e.g., bioactive glass) can enhance its osteoconductivity. In the present study, we therefore examined the impact of tailoring scaffold inorganic content and hydrophobicity through the photo-cure of star polydimethylsiloxane ($PDMS_{star}$) (hydrophobic inorganic polymer) and linear hydrophilic PEG on MSC differentiation. Results indicated a strong dependence of MSC fate on $PDMS_{star}$ M_n at relatively high $PDMS_{star}$ levels.

Methods: Materials. Pt-divinyltetramethyldisiloxane complex, tetrakis(dimethylsiloxy)silane (tetra-SiH), and octamethylcyclotetrasiloxane (D_4) were obtained from Gelest. Other reagents were obtained from Sigma Aldrich. **Synthesis of Macromers**. $PDMS_{star}$-MA was prepared in two synthetic steps. First, $PDMS_{star}$SiH was synthesized by the acid-catalyzed equilibration of D_4 with tetra-SiH. M_n was controlled by reaction stoichiometry. Allyl methacrylate was then added to each arm. PEG-DA was prepared by acrylation of corresponding PEG.[4] **Hydrogel Preparation.** Gels containing 1 mM acrylate-derivatized RGDS were prepared by the photopolymerization of aqueous mixtures of $PDMS_{star}$-MA (**2k, 7k**) and PEG-DA (**3.4 k**) macromers. Aqueous precursor solutions were prepared at 10 wt% with the following wt% ratios of $PDMS_{star}$ to PEG-DA: 0:100, 5:95, and 20:80. **Hydrogel Characterization.** Gel composition was characterized by XPS, and gel material properties were assessed by DMA, swelling, and serum protein adsorption analyses. **Cell Characterization.** Following three weeks of culture, the differentiation status of MSCs encapsulated within each hydrogel was examined using competitive ELISA.

Results: MSC differentiation toward osteoblast, adipocyte, and smooth muscle cell fates was evaluated by quantifying the levels of osteocalcin, A-FABP, and SM22α, respectively, across hydrogel formulations. Increasing the ratio of $PDMS_{star}$ to PEG from 0:100 to 5:95 appeared to have limited impact on MSC differentiation for both 2k and 7k $PDMS_{star}$ (**Figure 1**). In contrast, further increasing $PDMS_{star}$ levels to 20:80 resulted in marked shifts in MSC differentiation for both $PDMS_{star}$ M_n. However, the directionality of these shifts varied with $PDMS_{star}$ M_n. Specifically. 20:80 $PDMS_{star}$ (2k)-PEG gels were enriched in osteoblast-like cells, whereas MSC differentiation toward a smooth muscle cell phenotype was enhanced in 20:80 $PDMS_{star}$ (7k)-PEG gels.

To gain insight into material-based stimuli underlying observed differences in MSC differentiation, the modulus, swelling, and protein adsorption profiles (an indicator of hydrophobicity) of each hydrogel formulation was assessed. Comparison of gel mechanical properties demonstrated that the modulus of each $PDMS_{star}$ (7k)-PEG gel was statistically indistinguishable from the $PDMS_{star}$ (2k)-PEG gel of the corresponding weight ratio. In contrast, gel protein adsorption profiles, and therefore the biochemical stimuli presented to cells, varied markedly with $PDMS_{star}$ M_n.

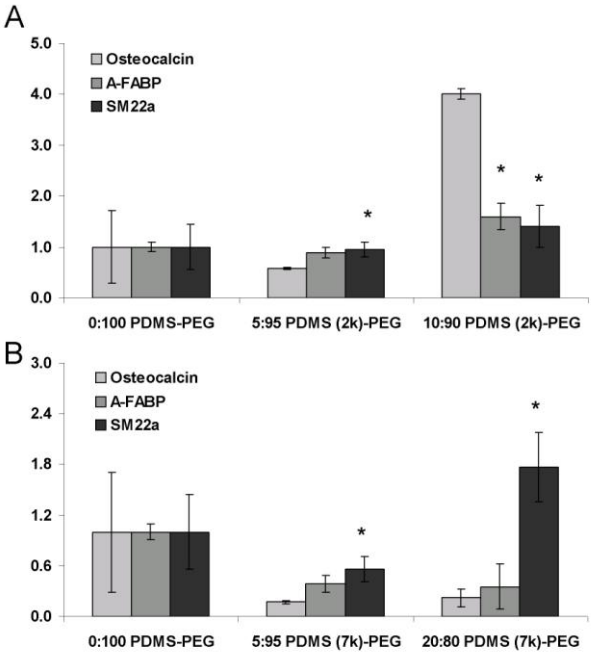

Figure 1: MSC differentiation in $PDMS_{star}$-PEG hydrogels with varying levels of $PDMS_{star}$ (A, B). Comparison of (A) and (B) gives insight into the potential impact of $PDMS_{star}$ molecular weight.

Conclusions: Results from the present study indicate that tuning scaffold inorganic content and hydrophobicity can serve as a powerful tool for directing MSC differentiation. Hydrogel characterization studies suggested that alterations in adsorbed serum proteins and/or calcium deposits with increasing $PDMS_{star}$ levels and M_n may underlie the present differentiation results. Future studies will explore the influence of $PDMS_{star}$ on MSC behavior over a broader M_n range toward identifying osteoinductive scaffold formulations.

USING SHAPE MEMORY POLYMER ACRYLATES TO DETERMINE THE IDEAL MECHANICAL PROPERTIES OF A THROMBECTOMY DEVICE

Andrea Muschenborn, Keith Hearon, Daniel Petty and Duncan J. Maitland
Texas A&M University, College Station Texas
amuschenborn@tamu.edu

Objective: Each year there are 15 million stroke occurrences worldwide. In the U.S. alone, approximately 638,000 cases are ischemic[1]. To date, the only FDA-approved drug to treat ischemic stroke, tissue plasminogen activator, is administered only to 2-5% of the patients because of a narrow treatment time window and other exclusion criteria[2]. Percutaneous mechanical embolectomy devices are an alternative treatment option and are often the only treatment option for patients. Device design is challenging because the devices must meet the size constraints necessary for catheter delivery; however, after delivery, the devices must be able to expand for clot retrieval. Furthermore, devices must be flexible enough to minimize the risk of vessel dissection while traveling through the tortuous vasculature, while also possessing the mechanical strength necessary to entrap the thrombus. Shape memory polymers (SMPs) are excellent candidate materials for embolectomy devices because SMP-based devices can exhibit the volume changes necessary for catheter-delivered thrombus removal and because the mechanical properties of SMPs can be finely tuned to meet specific application demands. The objective of this work was to determine the material properties necessary for the successful design of an SMP-based thrombectomy device. We designed a thermoset acrylic SMP system with tunable mechanical properties and machined devices out of the SMPs. To simulate the frictional forces that an actuated device would exert on an arterial wall, we will measure the frictional forces that our devices with varying recovery stresses exert on a thin-walled latex tube with a comparable modulus to that of arterial tissue. To determine the ideal recovery stress necessary for successful thrombus retrieval, we will attempt to extract phantom blood thrombi using devices with varying recovery stresses.

Methods: Devices were machined from amorphous thermoset acrylic SMPs containing ethyl methacrylate (EMA), butyl methacrate (BMA), and bisphenol A ethoxylate diacrylate (M_n~512, BPAEDA-512). For all samples, a 1:1 weight ratio of EMA:BMA was used, and BPAEDA-512 composition was varied from 1.0 mole% to 85 mole%. The co-monomers and crosslinker ratios were selected to produce devices with glass transition temperatures near 55°C (by DSC) and with rubbery modulus values between 1.0 and 60 MPa. Samples were UV-cured in 60 mL polypropylene syringes. The cured syringe casts were machined to 0.5 mm thick disks on a custom-made holder using a mini computerized numerical control machine (MDX540, Roland). 4x20x1 mm films were also machined from the cured samples for characterization by dynamic mechanical analysis. The design was patterned using a CO2 laser cutter (LS100, Gravograph). Friction tests were performed using an MTS Synergie tensile tester (50 N load cell; see Figure 1). Phantom blood clots containing 99 wt% acrylamide and 1 wt% N,N-methylene bisacrylamide in 5 wt% water solution were also synthesized by UV cure.

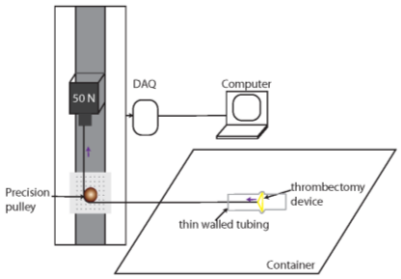

Figure 1. Experimental setup for friction tests.

Results: DMA results for machined films of the acrylic SMPs are provided in Figure 2. Rubbery moduli were tailorable between 1.0 and 50 MPa, and T_g remained close to 55°C for all samples except for those with very high crosslink densities (>66 mole% BPAEDA-512) A photograph of a machined device is provided in Figure 3.

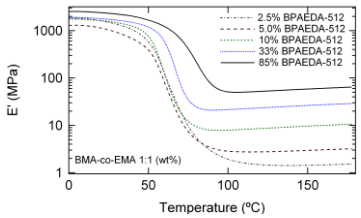

Figure 2: DMA results acrylic SMP samples

Conclusion: This research presents a fast, easy and inexpensive method of prototyping a thrombectomy device with different mechanical properties for testing. With these findings, we will be able to better tune the chemistry of other SMP systems, such as polyurethane SMPs, to target the mechanical properties that make the device more effective in retrieving a thrombus.

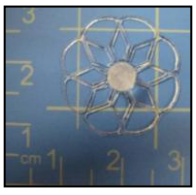

Figure 3: Fabricated thrombectomy device

1.Stead LG et al Arch Neurol 65, 1024 2008

2. Devin L Brown et al Annals of Emergency Medicine 46, 56 2005

INVESTIGATION OF THE MECHANICAL PROPERTIES OF POLYURETHANES FOR USE AS AN ELECROSPUN TISSUE ENGINEERED VASCULAR GRAFT

R. M. Nezarati, D. K. Dempsey, M. B. Browning, E. M. Cosgriff-Hernandez
Texas A&M University, College Station, TX
roya.nezarati@gmail.com

Objective: Current small-caliber (<4mm) vascular prostheses often re-occlude due to their inability to match the unique properties of native blood vessels. In regard to mechanical properties, current synthetic grafts are unable to meet both the compliance and burst pressure of native arteries. We have developed a multilayer vascular graft composed of a non-thrombogenic inner hydrogel layer surrounded by a reinforcing electrospun adventitial layer to decouple the effects of cell-material interaction and graft mechanical properties. In this study, we investigated the mechanical behavior of the reinforcing layer with the hypothesis that this information can be used to rationally choose a scaffold material with desirable biomechanical properties. Segmented polyurethanes (SPUs) were chosen due to their block copolymer structure and microphase separation which results in unique mechanical properties that have the potential to match those of arteries. Three SPUs were evaluated: two poly(carbonate urethanes) (Carbothane© and Chronoflex©) and a poly(ether urethane urea) (BioSpan©). Neat films and electrospun vascular grafts were fabricated and characterized to determine their potential for small-caliber prostheses.

Methods: ***Tensile Tests:*** Solvent-cast films were cut into standard dog bone specimens and uniaxially strained to failure at a rate of 100%/min. ***Electrospinning:*** Polymer solutions were prepared with 15 wt% concentrations in N-N-dimethylacetamide. The solutions were dispensed at a rate of 10 mL/hr as ~14 kV was applied at the needle tip. Fibers were collected on a rotating copper rod (4 mm diameter) placed 30 cm from the needle tip. Tubular grafts were removed from the rod and cut into 35 mm sections for testing. ***Compliance:*** Constructs were subject to a pressure ramp from 0 to 150 mmHg using a syringe pump. Intraluminal pressure was monitored using standard in-line strain gauge pressure transducers and outer diameter was measured with a He-Ne laser micrometer. ***Burst Pressure:*** A nonporous latex tube lining was inserted into grafts and deionized water was pumped through the graft at a rate of 140 mL/min. The pressure was measured downstream from the graft using a high pressure gauge. Infusion continued until graft failure, and the maximum pressure was recorded. ***Suture Retention:*** Tubular samples were cut lengthwise to obtain 12 mm wide strips. A 5.0 commercial PDS II monofilament suture was inserted 2 mm from the short end of the sample, looped, and tied. The lower end of the sample and the suture loop were secured in the grips of a uniaxial load test machine and extended at a rate of 100 mm/min until the suture pulled through the sample wall.

Table 1. Tensile properties of SPU films.

Polymer	Tensile Strength (MPa)	Ultimate Elongation (%)	Initial Modulus (MPa)
BioSpan	45.4 ± 2.3	776 ± 20	11.3 ± 0.1
Carbothane	33.9 ± 4.7	492 ± 24	7.1 ± 0.4
Chronoflex	58.8 ± 5.8	339 ± 18	19.8 ± 0.9

Results: The tensile data of the three polymers is summarized in **Table 1**. Preliminary biomechanical property data (compliance, burst pressure, and suture retention) of resultant electrospun grafts is shown in **Table 2**. Changing polyurethane chemistry resulted in very different biomechanical behaviors for each material. Carbothane had a 100% increase in burst pressure with only an 8% decrease in compliance compared to BioSpan. Chronoflex had both a higher burst pressure (35%) and compliance (66%) than BioSpan. Additional control over graft properties can be achieved by varying thickness (**Figure 1**). Decreasing graft thickness resulted in increased compliance that matched autologous vein grafts.

Table 2. Biomechanical properties of electrospun grafts.

Polymer	Compliance (%/mmHg X 10^{-4})	Burst Pressure (mmHg)	Suture Retention (gf)
BioSpan	3.5	672	203
Carbothane	3.2	1344	324
Chronoflex	5.8	905	25

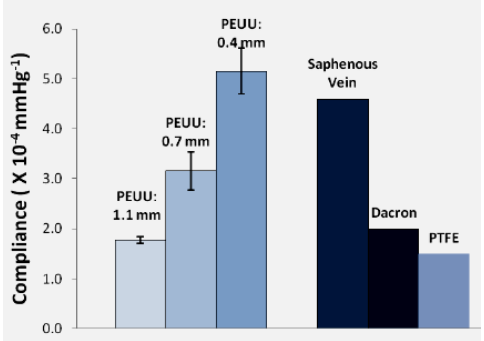

Figure 1. Compliance vs. graft thickness.

Conclusions: This study illustrates our ability to tune the mechanical properties of electrospun vascular grafts to those of native vasculature by altering the polymer chemistry. These data will be used to rationally choose a material with properties that can be further optimized to fabricate better vascular grafts. Initial investigations of these polymers show potential to improve on current synthetic options.

NANOSCALE DIFFUSION-LIMITING BIOPOLYELECTROLYTE MULTILAYERS

Jaebum Park and Mike McShane
Texas A&M University, College Station, TX
jbpark@tamu.edu

Objective

Biomaterial surfaces with nanometer scale control over their properties and functions have considerable importance to biomedical applications. In particular, implantable enzymatic biosensors and drug release systems require diffusion-limiting coatings to act as transport barriers for specific molecules. Layer-by-layer (LbL) self-assembly using alternative adsorptions between anionic and cationic biological polymers offers great potential, as it enables construction of nanocomposite films with biopolyelectrolyte multilayers (BPEMs) to provide more biomimetic matrices.

Methods

In this study, we explored diffusion-limiting nanofilms composed with various combinations of natural and/or synthetic biopolyelectrolytes such as alginate, dextran sulfate, heparin, poly(L-glutamic acid), poly(L-lysine), and chitosan. LbL process and properties of BPEMs were characterized by quartz crystal microbalance, ellipsometry, and contact angle measurements. Diffusion of a small target molecule (glucose) through BPEMs deposited on porous substrates was analyzed using side-bi-side diffusion cells.

Results

Components of the BPEMs strongly influenced contact angles (ranging from 14° to 72°) and thickness (ranging from 26 nm to 139 nm) of the nanofilms. Thin film coatings on the porous substrate with various BPEMs decreased diffusion coefficients of glucose (ranging from 4.4 X 10^{-10} cm^2/s to 3.4 X 10^{-9} cm^2/s) up to 4 orders of magnitude relative to diffusivity in water.

Conclusions

Permeabilities of the nanofilms were influenced by the composition of the films. In genral, crosslinking of multilayers led to decreases in permeability for chitosan-based films, but no clear trend for films containing PLL. Thin film coatings on the porous substrate with various BPEMs decreased diffusion coefficients of glucose up to 4 orders of magnitude relative to diffusivity in water. BPEMs have potential for use as biomimetic surfaces, to match the transport requirements of a variety of biomedical devices.

THERMORESPONSIVE DOUBLE NETWORK NANOCOMPOSITE HYDROGEL MEMBRANES

+Park, J.; Fei, R; George, J.T.; Grunlan, M.A.
+Texas A&M University, Dept. of Biomedical Engineering, College Station, TX
jeeparkmid5@gmail.com

Objective: Crosslinked poly(*N*-isopropylacrylamide) (PNIPAAm) hydrogels undergo a reversible volume phase transition in water from a swollen to a deswollen state above their volume phase transition temperature (VPTT; ~33 °C). This property has been exploited for the controlled detachment of cultured cells.[1] Extending the utility of PNIPAAm hydrogels as robust "self-cleaning" materials for implanted biosensor membranes requires enhancing their mechanical properties and rate of swelling/deswelling. In our previous work, incorporation of polysiloxane nanoparticles (~200 or 50 nm ave. diam.) enhanced PNIPAAm thermosensitivity.[2] Double network (DN) hydrogels typically produce enhanced mechanical strength and rigidity as well as swelling properties versus conventional hydrogels.[3] A DN hydrogel is synthesized in two steps with the first hydrogel highly crosslinked and the second hydrogel loosely crosslinked. In this study, we prepared nanocomposite DN hydrogels comprised of PNIPAAm and polysiloxane nanoparticles (~200 or 50 nm ave. diam.) introduced into the 1st or 2nd network. The impact of these variables on the mechanical properties and swelling/deswelling properties were evaluated.

Table 1. DN Hydrogel Compositions

	1st Network		2nd Network	
Notation	%BIS	%NP	%BIS	% NP
SN	2%	--	--	--
50-1 DN	4%	2%	0.2%	--
50-2 DN	4%	--	0.2%	2%
200-1 DN	4%	2%	0.2%	--
200-2 DN	4%	--	0.2%	2%

SN = single network (no 2nd network), **BIS** = wt% based on NIPAAm, **% NP** = wt % solids of nanoparticles with respect to NIPAAm weight.

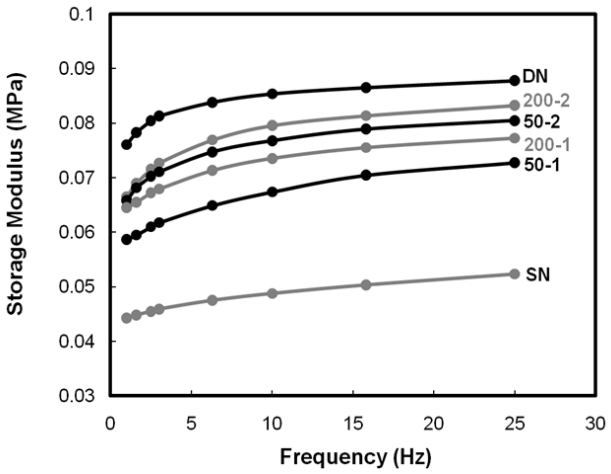

Figure 1. Compression moduli of hydrogels.

Methods: *Polysiloxane Nanoparticle Synthesis:* Crosslinked polysiloxane colloidal particles (~200 or 50 nm ave. diam.) were prepared by emulsion polymerization of D_4 and D_4^{Vi}.[2] *DN Hydrogel Fabrication:* The 1st network (i.e. SN) was obtained by the photocure (6 mW/cm^2, 365 nm, ~7 °C, 30 min) of aqueous precursor solutions containing NIPAAm monomer (1.0 g, 8.84 mmol), BIS crosslinker (0.04 g, 0.13 mmol), and Irgacure-2959 photoinitiator (0.08 g, 0.36 mmol) and DI water (the total volume equal to 7 mL including the volume of water optionally introduced by the nanoparticle emulsion) in a rectangular mold (1.5 mm thick) (**Table 1**). The designated 1st network was subsequently immersed in a 2nd precursor solution containing NIPAAm (6 g), Irgacure-2959 (0.24 g), BIS (0.012 g) and 21 mL DI Water for 1 day at 7 °C. The hydrogel sheet was then transferred to a mold (2.3 mm thick) and likewise photocured. *Characterization:* The VPTT, swelling and deswelling kinetics, morphology and mechanical properties of the hydrogels were measured.

Results: Compared to the SN hydrogel, the DN hydrogel exhibited enhanced swelling/deswelling kinetics and rigidity (G', by DMA). Thermosensitivity was enhanced by the addition of polysiloxane nanoparticles, particularly for "200-1" (**Table 1**). The storage moduli (G') of nanocomposite DN hydrogels was decreased somewhat compared to the DN hydrogel (i.e. no nanoparticles) but remained higher than that of the SN hydrogel (**Figure 1**).

Conclusions: PNIPAAm DN nanocomposites hydrogels were prepared with polysiloxane nanoparticles. Because of their enhanced strength and deswelling kinetics versus conventional PNIPAAm hydrogels, they may be particularly useful in applications requiring mechanical integrity and rapid cell-release such for biosensor membranes which self-clean in response to thermal modulation.

References:

1. Yamato, M.; Akiyama, Y.; Kobayashi, J.; Yang, J.; Kikuchi, A.; Okano, T. *Prog. Polym. Sci.* **2007**, *32*, 1123 -1133.
2. (a) Hou, Y.; Matthews, A.R.; Smitherman, A.M.; Bulick, A.S.; Hahn, M.S.; Hou, H.; Han, A.; Grunlan, M.A. *Biomaterials* 2008, *29*, 3175-3184. (b) Hou, Y.; Fei, R.; Burkes, J.C.; Lee, S.D.; Munoz-Pinto, D.; Hahn, M.S.; Grunlan, M.A. *in review*.
3. Gong, J. P.; Katsuyama, Y.; Kurokawa, T.; Osada, Y. *Adv. Mater.* 2003, 15, 1155-1158.

Fabricating Anatomically Correct Small Caliber Grafts for Vascular Tissue Engineering

Ibrahim Qattan, Richard T. Tran, and Jian Yang *

The Department of Bioengineering, The University of Texas at Arlington, Arlington, TX 76019, USA

The inability to precisely replicate the native vascular anatomy, compliance mismatch, thrombosis, and long *in vitro* culture times remain important limitations to the successful clinical implementation of tissue engineered small diameter blood vessels (SDBV) [1]. To address these issues, we are reporting on the development of a new biodegradable, strong, and elastic SDBV design, which closely mimics the stratified architecture of native vessels. The biomimetic SDBV incorporates three distinct phases to better mimic the native anatomy; 1) A submicron porous layer which provides the necessary topography for graft endothelialization in the tunica intima; 2) A porous internal elastic lamina layer whose porosity can be controlled to fine tune graft mechanical strength; and 3) An outer 150-250 μm pore size tunica media layer to accommodate for smooth muscle cells. The rationale behind the design is that the graft should provide an "off-the-shelf" readily implantable graft that can be combined with *in situ* tissue engineering approaches. In order to meet the strict mechanical requirements, the triphasic scaffolds were fabricated from a strong and elastic biodegradable crosslinked urethane-doped polyesters (CUPE) [2]. Scaffolds were characterized by scanning electron microscope and for tensile properties, burst pressure, and suture retention to determine if the scaffolds met the requirements for immediate implantation. Mechanical studies confirm that the mechanical properties of the triphasic scaffold resemble or are superior to those of the native vessel. The combined mechanical properties and previously demonstrated anti-thrombogenic nature of CUPE may serve as a viable graft material for blood vessel tissue engineering.

References

1. Yang, J.; Motlagh D.; Webb A.R.; Ameer G.A. Novel biphasic elastomeric scaffold for small-diameter blood vessel tissue engineering. *Tissue Eng* **2005**, *11*(11-12), 1876-86.

2. Dey, J.; Xu H.; Shen J.; Thevenot P.; Gondi S.R.; Nguyen K.T.; Sumerlin B.S.; Tang L.; Yang J. Development of biodegradable crosslinked urethane-doped polyester elastomers. *Biomaterials* **2008**, *29*(35), 4637-49.

INTEIN-MEDIATED PROTEIN TRANS-SPLICING FOR IN SITU HYDROGEL FORMATION

Ramirez, M; Chen, Z
Texas A&M University, College Station, TX
Mar227@tamu.edu

Objective:

The objective of our project is to synthesize a highly stable protein hydrogel capable of undergoing gel formation at physiological conditions. Gelation is driven by auto catalytic mini-intein trans-splicing of hydrophilic protein constructs. It is intended to use this technique for *in situ* gel formation for drug delivery applications of therapeutic proteins and UV/heat sensitive drugs.

Methods:

For the formation of the intein-mediated hydrogel, two different protein constructs were synthesized: CutA-L-NpuN and NpuC-S-CutA. CutA is a highly stable triangular trimeric protein. NpuN and NpuC are the mini-inteins of Npu's DnaE protein. The highly water soluble "S" fragment is a synthetic peptide composed of repeating aminoacid units [(AG)3PEG]. Upon mixing, intein splicing reaction yields construct CutA-L-S-CutA, a highly hydrophilic, cross-linkable protein.

Traditional recombinant DNA technology was used for the constructs syntheses. Proteins were expressed in E. coli and purified by affinity chromatography. Reactions were done by mixing constructs at high concentrations in equimolar ratios. Gel formation was determined by upside vial test. Erosion was carried out by adding PBS buffer to gels and measuring protein concentration in supernatant at different time intervals.

Results:

Constructs were successfully cloned, expressed in e Coli, and purified by affinity chromatography. Intein activity was corroborated with splicing yields above 90%. Protein constructs were mixed at high concentrations (above 10 wv%) and gel formation was corroborated. The erosion profile obtained from the gels showed a fast erosion rate within the first day, presumably reaction by-products and unreacted proteins. A much slower erosion rate was observed in the subsequent days.

Conclusions:

We demonstrated the synthesis of highly stable protein hydrogels via self-splicing mini inteins. The hydrogels showed high resistance to erosion. By using self-catalytic intein trans-splicing reactions, cross linking of protein in physiological conditions allows for integration of heat/UV sensitive drugs and proteins into hydrogels. Moreover, cross-linking reactions happen immediately upon mixing of two constructs, making the gel suitable for injectable applications.

MICROENCAPSULATION AS A MEANS TO MODULATE NANOMATERIAL-CELL INTERACTIONS

+Dustin Ritter, Amy Romoser, Ravish Majithia, Mike McShane, Christie Sayes, Ken Meissner
+Texas A&M University, College Station, TX
dritter918@hotmail.com

Objective

A variety of colorimetric and fluorometric assays have been developed to quantify medically-relevant biochemicals *in vitro*. For example, our lab has previously developed an *in vitro* glucose sensing assay based on competitive-binding and Förster resonance energy transfer to transduce binding events. High glucose sensitivity has been reported; however, the current embodiment has limitations that complicate efficient energy transfer (*e.g.*, poor photostability, narrow excitation bands, broad emission bands, *etc.*) due to the organic dyes that are employed. A potential route by which these limitations might be overcome is to use quantum dots (QDs), which are inorganic nanocrystals that possess excellent optical properties such as broad absorption, narrow and size-tunable emission, high quantum yield, a long fluorescence lifetime, and resistance to photobleaching. However, toxicity of Cd-based QDs is currently in question. To enable usage of such reagents for chronic monitoring *in vivo*, suitable materials and structures must be developed to spatially confine the sensing assay to an injection or implantation site and modulate the interactions with the physiological environment. Sequestering of the sensing assay inside a biocompatible microcapsule could enable safe deployment of nanomaterials that enhance sensor function.

Methods

To test our hypothesis that encapsulation mitigates toxicity, branched polyethylenimine-coated CdSe/ZnS QDs were synthesized and encapsulated in polyethylene glycol-terminated polyelectrolyte multilayer microcapsules. Cells were exposed to both encapsulated and free QDs for up to 48 hrs, and cell viability and indicators of oxidative stress were used to compare the cellular response.

Results

QD encapsulation efficiency was determined to be ~30%, resulting in ~9 x 10^6 QDs/capsule; at this concentration, the encapsulated QD volume is ~0.1% of the total microcapsule interior volume. Confocal micrographs indicate that cells phagocytose free QDs; however, encapsulated QDs are not phagocytosed and exposed cells remain viable for up to 48 hrs. Western blots show a higher expression of TNF-α from cells exposed to free QDs as compared to those exposed to encapsulated QDs, indicating that free QDs promote apoptosis and inflammation. Finally, a resazurin assay reveals a dose-dependent decrease in metabolic activity with free QD concentration, whereas no such decrease is observed with encapsulated QDs.

Conclusions

While free QDs did result in specific toxicities along with oxidative stress and heavy metal effects over increased time and concentration, the encapsulated QDs did not induce these toxicities at any time point or dosing concentration. These results support incorporation of inorganic nanomaterials - sequestered using appropriate microencapsulation methods - into biochemical sensing assays.

FUNCTIONAL PROPERTIES OF NANO-SCALED SENSING SCAFFOLDS MADE FROM ALGINATE

[*]Roberts, J R; [*+]McShane, M J
[*]Department of Biomedical Engineering, Texas A&M University, College Station, TX
[+]Department of Material Science and Engineering, Texas A&M University, College Station, TX
jasonrr@tamu.edu

Objective(s): Nanosensors have many distinct advantages over macro-scale sensors including their high surface area to volume ratio, their ability to access normally inaccessible regions of interest such as the interior of cells, and their ability to be administered by injection rather than more invasive implantation. However, reduced size can lead to other functional issues that must be evaluated. In this work, glucose sensing chemistry, the oxidative enzyme glucose oxidase (Gox), is immobilized in alginate matrices in the micro and nanoscale. Nanoparticle scaffold and loaded enzyme properties including size, morphology, loading efficiency, and loaded enzyme activity are determined and compared to those of micro-scaled sensors.

Methods: Multiple batches of both micro and nanoparticle alginate scaffolds were made using emulsion methods. Microparticles containing Gox were constructed using an emulsion / external gelation method while nanoparticle alginate scaffolds containing Gox were manufactured by emulsion/solvent evaporation technique. In both cases, enzyme was physically entrapped within the matrix by the emulsion method. After manufacture, particles were washed and exposed to N-(3-dimethylaminopropyl)-N'-ethylcarbodiimde hydrochloride (EDC) and N-hydrosulfosuccinimide (NHS) to immobilize the entrapped protein within the matrix. Particles were washed and lyophilized for evaluation. Nanoparticle size distribution was determined by dynamic light scattering (DLS) and scanning electron microscopy (SEM), while microparticle sizing was evaluated using a Coulter-principle counter. Enzyme loading was evaluated using a Lowry Assay for protein quantification in a set mass of particles. Enzyme activity was determined by o-dianisidine colorimetric assay with controlled masses of particles and compared to free enzyme activity for relative activity.

Results: Microparticles were spherical with an average diameter of 5.4± 0.30μm (α=.05) while nanoparticle batches were spheroid with a peak diameter 30-50nm. Enzyme loading for the microparticle alginate was 147± 2.7μg enzyme/mg particle (88% of theoretical maximum), with relative activity of 84%. For the nanoparticles, the enzyme loading was 76±15 μg enzyme/mg particle (15% of theoretical maximum) with a relative activity of 5%.

Conclusions: Both methods of manufacture seem to produce uniform particles with repeatable loading and activity from batch to batch. Nanoalginate particles have slightly lower enzyme concentrations and considerably lower enzyme activity compared to microparticles sensors. The relative activity is much lower for nanoparticles, signifying that a majority of the enzyme has been inactivated in the process of particle manufacture. However, if enzyme deactivation could be reduced or enzyme loading increased, nanoparticle alginate could prove to be an effective matrix for glucose-sensing chemistry. The next step for nanoparticle formulation optimization is a post-emulsion enzyme immobilization reaction involving free enzyme and the particle surface which is hypothesized to increase the amount of loaded enzyme as well as the relative activity.

OPACIFICATION OF POLYURETHANE SHAPE MEMORY POLYMER FOAMS

+Rodriguez, J N; +Yu, Y A; *Miller, M W; +*Wilson, T S; +/**Grunden, D T;**Clubb, F J; ++Hartman, J; +Maitland, D J
+Texas A&M University, College Station, TX, *Texas A&M Institute for Preclinical Studies, College Station, TX, +*Lawrence Livermore National Laboratory, Livermore, CA, **Cardiovascular Pathology Laboratory, College Station, TX, ++Department of Neurosurgery, Kaiser Permanente Medical Center, Sacramento, CA
jennifernrodriguez@tamu.edu

Objective:, It has been proposed that shape memory polymers (SMP) be used for the treatment of intracranial aneurysms[1], and more recently, that these materials be radio-opaque[2]. The objective of this work was to obtain the minimal amount of loading of an SMP foam matrix with particulate tungsten to induce clinically useful radio-opacity while not negatively impacting the mechanical properties of the original formulation. The least invasive method for delivery of aneurysm filling device, involves usage of a microcathter using the aid of fluoroscopic imaging for optimal positioning and subsequent device deployment. Adequate loading of SMP foam with a radio-opaque filler would increase the likelihood of these materials being used to treat intracranial aneurysms in humans.

Methods: Solid polyurethane based SMP[3] was fabricated with increasing volume percentages of tungsten loading (do you need to include the word "loading"). Samples were cut in to increasing thicknesses and imaged using fluoroscopy both with and without a pig's skull to determine visibility of the minimal thickness and loading. Using these results, percentage of loading for foam fabrication was determined. Foams were cut into increasing thicknesses, in a manner similar to the solid polymer, and were imaged both with and without a pig's head for reference opacity. The increase in image contrast was quantified using Matlab after individual samples were imaged in the same location on the animal. Material properties, such as mechanical testing and average pore cell sizes were obtained to determine effects of the addition of tungsten to the polymer foam matrix.

Results: Loading 4% by volume of tungsten to the SMP foam matrix elicited radio-opactiy through a pig's skull thickness (Figure 1), when the material thickness was greater than 8 mm (Figure 2). Material charecterization determined that the addition of tungsten almost doubled the breaking tensile strength, and increased the breaking strain by greater than one and a half times the non-tungsten loaded foams (Table 1). The addition of tungsten increased heterogeneity of the 4% by volume of foam, when compared to the control.

Conclusions: The addition of 4% by volume of tungsten to SMP foam created a clinically useful level of fluoroscopic contrast. The level of contrast was sufficient to be visible through the thickness of a skull and tissue of a pig. These results are very promising for the advancement of this material to become a viable medical device for the treatment of aneurysms as an alternative to current filling methods. The increase in mechanical properties of the foam shows that the addition of 4% by volume of tungsten does not negatively impact the material, further advancing this material toward market. Although the results of this work represent a significant step toward getting this device to market additional in-vivo studies would need to be conducted to prove safety and efficacy of this material.

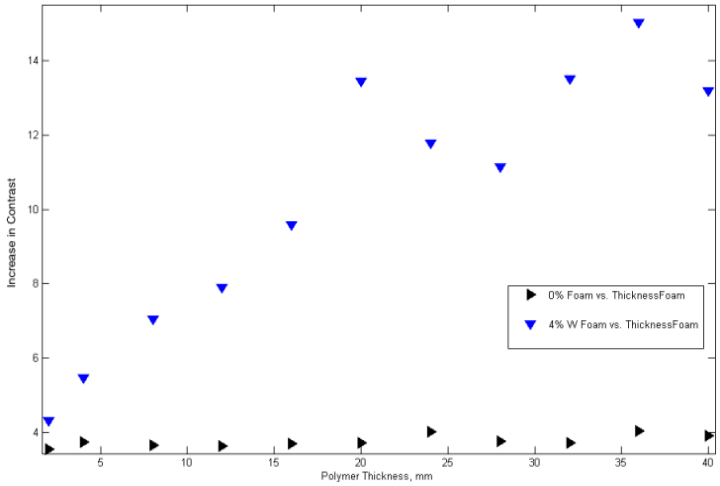

Figure 1: Increase in Contrast via Tungsten Doping of SMP Foam

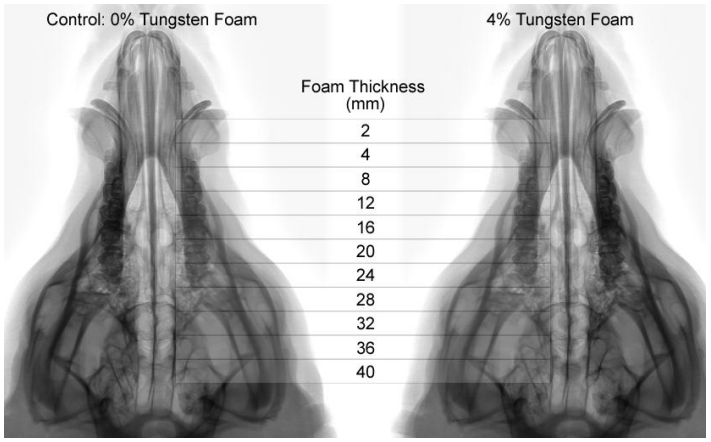

Figure 2: Radio-Opacity of 0% and 4% SMP Foam

Table 1: Mechanical Testing of Foams

	Breaking Tensile Strength (kPa)	Breaking Strain (%)	Young's Modulus (MPa)
0% Tungsten Foam	80 +/- 30	10 +/- 3	0.8 +/- 0.4
4% Tungsten Foam	130 +/- 30	16 +/- 4	0.8 +/- 0.2

References: 1. Metcalfe, A., Biomaterials 24:491-497, 2003. 2. Hampikian, J. M., Materials Science and Engineering: C 26:1373-1379, 2006. 3. Wilson, T. S., J Appl Polym Sci 106:540–551, 2007.

AMPHIPHILIC PEG-SILANE TO PREVENT THROMBOSIS ON PCU

+Rufin M.A.; Giese, M.L.; Grunlan, M.A.
Texas A&M University, Dept. of Biomedical Engineering, College Station, TX
rufinm@tamu.edu

Objective: Catheters are increasingly being utilized for vascular access for hemodialysis despite their increased risk of thrombosis which is associated with catheter dysfunction, infection and embolism.[1] Anti-coagulant therapies (e.g. heparin locks) are used to prevent thrombosis, but have limited efficacy[2] and are associated with bleeding complications.[3] Hemodialysis catheters prepared from polycarbonate-polyurethane copolymers (PCU) are gaining popularity over silicone catheters due to their unique mechanical and chemical properties.[4] FDA-approved PCU catheters with complex heparin-grafted coatings are available but have yet to prove their efficacy and are associated with high costs and risks like that associated with free heparin. A "heparin-free" "stealth" coating that could be applied the surfaces of PCU catheters is an attractive alternative to diminish thrombosis which begins with the adsorption of blood proteins. Although poly(ethylene oxide) (PEO; or poly(ethylene glycol) PEG) exhibits exceptional protein resistance *in vitro*, its performance *in vivo* has been disappointing. Thus, we developed a novel PEG-silane in which PEG molecular mobility is enhanced and the chain rendered amphiphilic by incorporation of a hydrophobic, flexible siloxane tether (**Figure 1**). A PCU was modified with the PEG-silane amphiphile via surface-grafting and bulk modification.

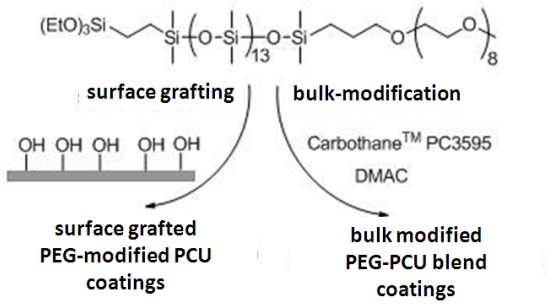

Figure 1. Surface and bulk modification of PCU with PEG-silane amphiphile.

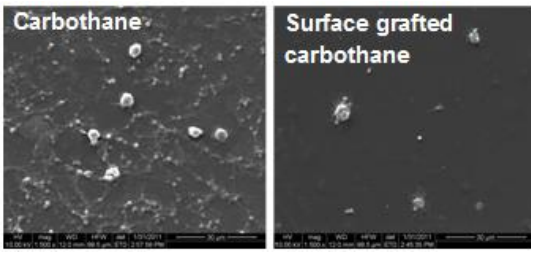

Figure 2. Whole blood (pig) adhesion under flow conditions (15 min).

Methods: *PEG-Silane Amphiphile Synthesis*: The PEG-silane amphiphile was prepared as previously reported.[5] *Surface-grafted Coatings*: Carbothane™ PC3595 (Lubrizol), a PCU utilized to prepare FDA-approved hemodialysis catheters, was solvent cast (10% in dimethylacetamide, DMAC) onto glass microscope slides previously modified with (3-glycidoxypropyl)trimethoxysilane and dried *in vacuo* (< 1mTorr, RT, 72h). Following plasma treatment (1 min, air), the coated slide was exposed to 5 mM grafting solution (hexane) for 2 hr followed by rinsing with hexane and water. *Bulk-crosslinked Coatings*: Carbothane™ PC3595 was combined with DMAC (1:10 wt% ratio) and the PEG-silane added at varying wt% based on PCU wt (0, 1, and 5 wt%). *Protein Adhesion*: Fibrinogen adhesion studies were conducted as previously reported.[5] *Whole Blood Adhesion*: Under static conditions, 1 mL of whole blood (pig) was applied to a silicone isolator (diameter = 23 mm) for 1 h. Coatings were exposed to whole blood under flow conditions using a parallel plate flow chamber. For 15 min, blood flow was maintained at 0.825 mL/min which generated a mean wall shear stress of 60 dyne/cm^2. Following exposure to whole blood, these surfaces were imaged using scanning electron microscopy (SEM) to visualize platelet adhesion and aggregation. *Surface Characterization*: Surface properties were examined via contact angle analysis (KSV CAM-200) and ATR-FTIR.

Results: Contact angle measurements revealed significant differences in the wettability of PCU versus that modified with the PEG-silane amphiphile both at the surface and throughout the bulk. SEM images confirmed that the PCU surface grafted with the PEG-silane amphiphile adsorbed much fewer platelets and protein (**Figure 2**).

Conclusions: The PEG-silane amphiphiles are useful to improve the clot resistance of PCU. Both the surfaces as well as the bulk may be modified with the PEG-silane amphiphile. In future work, we will study the effects of varying the PEG length of the PEG-silane amphiphile.

References:

1. Tal, M.G.; Ni, N. *Tech. Vasc. Interv. Radiol.* **2008**, *11*, 186-191.
2. Icenogle T.B.; Smith R.G.; Cleavinger M.; Vasu M.A.; Williams R.J.; Sethi G.K. Copeland J.G. *Art Org.* **1989**, *13*, 532-538.
3. Levine M.N.; Raskob G.; Beyth R.J.; Kearon, C.; Schulman, S. *CHEST* **2004**, *126*, 287S-310S.
4. Schwab, S.J.; Beathard, G. *Kidney Int.* **1999**, *56*, 1-17.
5. Murthy, R.; Cox, C.D.; Hahn, M.S.; Grunlan, M.A. *Biomacromolecules*, **2007**, *8*, 3244.

AMPHIPHILIC INTERPENETRATING NETWORKS FOR ORAL ANTICANCER DRUG DELIVERY

Cody A. Schoener and Nicholas A. Peppas
University of Texas at Austin, Austin, TX, 78712, USA
schoener@che.utexas.edu

Objective: Intravenous (I.V.) administration of chemotherapeutics is adjunct to patients who underwent surgical removal of tumors, however this systemic flow of harmful drugs throughout the body destroys cancerous and healthy cells non-discriminately. Thus, patients experience undesirable side effects resulting in altered treatment plans which may ineffectively diminish or oblate remaining tumor cells. New oral methods of delivering anticancer agents via polymer carriers may improve current treatment regimes, but must overcome physiological barriers faced during oral transit. We recently developed sequential interpenetrating networks (IPN) composed of hydrophilic, pH-responsive poly(methacrylic acid-grafted-ethylene glycol) (P(MAA-g-EG)) and hydrophobic poly(n-butyl acrylate) (PBA) which may give rise to a unique set of properties appropriate for the oral delivery of chemotherapeutics.

Methods: IPNs were prepared by sequential photo-polymerizable methods. First, methacrylic acid, poly(ethylene glycol methyl methacrylate) (PEGMMA; MW ~1000 g/mol), tetraethylene glycol dimethacrylate (TEGDMA; crosslinker), and 1-hydroxycyclohexylbenzophenone (Irgacure 184, photocatalyst) were dissolved in ethanol/water and exposed to UV light. Second, n-butyl acrylate, TEGDMA, and Irgacure 184 were dissolved in a solvent composed of 80, 75, or 70% (w/w) ethanol in water. A P(MAA-g-EG) disc from the first step was placed in this solution overnight and then exposed to UV light resulting in three unique IPNs: 80/20 IPN, 75/25 IPN, 70/30 IPN. IPNs were washed and dried. Swelling profiles were determined by swelling discs in buffers between pH 3.2 and 7.6. Contact angle measurements on IPN surfaces were used to determine difference in hydrophobicity. Fluorescein, a cancer drug analogue, was loaded into crushed IPN particles by imbibing and released in a dissolution apparatus. Cytotoxicity on Caco-2 cells determined if blank and loaded IPN particles were biocompatible.

Results: Equilibrium mass swelling experiments illustrated the influence of PBA on resulting IPNs as compared to pure P(MAA-g-EG). As the amount of PBA increases in the IPNs there is a greater degree of entanglement between the polymer networks resulting in decrease swelling. All carriers demonstrated a collapsed state at low pH's thus protecting the loaded drug from harsh stomach contents. Contact angles measured 47 ± 1°, 62 ± 1°, 68 ± 1°, 106 ± 1° for P(MAA-g-EG), 80/20 IPN, 75/25 IPN, 70/30 IPN, respectively, confirming the difference in degrees of hydrophobicity. Loading efficiencies ranged from 25-45% and percent released ranged from 80-99% (Figure 1). 75/25 IPN showed exceptionally high loading levels (45%) due to an optimized balance of hydrophobic and swelling properties. All IPNs were biocompatible.

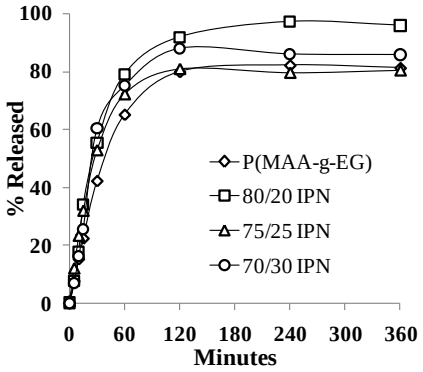

Figure 1. Percent Released of IPNs and P(MAA-g-EG)

Conclusions: These novel IPNs of P(MAA-g-EG) and PBA demonstrate their potential to protect and deliver chemotherapeutics orally. We are currently releasing Fluorescein loaded IPN particles in low pH, then high pH to mimic the transition from stomach to upper small intestine. Furthermore, we are developing experimental procedures for the loading of Doxorubicin, a cancer drug.

SYNTHESIS OF A CELL-RESPONSIVE BIODEGRADABLE POLYUREA FOR LIGAMENT TISSUE ENGINEERING

Sears, N; Benhardt, H; Touchet, T; Cosgriff-Hernandez, E
Texas A&M University, College Station, TX

Objective: Many scaffold fabrication techniques have been used to formulate ligament scaffolds for the replacement of injured tissue. Synthetic, nonbiodegradable scaffolds have the innate problem of eventual failure as we have not developed a material that can withstand physiological loads for extended periods of time. Biodegradable scaffolds usually incorporate a biodegradable polymers that undergo nonspecific hydrolysis which does not match the body's rate of degradation and tissue regeneration. We propose the inclusion of a cell-responsive biodegradable oligopeptide in order to enable synthetic polymers to integrate into the native remodeling processes and thus promote enhanced tissue formation. We propose to develop a series of polyureas which include a collagen-mimetic oligopeptide in their backbone that combine the strength and tunability of synthetic elastomers and the cell-responsive degradation of native collagen. In this study functionalization of poly(ethylene glycol) (PEG) with amine end groups (NH2) was achieved.

Methods: *Prepolymer Synthesis:* PEG diol, MW = 6000 (PEG 6K OH) was reacted with succinic anhydride to form PEG 6K Diacid (PEG 6K COOH) in methods previously described[1]. PEG 6K COOH was then activated with a leaving group. PEG 6K COOH was dissolved in dimethylformamide at 10 weight percent and N,N'-Dicyclohexylcarbodiimide (DCC), and N-Hydroxysuccinimide (NHS) were added in molar ratios (relative to PEG 6K COOH) of 13 and 10, respectively. After 2-3 hours of activation, PEG 6K NHS was added dropwise to a solution of 6:1 molar ratio of ethylenediamine (EDA) in DMF with 10 weight percent triethylamine (TEA). After one hour of reacting PEG 6K NHS with excess EDA.*Polymer Synthesis*: Hexane diisocyanate (HDI) was added as a chain extender in a 5:1 molar ratio (relative to PEG) to form a polyurea (PU) represented by the diagram below. The PU was characterized with gel permeation chromatography (GPC) using the reaction solvent, DMF, as the mobile phase.

Results: Synthesis of PEG COOH and activation with DCC/NHS was accomplished **efficiently** and confirmed with fourier transform infrared spectroscopy (FTIR). Formation of PEG COOH showed creation of a peak at 1737cm^{-1} (C=O) ester. Reacting the activated PEG NHS with EDA showed creation of a peak at 1645cm^{-1} C=O (amide I band), indicating endcapping of the PEG with EDA. The resulting diamine and excess EDA were reacted by adding a solution of HDI in DMF dropwise to form the PU. Polymerization was monitored after the presence of HDI was no longer detectable with IR spectroscopy. Molecular weight characterization was done using a polymethyl methacrylate (PMMA) as a standard using multidetector calibration using the refractive index response and light scattering.

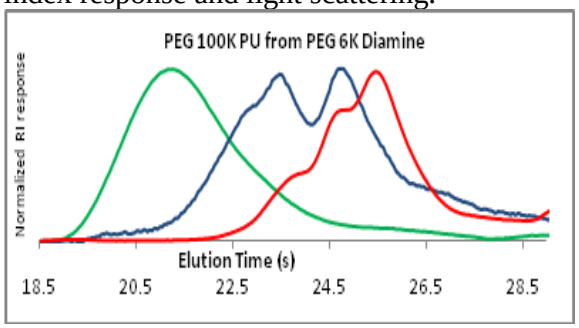

Figure 2. RI response vs. elution of 3 PU samples. Right to left: 4 hours (Mp=7060 Da), 10 hours (Mp=13754/29561 Da), 18H (Mp=115726 Da).

Conclusions: Synthesis of the PU from PEG prepolymers and the formation of amide linkages allows reactivity with diamine molecules such biodegradable oligopeptides. We have successfully synthesized a PU with appropriate chemistry to allow inclusion of a collagen mimetic oligopeptide. MW characterization of the PU shows over 100 KDa. Future work will include synthesis of the prepolymer inclusive of the biodegradable oligopeptide, as well as PU synthesis with the biodegradable prepolymer.

[1] Ma et al. "Interaction of heparin with polyallylamine-immobilized surfaces." J Biomed Mater Res, 27: 357-365.

DESIGN AND DEVELOPMENT OF TARGETED CATIONIC DEGRADABLE SHELL CROSSLINKED NANOPARTICLES FOR MEDIATING HIGHLY EFFICIENT DELIVERY OF NUCLEIC ACIDS

[+]Shrestha, R.; [+]Samarajeewa, S.; [*]Shen, Y.; [+]Florez, S.; [*]Taylor, J-S. A.; [+]Wooley, K. L.
[+]Department of Chemistry and Chemical Engineering, Texas A&M University
[*]Department of Chemistry, Washington University in Saint Louis
ritu.shrestha@chem.tamu.edu

• Objective

This presentation will highlight the progress toward the design and development of targeted cationic degradable shell crosslinked knedel-like (SCK) nanoparticles for efficient and effective delivery of gene and nucleic acids *in vivo*. SCKs are robust nanostructures that are created by the self assembly of functional amphiphilic block copolymers followed by crosslinking of the hydrophilic shell region for providing stability to the nanoparticles against infinite dilution. In the recent years, cationic SCKs (cSCKs) that possess positive charge on the surface of the nanoparticles have been demonstrated as a highly efficient agent for cell transfection. The positive charges presented on the surface offer a dual advantage – firstly, it allows for electrostatic binding of nuclei acids and secondly promotes the mediation of the nanoparticles across the cell membrane. Modification on the block copolymer precursor of cSCKs allows the grafting of polyethylene oxide (PEO) moieties for enhanced biodistribution. Additionally, the chain end termini of PEOs can be altered to bear functional handles for the covalent conjugation of peptides and proteins to facilitate site-specific targeting. Furthermore, block copolymer precursors with hydrolytically cleavable ester linkages can be exploited to incorporate degradability into the resulting nanoconstructs for biological clearance *in vivo*. Herein, progress towards the synthesis of functional cSCKs, tethering of targeting ligands, and incorporation of degradability into the nanostructures will be discussed. Furthermore, integration of all these strategies to create a hierarchical multifunctional system will be described.

• Methods

As illustrated in Figure 1A., amphiphilic diblock copolymer of poly(acrylic acid)- *b* –polystyrene (PAA-*b*-PS) underwent amidation with *N*-Boc-ethylenediamine followed by removal of the protecting groups using trifluoroacetic acid to reverse the negatively charged PAA-*b*-PS to positively charged poly(acrylamidoethylamine)-*b*-polystyrene (PAEA-*b*-PS). The resulting block copolymer was dissolved in DMSO followed by dialysis against nanopure water to obtain micelles. The micelles were crosslinked in the shell region with a diacid crosslinker at pH 8.0 to form cSCKs. cSCKs were then mixed with DNA at various N/P ratios (Figure 1B) to demonstrate the electrostatic interaction between positively charged cSCK and negatively charged DNA.

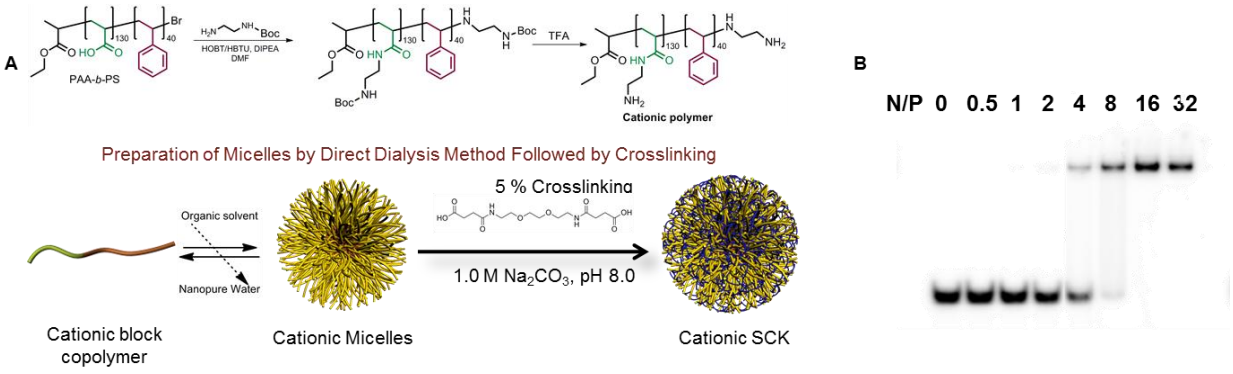

Figure 1. A) Synthesis of cationic block copolymer and their self assembly and crosslinking to form cSCKs **B)** Gel retardation assay of SCK/DNA complex at various N/P ratios

• Results

The sizes of the nanoparticles were analyzed by dynamic light scattering and were found to be $((D_h)_{num}) = 10 \pm 3$ nm for micelles and 14 ± 4 nm for cSCKs. The zeta potential measurement for nanoparticles showed $\zeta = 16 \pm 3$ mV for micelles and $\zeta = 8 \pm 2$ for cSCKs which confirmed that the charges of the particles were reversed by amidation. Agarose gel retardation assay verified that positively charged cSCKs show electrostatic attraction with negatively charged DNA at N/P ratio of 4:1 showing strong binding of DNA with cSCKs to form SCK-DNA complex.

• Conclusions

In this work, we have demonstrated formation of cSCKs with positive ζ values that show great binding to DNA at N/P ratio of 4:1. This system will be further modified to bear degradable units and targeting ligands to further study the system *in vivo*.

CRITICAL SIZE DEFECT REPAIR THROUGH A GENE THERAPY APPROACH

Simpson, CL; Sonnet, C*; Sullivan, K*; Olabisi, R; Davis, AR*; Olmsted-Davis, EA*; West, JL

Rice University, Houston, TX

*Baylor College of Medicine, Houston, TX

CLS4@RICE.EDU

Objectives: There is a great clinical need for a bone regeneration system to treat critical size fractures that will not heal leading to disability, deformity or amputation. Previous work established a system in which adenovirus-transduced BMP-2 expressing fibroblasts were encapsulated within poly(ethylene) glycol diacrylate (PEGDA) microsphere hydrogels, which allowed the diffusion of sufficient amounts of BMP-2 protein from the cell-seeded hydrogels to induce heterotopic bone formation *in vivo* in a murine model. Placement via injection is possible with the microsphere structures and microencapsulated cells induced greater volumes of bone formation than when these cells were directly injected. We are now using our established model for heterotopic bone formation in a critical size defect model.

Methods: Wistar skin fibroblasts (WSF) were cultured in DMEM supplemented with FBS and Pen/Strep then trandsuced with human type 5 adenovirus (Ad5) constructed to contain cDNAs for human BMP2. WSFs (2×10^7) were then combined with 0.1 g/ml PEGDA with 1.5% (v/v) triethanolamine/HEPES buffered saline (pH 7.4), 37 mM 1-vinyl-2-pyrrolidinone and 0.1 mM eosin Y to form a hydrogel precursor solution. The hydrogel precursor solution and sterile mineral oil with 3 µl/ml of 2,2-dimethoxy-2-phenyl acetophenone in 1-vinyl-2- pyrrolidinone (300 mg/ml) were emulsified by vortex while exposing to white light. Microspheres were isolated, collected and injected into rat femoral critical size defects (~5 mm). The defect was injected with either 1) Ad5BMP2-transduced autologous cells; 2) Ad5BMP2-transduced microencapsulated allogenic cells; or 3) no treatment.

Results: BMP-2 ELISA results show significant BMP-2 expression of Ad5BMP2-transduced microencapsulated cells compared to control. Microencapsulated cells also remain 70% viable after 24 hours incubation. Two weeks following surgery, animals which received no treatment or AdBMP2-transduced autologous WSFs did not show any healing. In contrast, animals receiving microencapsulated Ad5BMP2-transduced allogenic WSFs show significant bone growth at 2 wk. Histological analysis shows significant new bone formation surrounding the implanted beads as well as fusion of skeletal bone with new bone. Preliminary mechanical testing shows stiffness and strength of repaired femurs are similar to that of the contralateral skeletal bone.

Conclusions: The use of autologous Ad5BMP2-transduced cells did not treat critical size defect while injections of microencapsulated allogenic Ad5BMP2-transduced cells formed significant amounts of bone. The data suggest that the PEGDA microspheres provide immunoprotection of the transduced allogenic cells, permitting them to release sufficient amounts of BMP2 to induce bone formation. Ongoing studies include an extensive time course and examination of mechanical stability of the newly formed bone.

Tuning the Young's Modulus of Multiphoton Fabricated Hydrogels

*Spivey, E C; *Schmidt, C E; **Shear, J B
*Department of Biomedical Engineering
**Department of Chemistry and Biochemistry
The University of Texas at Austin

Objective

Cell growth and development is dependent on numerous and diverse properties of the local microenvironment. Recent research has shown the particular importance of substrate modulus on cell behavior and fate. We show that multiphoton lithography can be used to fabricate hydrogels with tunable moduli. Here, we examine the mechanical properties of micron-scale hydrogels fabricated from solutions of bovine serum albumin (BSA), hyaluronic acid (HA), and polyethylene glycol (PEG). Both BSA and HA are natural biomaterials that are abundant in blood and extracellular matrix, PEG is a synthetic, FDA-approved biomaterial. We are particularly interested in how different concentrations of these macromolecules influence the Young's modulus and swelling ratios of the resulting hydrogels. Preliminary results indicate that we can tune moduli over several orders of magnitude by altering fabrication parameters. Ultimately, this will allow us to fabricate cell scaffolds over a range of moduli representing all tissue types, and may also allow us to fabricate scaffolds with micron-scale modulus gradients.

Methods

Our multiphoton lithography method exploits multiphoton excitation (MPE) generated by focused, mode-locked Ti:S laser to promote photochemical crosslinking (via a photosensitizer) in a solution of macromolecules and photosensitizer[1,2]. Excited-state interactions between the photosensitizer and macromolecule lead to the creation of a solid, micron-scale hydrogel matrix around the focal point of the laser-focusing optics. By scanning the focal point, we fabricated 35x40 µm hydrogel blocks from solutions containing different concentrations of BSA (0-30 % w/v), methacrylated HA (GMHA, 0-5% w/v), and PEG diacrylate (PEGDA, 0-50% w/v). BSA and PEGDA were used as purchased, GMHA was conjugated and characterized using previously published methods[3]. Solutions were made by adding stock to 5 mM rose bengal (RB) in 20 mM HEPES buffered saline (HBS). The hydrogels were fabricated on the surface of a #1 cover glass, the Ti:S laser was tuned to 740 nm with an average power of 10-100 mW. Structures were rinsed thoroughly with HBS and measured with an atomic force microscope (AFM, Asylum MFP-3D), using cantilevers with 0.75-2.5 µm radius borosilicate bead tips and spring constants (k) of 5-40 N/m. We acquired measurements of the thickness of the structure and the forces required to indent the structure with the bead. Force and indentation measurements were then used with bead radius (R) to calculate Young's Modulus by a least-squares fit of the experimental data to the Hertz model.

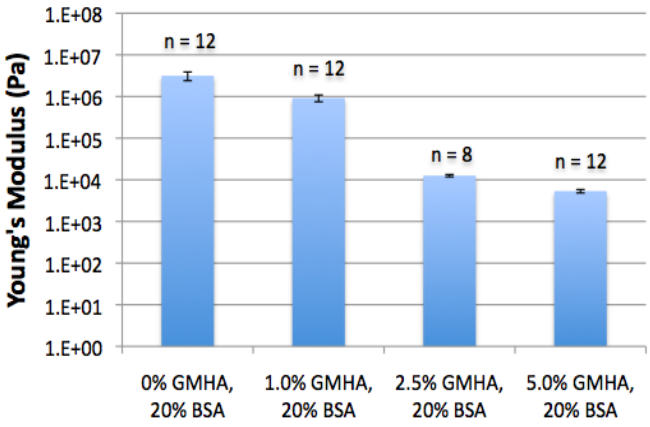

Results

Results shown are for a series of hydrogels fabricated using a 20% solution of BSA, with 0-5% GMHA. The cantilever used to acquire this data has k = 6.2 N/m and R = 0.85 µm. The effect of GMHA concentration on the hydrogel modulus is significant, but does not appear to be linear. Data were acquired from 12 total locations on three separate hydrogel blocks of each type. All data shown have r^2 values > 0.99, most are ≥ 0.995. Subsequent experiments have revealed that for a given cantilever spring constant and bead size, there is an optimal range of moduli that can be measured. We are currently examining the effect of this phenomenon on our existing results, and are integrating our findings into future experiments.

Conclusions

Multiphoton fabrication shows promise as a tool for both investigational and clinical work in tissue engineering, but the mechanical properties of the resulting hydrogel microstructures must be fully characterized. We contend that with the current body of knowledge, we can develop a system that accurately measures the moduli of multiphoton fabricated BSA and GMHA hybrid microstructures, and use it to determine the parameters by which the moduli of the microstructures can be tuned. Characterization of the relationship between fabrication parameters and the modulus of the resulting hydrogel will allow the rational design of mechanically appropriate scaffolds, with a degree of control over the range and scale of variations in modulus that is not currently possible.

1. Allen, R. *Anal. Chem.*, **2005**. 77(16); 5089-5095.
2. Nielson, R. *Small*. **2009**. 5(1); 120-125.
3. Leach, J.B. *Biotech. Bioeng*, **2003**, 82(5); 578-589.

THERMALLY RESPONSIVE POLYMER-NANOSHELL COMPOSITES FOR CONTROLLED CHEMOTHERAPUETIC DELIVERY

Strong, L E; Bikram M; Sershen S; West J L
Rice University, Houston, TX
laura.strong@rice.edu

Objective: Despite the efficacy of various chemotherapeutic agents toward cancerous tumors, many patients have to cease treatment due to offsite toxicity. A controlled delivery system that provides a burst release of chemotherapeutics targeted only to malignant tissue would be advantageous to decrease these undesirable systemic effects. This study aims to develop a controlled delivery system by loading drug molecules into a thermally responsive poly(N-isopropylacrylamide-co-acyrlamide) (NIPAAm-co-AAm) hydrogel and using optically active gold-silica nanoshells to trigger delivery. Poly(NIPAAm-co-AAm) hydrogels display property changes at a lower critical solution temperature (LCST). Below this temperature the gels are in a highly swollen state, but when heated, a burst release of water and any absorbed molecules occurs. This temperature change can be achieved by external heating methods or by irradiation of the imbedded gold-silica nanoshells. In the latter case, exposure to near infrared (NIR) light, which can penetrate biological tissue with little attenuation or damage to tissue, triggers a rapid temperature increase, polymer collapse, and drug expulsion.

Methods: Gold-silica nanoshells were synthesized in a four-step process: 1) silica core synthesis, 2) amine functionalization of cores, 3) absorption of gold colloid onto cores, and 4) gold shell growth. Poly(NIPAAm-co-AAm) hydrogels were synthesized via free radical polymerization of a prepolymer solution (95:5 molar ratio of NIPAAm:AAm with a 1:750 ratio of the crosslinker methylenebisacrylamide to the monomers) and $8 \cdot 10^9$ nanoshells/mL gold-silica nanoshells. Ammonium persulfate (APS) and tetramethylethylenediamine (TEMED) were added to initiate polymerization. The LCST of the hydrogels was determined by incubating gels in a water bath at increasing temperatures and weighing to analyze deswelling behavior. Both incubating the gels at 50 $^{\circ}$C and exposing the gels to an 808 nm laser at 8 W/cm^2 were used to further analyze the thermal behavior of the hydrogels. For drug release studies, hydrogels were dried and then swollen in a solution containing 0.5 mg/mL doxorubicin (580 Da) and transferred to TRIS buffer. Temperature was then altered by either incubation in a 50°C water bath or exposure to an 808 nm laser at 8 W/cm^2. Samples of buffer solution were taken at various time points and analyzed via UV-Vis spectroscopy for drug content.

Results: The LCST of the poly(NIPAAm-co-AAm) hydrogels was determined to be from 39-45°C, or slightly above physiologic temperature. Similar profiles are seen for gels with and without nanoshells, indicating incorporated nanoshells do not hinder hydrogel collapse or drug release. Collapse of the hydrogels containing nanoshells is seen to follow both incubation at 50 $^{\circ}$C and irradiation with the NIR laser. Doxorubicin delivery from irradiated hydrogels containing nanoshells is significantly higher than irradiated hydrogels without nanoshells and hydrogels left at room temperature ($p<0.05$) at all times $t>0$.

Conclusions: Burst release of the chemotherapeutic doxorubicin can be triggered by NIR irradiation of nanoshell containing poly(NIPAAm-co-AAm) hydrogels. Future applications of this project include incorporating this hydrogel as a thin coating onto individual nanoshells as to create an injectable, targeted drug delivery system.

SYNTHESIS, FABRICATION AND DEGRADATION OF POLY(ETHYLENE GLYCOL)-POLY(CAPROLACTONE) BIODEGRADABLE HYDROGELS

Touchet, T, Cosgriff-Hernandez, E. M.
Texas A&M University, College Station, TX
tytouchet@tamu.edu

Objective: The traditional tissue engineering paradigm involves the seeding of stem cells onto a three dimensional scaffold with bioactive agents to promote neoplasia of native tissue. The scaffold is degraded and ultimately replaced with autologous tissue. Tissue engineered scaffolds are investigated due to the complexity of developing an analog that meets the properties of native tissue. PEG based hydrogels have been extensively investigated as potential candidates for soft tissue repair. PEG hydrogels intrinsically resist protein adsorption and cell adhesion providing a biological "blank slate" that can be used to carefully control cell-material interactions through the selective addition of bioactive molecules. However, traditionally PEGDA hydrogels are considered non-degradable and therefore not ideal for tissue engineering. To address this, biodegradable polymers such as polycaprolactone (PCL) or poly(glycolic acid) (PGA) can be incorporated into these hydrogels to create a degradable tissue engineered scaffold. In the current study, the synthesis, fabrication and the degradation profile of PEG and PEG/PCL hydrogels is reported.

Methods:

Synthesis of PEG-diacrylate (PEGDA): PEG 3.4K OH acrylated using standard protocols[1]. Briefly, the terminal hydroxyls were reacted with acryloyl chloride to form an ester linkage and acrylate end groups. The excess acryloyl chloride was neutralized, and the product was precipitated in cold diethyl ether. The structure was confirmed with NMR and FTIR spectroscopy. *Synthesis of PCL-diacrylate (PCLDA):* PCL 2K OH was acrylated using standard protocols. Briefly, the terminal hydroxyls were reacted with acryloyl chloride to form an ester linkage and acrylate end groups. The excess acryloyl chloride was neutralized, and the product was precipitated in cold diethyl ether. The structure was confirmed with NMR and FTIR spectroscopy. *Fabrication of PEG-PCL hydrogels*: PEGDA and PEGDA/PCLDA 20 wt % solution were made in DCM. A photoinitiator (2,2-Dimethoxy-2-phenylacetophenone) was added at a concentration of 10 mg/ml, and the solution was crosslinked between plates spaced 1.5mm via 6 min exposure to 365 nm UV light (Transilluminator, 9 mW/cm^2). After crosslinking was complete, the gels were transferred to water for three days to leach out DCM. *Degradation Study:* Punches of PEGDA and PEGDA/PCLDA gels (n=6) were placed in either 1X PBS or 0.05M NaOH. The PBS group was changed weekly and this study was continued for six weeks. The solutions for the NaOH group were changed daily and the study was continued until the gels fully degraded. Degradation was reported as increase in the swelling ratio (Q) and was determined by dividing the swollen weights at each time points with the original dry weights.

Results: Successful syntheses of all the polymer components were characterized by using FTIR and H^{1}NMR. Functionalization of PEGDA was found to be approximately 85% and functionalization PCLDA was found to be 95% using H^{1}NMR. Hydrogels with PCLDA components degraded significantly more than PEGDA hydrogels under accelerated conditions, Figure 1. No significant degradation was seen for any gels in PBS over the six week study.

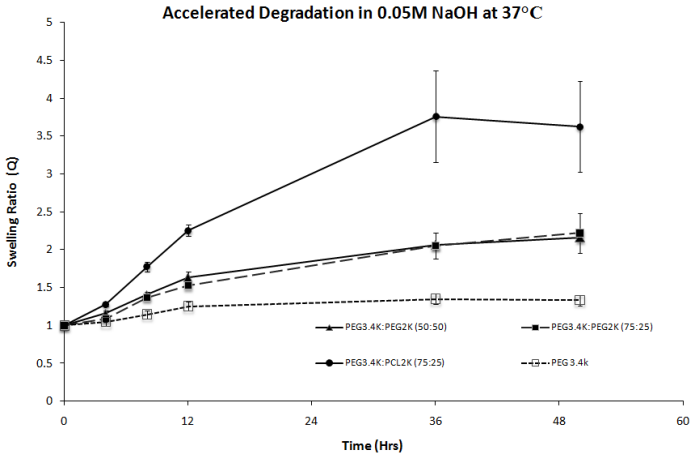

Figure 1: Swelling ratios of PEGDA and PEGDA/PCLDA hydrogels in the accelerated degradation study.

Conclusions: By incorporating a hydrolysable component into a traditionally stable hydrogel, a biodegradable gel was successfully fabricated with a degradation rate that is significantly faster than the standard stable PEGDA hydrogels. These biodegradable hydrogels are excellent candidates as scaffolds for tissue engineering.

References:

[1] West JL. Advanced Materials 18, 2679-2684 (2006).

Efficacy of a Novel Two-Component Polymer Drug-Eluting System for EMR

Richard T. Tran,[1] Michael Palmer,[1] Shou-Jiang Tang,[2] Jian Yang,[1,*]

1. Department of Bioengineering, The University of Texas at Arlington, Arlington, TX 76019-9800, U.S.A.

2. Department of Medicine, The University of Mississippi Medical Center, Jackson, MS 39216-4500, U.S.A.

Background: Biodegradable injectable hydrogels able to deliver therapeutic payloads show great potential for use in EMR to yield improvements in safety, efficacy, and mucosal regeneration.

Objective: Our purpose was to assess the efficacy of an injectable two-component polymer drug-eluting system (TPDS) as a submucosal injection material.

Design: Comparative study among 3 different solutions for EMR using material characterization tests, ex vivo, and in vivo porcine models.

Interventions: A total of 30 gastric submucosal cushions were performed in ex vivo porcine stomachs with saline (0.9%), sodium hyaluronate (0.4%), and TPDS (n = 10). Four in vivo porcine stomach EMRs were then performed.

Main outcome measurements: Material characterization and Rebamipide release profiles were assessed in vitro. Submucosal cushion height and duration were measured ex vivo, and efficacy was assessed by in vivo en bloc resection.

Results: No significant difference in injection pressures between TPDS (28.9 ± 0.3 PSI) and sodium hyaluronate (29.5 ± 0.4 PSI, $P > .05$) was observed. TPDS gels displayed a controlled release of Rebamipide for up to 5 days in vitro. After 30 minutes, the elevation height of TPDS (5.7 ± 0.6 mm) was higher than saline (2.6 ± 0.4 mm, $P < .01$) and SH

THERMOMECHANICAL CHARACTERIZATION AND MODELING OF THERMOSETTING POLYURETHANE SHAPE MEMORY POLYMERS FOR USE IN BIOMEDICAL DEVICES

Volk, B L; Lagoudas, D C; Maitland, D J
Texas A&M University, College Station, TX
brentvolk@tamu.edu

I. OBJECTIVE

The objective of this work is to calibrate a large deformation model using experimental data from testing performed on a polyurethane SMP that is being considered for biomedical applications and then validate the model predictions by comparing to experimental data at different strain values and recovery conditions.

II. METHODS

In this work, both experimental and computational methods are used. Experimentally, thermomechanical tests are performed on thermosetting polyurethane shape memory polymers. Free recovery and constrained recovery tests up to 25% extension are performed to measure the maximum shape recovery and blocking stress of the material, respectively.

Computationally, a finite deformation model is implemented in MATLAB® in 1-D. The material properties necessary to calibrate the model, namely the elastic modulus and coefficient of thermal expansion in each the rubbery and glassy phases and the frozen volume fraction, are calculated from a single free recovery experiment. The calibrated model is used to predict the material response at different values of extension and the predictions are validated by comparing to the experimental data.

III. RESULTS

The complete free recovery behavior was observed for extensions up to 25%, and the recovery was observed to occur at the same temperatures, regardless of the value of applied deformation. In constrained recovery, the polyurethane SMP was able to recover a stress of 4.2 MPa at 25% extension, and this recovery value is higher than current values reported in the literature. The calibrated model was observed to predict well the material response for the polyurethane SMPs at different deformations and recovery conditions. The comparison of the model predictions to the experimental recovery data is presented in Figure 1.

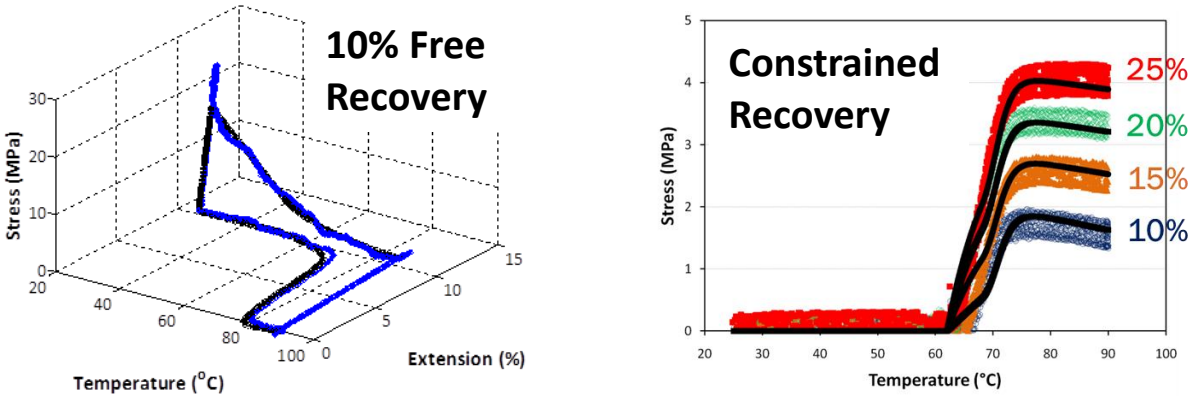

(a) (b)

Figure 1 - (a) Simulation of the 10% free recovery experiment from which the material properties were calibrated and (b) constrained recovery predictions for extensions of 10%, 15%, 20%, and 25%. These results are a subset of the experimentally validated predictions using the model that was calibrated from a single experiment.

IV. CONCLUSIONS

Free recovery and constrained recovery experiments were performed on a polyurethane SMP. A large deformation model was calibrated from a single 10% free recovery experiment and then observed to predict well the material response for free and constrained recovery tests at different extensions. The experimental validation of the large deformation, thermoelastic model for shape memory polymers provides a valuable step toward the three-dimensional, finite element modeling (analysis, design, and optimization) of biomedical devices made out of such materials.

THERANOSTIC NANOPARTICLES FOR CANCER MANAGEMENT

+*Wadajkar, A S; +*Kadapure, T; +*Zhang, Y; **Cui, W; +*Nguyen, K T; +*Yang, J
+Dept of Bioengineering, University of Texas, Arlington, TX
*Joint Biomedical Engineering Program, University of Texas at Arlington and University of Texas Southwestern Medical Center at Dallas, TX
**Dept of Radiology, University of Texas Southwestern Medical Center, Dallas, TX
jianyang@uta.edu

- **Objective:** Significant challenges in cancer management remain on the development of an effective theranostic system that enables efficient imaging and targeting drug delivery for cancer treatment. The aim of this research was to develop novel biodegradable photoluminescent polymer (BPLP)-coated magnetic nanoparticles (MNPs) that can serve as a theranostic nanoparticle system with dual-targeting and dual-imaging capabilities.
- **Methods:** The physicochemical properties of the BPLP-coated MNPs were characterized using dynamic light scattering (DLS), zeta potential analyzer, transmission electron microscope (TEM), and Fourier transform infrared microscope (FTIR). Imaging capability of nanoparticles was tested by an enhanced optical microscope and magnetic resonance imaging (MRI). The magnetic properties were tested using SQUID-based magnetometer. Finally, cytotoxicity on human dermal fibroblasts (HDFa) and cellular uptake of nanoparticles by prostate cancer cells (PC3 and LNCaP) were evaluated by MTS, iron, and pico-green DNA assays.
- **Results:** Our BPLP-coated MNPs were spherical in shape and approximately 230 nm in the diameter as estimated by DLS and TEM. The nanoparticles were stable with negative surface charge. FTIR confirmed the presence BPLP coating on MNPs from the characteristic peaks. Our nanoparticles emitted a bright fluorescence under optical microscope while MRI showed that our nanoparticles produced a bright contrast even at a very low concentration. SQUID-based magnetometer measurements revealed that the magnetic properties of the bare MNPs were maintained even after polymer coating. Moreover, BPLP-coated MNPs were cytocompatible up to a concentration of 500 µg/ml on HDFa, and the cellular uptake of these nanoparticles by PC3 and LNCaP was dependent on the particle dose and magnetic field.
- **Conclusion:** Dual-targeting strategy allows the recruitment of nanoparticles at the targeted tumor site by magnetic targeting and the facilitated uptake of drug-loaded nanoparticles by cancer cells through receptor-mediated targeting. In addition, via dual imaging modalities - magnetic resonance and fluorescence imaging, these nanodevices provide extraordinary tools to diagnose and monitor cancer during the treatment. Our preliminary results confirm the potential of BPLP-coated MNPs as theranostic nanoparticle system. Future studies include the evaluation of these particles for their targeting and drug delivery efficiency *in vitro* and *in vivo* using various cell culture and animal models, respectively.

MOISTURE ABSORPTION EFFECT ON THE SHAPE MEMORY POLYMER FOAMS

*Yu, Y J; *Hearon, K; +Wilson, T S; *Maitland, D J

*Texas A&M University, College Station, TX;
+Lawrence Livermore National Laboratory, Livermore, CA.
yu1122@tamu.edu

◆ Objective:

Polyurethane (PU) SMP foams are being investigated for numerous biomedical device applications because of their excellent biocompatibility and high volume expansion capabilities. With our ultimate goal of engineering SMP PU foams for use in blood contacting environments, we have investigated the effects of moisture exposure on the physical properties of PU foams. To our best knowledge, this study is the first to investigate the effects of moisture absorption at varying humidity levels (non-immersion and immersion) on the physical properties of PU SMP foams. Water uptake, shifts in T_g, stress-strain behavior, and shape memory behavior of the foams were investigated for PU SMP foams that were exposed to 40%-100% humidity levels for varying lengths of time.

◆ Methods:

Polyurethane SMP foams were made from hexamethylene diisocyanate, N,N,N',N'-tetrakis(2-hydroxypropyl) ethylenediamine, and triethanolamine; however, the details of the synthesis are proprietary. Foam samples were placed in an environmental chamber at 25 °C, with controlled humidities of 40 %, 60 %, and 80% for time periods of 12 h, 24 h, 48h, and 96 h. For 100% humidity, the samples were immersed in a water bath at control temperatures of 25 °C and 37 °C. To measure the water uptake of the foams, TGA experiments were run on the foam samples, and mass decrease up to 150 °C was defined as water loss. To evaluate the effect of moisture absorption on T_g, DSC experiments were run. To determine the effects of moisture uptake on the stress-strain behavior and maximum recoverable strain of the samples, strain to failure and free strain recovery experiments were run.

◆ Results:

TGA results demonstrated that the foams exhibited a maximum water uptake of 8.0% (by mass) after exposure to 100% relative humidity for 96 h. For the lower humidities, distinct saturation levels were evident, and the effects of humidity level and moisture exposure time on water uptake. DSC results demonstrated that water absorption significantly decreased the T_g of the foams, with maximum water uptake shifting the T_g from 67 °C to 5 °C. Free strain recovery results demonstrated recovery ratios approaching 100% for samples strained to 25% or lower. Tensile testing results demonstrated that water uptake caused plasticization in the foams: samples exposed to 100% humidity for 96 h exhibited 100% increases in failure strains and 500% decreases in failure stresses.

◆ Conclusions:

The results of this study have implications in both the storage and use of PU SMP foam devices. The water uptake of the polyurethane SMP foams increased with increased humidity exposure time, increased humidity, and increased temperature. The T_g of the PU foams decreased upon moisture absorption, and a maximum shift from 67 to 5 °C occurred after 8% water uptake. These PU SMP foams thus maintain good shape memory behavior after moisture exposure and consequently appear to be useful in biomedical device applications that will subject the foams to physiological conditions.

In vitro Study of pH Sensitive and Biodegradable Dextran based Hydrogels for Oral Delivery of Nanoparticles

Xiao Yu[1], Michael V. Pishko[1]

[1]Department of Chemical Engineering, Texas A&M University, College Station, TX, 77843-3122, U.S.A

asteryu@neo.tamu.edu

Objective

Preparation of pH sensitive, biodegradable polysaccharide based hydrogels for oral delivery of nanoparticles and its *in vitro* release studies.

Methods

Dextran based hydrogels were prepared by UV irradiation with proper photoinitiators. Tunable release profiles of nanoparticles (fluorescent polystyrene nanoparticles, PS NPs) from the hydrogels could be achieved by varying the gel composition, or copolymerizing it with another macromer. *In vitro* release experiments were performed in a shaking water bath at 37 ºC, with enzyme added in the medium (enzyme used to degrade the hydrogel).

Results

Two different kinds of dextran based hydrogels were synthesized. Hydrogels of both kinds were stable in SGF (simulated gastric fluid, pH=1.2), and prone to swelling and degradation in the absence or presence of dextranase in SIF (simulated intestinal fluid, pH=6.8). Controlled releases of fluorescent nanoparticles were achieved by adjusting the degradation rate of the hydrogels, which was influenced by the hydrogel composition.

PS NPs loaded within the gels could be released totally within 6 hrs from the hydrogel prepared by 5 min UV irradiation, while it takes more than 8 hrs to break down the hydrogel prepared by 30 min UV irradiation. Sustained release profiles of fluorescent nanoparticles could be obtained by copolymerizing with another macromer that cannot be degraded by the enzyme. In our case, only 15 μL/mL of PEG-diacrylate (Mw 575) copolymerized within the hydrogel could extend the degradation time to 22 hrs.

Conclusions

Polysaccharide dextran was modified to form a pH sensitive hydrogel and nanoparticles were loaded within the hydrogel network. Releases of these nanoparticles from the hydrogels were observed and adjustable profiles were obtained by changing the hydrogel composition.

MOISTURE ABSORPTION EFFECT ON THE SHAPE MEMORY POLYMER FOAMS

*Yu, Y J; *Hearon, K; +Wilson, T S; *Maitland, D J

*Texas A&M University, College Station, TX;
+Lawrence Livermore National Laboratory, Livermore, CA.
yu1122@tamu.edu

Objective:

Polyurethane (PU) SMP foams are being investigated for numerous biomedical device applications because of their excellent biocompatibility and high volume expansion capabilities. With our ultimate goal of engineering SMP PU foams for use in blood contacting environments, we have investigated the effects of moisture exposure on the physical properties of PU foams. To our best knowledge, this study is the first to investigate the effects of moisture absorption at varying humidity levels (non-immersion and immersion) on the physical properties of PU SMP foams. Water uptake, shifts in T_g, stress-strain behavior, and shape memory behavior of the foams were investigated for PU SMP foams that were exposed to 40%-100% humidity levels for varying lengths of time.

Methods:

Polyurethane SMP foams were made from hexamethylene diisocyanate, N,N,N',N'-tetrakis(2-hydroxypropyl) ethylenediamine, and triethanolamine; however, the details of the synthesis are proprietary. Foam samples were placed in an environmental chamber at 25 °C, with controlled humidities of 40 %, 60 %, and 80% for time periods of 12 h, 24 h, 48h, and 96 h. For 100% humidity, the samples were immersed in a water bath at control temperatures of 25 °C and 37 °C. To measure the water uptake of the foams, TGA experiments were run on the foam samples, and mass decrease up to 150 °C wasdefined as water loss. To evaluate the effect of moisture absorption on T_g, DSC experiments were run.

Results:

TGA results demonstrated that the foams exhibited a maximum water uptake of 8.0% (by mass) after exposure to 100% relative humidity for 96 h. For the lower humidities, distinct saturation levels were evident, and the effects of humidity level and moisture exposure time on water uptake in Fig. 1. DSC results demonstrated that water absorption significantly decreased the T_g of the foams, with maximum water uptake shifting the T_g from 67 °C to 5 °C in Fig. 2.

Conclusions:

The results of this study have implications in both the storage and use of PU SMP foam devices. The water uptake of the polyurethane SMP foams increased with increased humidity exposure time, increased humidity, and increased temperature. The T_g of the PU foams decreased upon moisture absorption, and a maximum shift from 67 to 5 °C occurred after 8% water uptake. These PU SMP foams thus maintain good shape memory behavior after moisture exposure and consequently appear to be useful in biomedical device applications that will subject the foams to physiological conditions.

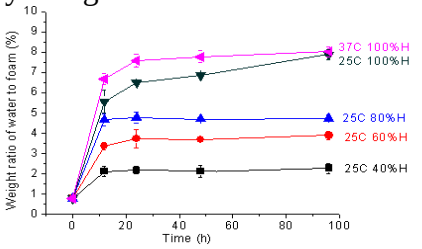

Figure 1. The effect of humidity exposure time up moisture absorption, measured by TGA

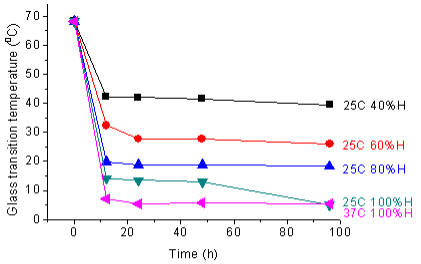

Figure 2. The effect of moisture absorption on T_g

POROUS INORGANIC-ORGANIC SHAPE MEMORY POLYMERS

+Dawei Zhang, William L. Burkes, Cody A. Schoener and Melissa A. Grunlan
Texas A&M University, Department of Biomedical Engineering,
Materials Science and Engineering Program, College Station, TX, +zhangdavei@tamu.edu

Objective: Thermoresponsive shape memory polymers (SMPs) are "smart" materials whose shape is modulated by thermal changes.[1] SMPs have been fabricated in the form of thin films and porous foams.[2,3] Compared to solid SMPs, porous SMPs are lightweight, highly compressible and more permeable to heat.[4] We have recently reported a new class of "inorganic-organic" SMPs that can be prepared via photochemical cure of macromers comprised of an organic poly(ε-caprolactone) (PCL) "switching segment" and an inorganic polydimethylsiloxane (PDMS) "soft segment" (AcO-PCL_n-*block*-$PDMS_m$-*block*-PCL_n-OAc).[5,6] The melting transition of the PCL crystalline domains served as the transition temperature ($T_{trans} = T_m$ = ~50 ºC). These solid SMPs exhibited excellent shape memory abilities and highly tunable physical properties resulted from varying the PCL and PDMS segment lengths. In this study, we fabricated SMP foams by photocuring CH_2Cl_2-based precursor solutions of AcO-PCL_{40}-*block*-$PDMS_{37}$-*block*-PCL_{40}-OAc in the presence of leachable water-fused NaCl particles. The pore morphology, mechanical and shape memory properties of these foams were tailored by changing the macromer concentration, extent of salt fusion and salt size.

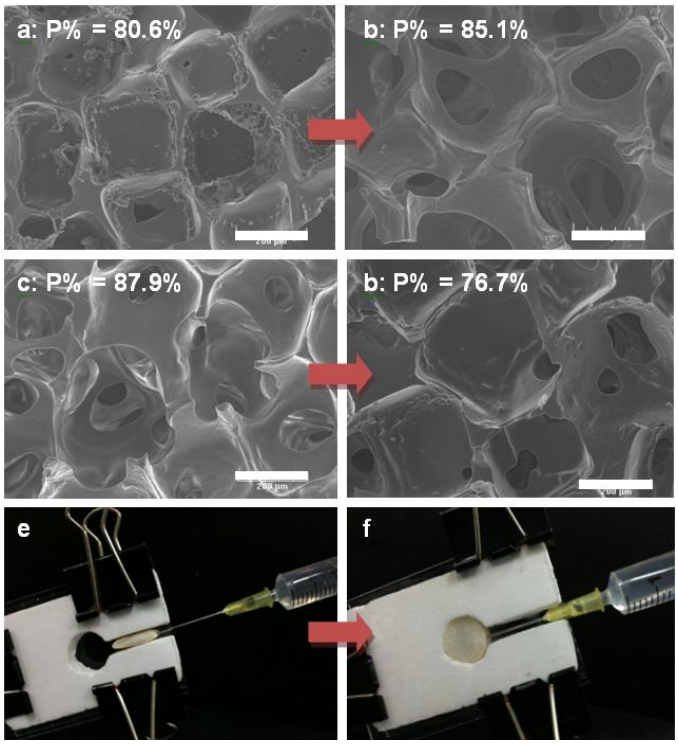

Figure 1. SEM images: *Top row*: (0.15 g/mL) with increased salt fusion from (**a**) 0 wt% to (**b**) 7.5 wt% water; *Middle row:* SMP foams (5 wt% water) with increased macromer concentration from (**c**) 0.1g/mL to (**d**) 0.3 g/mL; *Bottom row*: **e-f:** deploying SMP foam (0.15 g/mL; 5 wt% water) in a model defect. (Scale bars = 200 µm).

Methods: NaCl salt (particle size: 459 ± 69 µm) was "fused" by adding DI water (0, 2.5, 5 or 7.5 wt% based onto 1.8 g salt) inside a glass vial (OD = 14.7 mm). Macromer precursor solution (0.1, 0.15, 0.2 and 0.3 g/mL in CH_2Cl_2) was added to cover the fused salt and photocured for 3 min (6 mW/cm^2, 365 nm). After air-drying overnight, the salt was removed by soaking in a water/ethanol (1:1 vol:vol) for 4 days with daily changes of solvent and sequentially dried in air overnight. Finally, the foam was annealed at 85 °C for 1 hr.

Results: Pore interconnectivity and % porosity (P%) increased with increased extent of salt fusion (i.e. increased wt% water) and with decreased concentration of macromer in the precursor solution (**Figure 1: a-d**). Strain-controlled thermal mechanical compression tests revealed that the foams exhibited ~100% shape fixity and shape recovery between ~91-98% (after an initial "pre-cycle") depending on porosity and macromer concentration in the precursor solution. Compression tests of foams showed that the elastic modulus could be tuned from 0.8 to 4.2 MPa depending on fabrication variables.

Conclusions: In this study, we have successfully fabricated porous inorganic-organic SMPs with controllable pore interconnectivity, porosity, mechanical and shape memory properties. These SMP foams have potential use as self-fitting scaffolds delivered via minimally invasive surgery to heal bone defects (**Figure 1: e-f**).

References:

1. Lendlein, A.; Kelch, S. *Angew. Chem. Int. Ed.*, 2002, 41, 2034-2057.
2. Nagata, M.; Sato, Y. *J. Polym. Sci., Part A: Polym. Chem.*, 2005, 43, 2426-2439.
3. Maitland, D. X.; Metzger, M. F.; Schumann, D.; Lee, A.; Wilson, T. S. *Lasers Surg. Med.*, 2002, 30, 1-11.
4. Chung, S. E.; Park, C. H. *J. Appl. Polym. Sci.*, 2010, 117, 2265-2271.
5. Schoener, C. A.; Weyand, C. B.; Murthy, R.; Grunlan, M. A. *J. Mater. Chem.*, 2009, 20, 1787-1793.
6. Zhang, D.; Giese, M. L.; Prukop, S. L.; Grunlan, M. A. *J. Polym. Sci., Part A: Polym. Chem.*, 2011, 49, 754-761.

Novel Elastomeric Particle Reinforced Biodegradable Composites for Orthopaedic Implant/Fixation Devices

Chang Zhang[1], Richard T. Tran[1], Sthanu Mahadev[2], Dragos-Stefan Dancila[2], Jian Yang[1]*

[1]Department of Bioengineering and [2]Department of Mechanical & Aerospace Engineering

The University of Texas at Arlington, Arlington, TX 76010

Abstract

Orthopedic surgeons often use tissue fixation devices such as pins, plates, and screws or bone implants made from biodegradable poly(L-lactide) (PLLA). Although biodegradable medical devices can have significant advantages over their metal counterparts, there are concerns such as slow degradation rates and their inability to fully integrate with the bone, which can be problematic and require revision surgeries. A strategy to improve the osteointegration ability of polymers has been to blend polymers with hydroxyapatite (HA), a bioceramic that is proven to be osteoconductive. However, HA is very brittle and hard to process into fixation devices with sufficient strength and fatigue resistance. Even through significant work has been devoted to working with polymer/HA composites, none of the investigated formulations could provide the required mechanical properties for the resulting orthopedic devices, which are subject to high stress and often undergo cyclic mechanical loading (e.g. intervertebrate disks).

In the present work, we formulated novel elastomeric/HA composites based upon our recently developed citric acid-based biodegradable elastomers, crosslinked urethane-doped polyesters (CUPEs) [1], and poly(diol citrates) (POC). POC/HA composites formulated previously have demonstrated biocompatibility and osteoconductivity *in vivo* but lack of sufficient strength for some orthopedic applications such as bone screws [2]. Incorporating mechanically stronger CUPE into the POC/HA composites greatly enhance the mechanical strength without sacrificing elasticity, osteoconductivity and cytocompatibility in vitro, and homogeneity of the composites. The new CUPE/POC/HA composites are rigorously characterized in terms of their biodegradation, mineralization, and mechanical properties (tensile, compressive, bending, shear, etc.). The development CUPE/POC/HA elastomeric composites provides viable candidates for many orthopedic applications such as bone fixation devices and bone tissue engineering implants.

References

[1] Jagannath Dey, Hao Xu, Jinhui Shen, Paul Thevenot, Sudershan R. Gondi, Kytai T. Nguyen, Brent S. Sumerlin, Liping Tang, Jian Yang. Development of biodegradable crosslinked urethane-doped polyester elastomers. *Biomaterials* 2008, 29:4637-4649.

[2] Hongjin Qiu, Jian Yang, Pradeep Kodali, Jason Koh, Guillermo A. Ameer. "A citric acid-based hydroxyapatite composite for orthopaedic implants." *Biomaterials*, 2006, 27, 5845-5854.

ANTIBACTERIAL ACTIVITIES OF GOLD AND SILVER NANOPARTICLES AGAINST *ESCHERICHIA COLI* AND BACILLUS CALMETTE-GUÉRIN

Zhou, Y[1]; Kong, Y[2]; Kundu, S[1,3]; Cirillo, J D[2]; Liang, H[1,3]

1. Materials Science and Engineering, Texas A&M University, College Station, TX

2. Department of Microbial and Molecular Pathogenesis, Texas A&M Health Sciences Center, College Station, TX

3. Department of Mechanical Engineering, Texas A&M University, College Station, TX

Email: yanzhou@tamu.edu

Objective

The objective of our research is to investigate effects of gold and silver nanoparticles (NPs) on bacillus Calmette-Guérin (BCG) and *Escherichia coli*.

Methods

Experimentally, particle size and shape were characterized using transmission electron microscope (TEM). Different concentrations of NPs were applied in bacteria culture. The growth of *E. coli* was monitored through colony forming units (CFU). Inhibitory effects on BCG growth were observed by recording fluorescent protein expression levels. Dynamic interaction between NPs and bacteria was analyzed through bacteria thin sections followed by TEM.

Results and Conclusions

The results suggest NPs have a potential application as antibacterial compounds. The antibacterial effects and mechanism of action for NPs were dependent upon composition and coating agents.

TUNABLE, ULTRA-SENSITIVE PH RESPONSIVE NANOPARTICLES TARGETING SPECIFIC ENDOCYTIC ORGANELLES IN LIVING CELLS

[+]Zhou, K; [+]Wang, Y; [+]Huang, X; [*]Poudel, M; [+]Gang, H; [*]Luby-Phelps, K K; [**]Sumer, B D; [+]Gao, J.
[+]*Harold C. Simmons Comprehensive Cancer Center,* [*]*Department of Cell Biology and* [**]*Department of Otolaryngology, the University of Texas Southwestern Medical Center, Dallas, TX. USA*
kejin.zhou@utsouthwestern.edu

Objective

It will be developed a set of tunable, pH-activatable micellar (pHAM) nanoparticles based on the self-assembly of ionizable copolymers which can be selectively activated in specific endocytic compartments such as early endosomes or lysosomes in human cells.

Methods

It was synthesized two series of block copolymers (PEO-*b*-PR) with tertiary amine-containing (PR) and poly(ethylene oxide) (PEO) segments by atom transfer radical polymerization. A pH-insensitive dye, tetramethyl rhodamine (TMR), was used as a model fluorophore and conjugated in the PR block as an imaging beacon to investigate the pH responsive properties.

Results

These nanopartilces have fast temporal response (<5 ms), large increase of emission intensity between ON/OFF states (up to 55 times), and only require <0.25 pH for activation. The nanoparticles with pH transitions at 6.3 and 5.4 can be selectively activated in different endocytic compartments such as early endosomes (pH 5.9-6.2) and lysosomes (5.0-5.5).

Conclusions

It is successfully established a series of pH-activatable micellar nanoparticles with tunable and ultra-sensitive pH response in the physiological range (5.0-7.4). These nanopartilces can be selectively activated either in early endosomes or in lysosomes. This nanoplatform may offer some exciting opportunities in the development of nonlinear ON/OFF nanosystems for diagnostic imaging and drug delivery applications.